Synthesis and electrochemical study of aromatic manganese carbonyl complexes and applications in hydrogen storage & proton reduction catalysis

By Wei Dai

B.S. Unitersity of Science and Technology of China 2006

A Dissertation Submitted in Partial Fulfillment of the
Requirements for the Degree of Doctor of Philosophy
in the Department of Chemistry at Brown University

Providence, Rhode Island
May 2012

This dissertation by Wei Dai is accepted in its present form
by the Department of Chemistry as satisfying the dissertation requirement
for the degree of Doctor of Philosophy.

Date_____ _____

Dwight A. Sweigart, Advisor

Recommended to the Graduate Council

Date_____ _____

Shouheng Sun, Reader

Date_____ _____

Eunsuk Kim, Reader

Approved by the Graduate Council

Date_____ _____

Peter Weber, Dean of the Graduate School

VITA

Wei Dai was born on Jan. 12, 1984 in lianyungang, Jiangsu. He attended the USTC from Sep. 2002 to June 2006, graduating with a B. S. in Chemistry Department. He has been a research assistant in Dr. Yi Xie's lab since summer in 2004, and has co-authored a few publications in peer-reviewed journals. In 2006, he was admitted to the Department of Chemistry of Brown University. In December of 2006, he began to work toward the degree of Doctor of Philosophy in the area of organometallic electrochemistry under the supervision of Professor Dwight A. Sweigart. During this time, he held positions as research and teaching assistant. During his 5 years at Brown, he published 1 paper and 2 more in process. He won the poster price in 2010 of the chemistry department. Right now he is exited about the new discovery of proton couple reduction catalyzed by aromatic manganese complexes. He will continue his academic career as an electrochemist in organometallics.

Publications at Brown University

1. Wei Dai, Sang Bok Kim, Robert D. Pike, Christopher L. Cahill and Dwight A. Sweigart*. "Electrochemical study of manganese and rhenium arene complexes (C6R6)M(CO)3+ (R= Me, Et)". *Organometallics* **2010** 29(21), 5173-5178
2. Wei Dai and Dwight A. Sweigart*. "Electrocatalytic proton reduction by aromatic manganese carbonyl complex". Manuscript in preparation
3. Wei Dai, Robert D. Pike, Dwight A. Sweigart*. "Direct synthesis and characterization of (η^6-aniline) manganese tricarbonyl cation and its analogs". Manuscript in preparation
4. Weibin Li, Gerald Kagan, Huan Yang, Chen Cai, Russell Hopson, Wei Dai, Dwight A. Sweigart and Paul G. Williard*. "Accurate Formula Weight Determination in Physically Separated Systems by Diffusion Coefficient−Formula Weight Correlation". *Organometallics* **2010** 29(6), 1309-1311

Acknowledgements

First of all, I am grateful to have Dr. Sweigart as my advisor. I knew nothing about organometallics before joining his group, he teached me electrochemistry of organometallics which is a very useful technique. He inspired me with great ideas about new directions of my study. Without his fully support, I could not survive through these five years.

Secondly, I would like to express my gratitude to my research committee members: Dr. Sun, I appreciate your kind help as my reference, for your helpful advise in my study; Dr. Suggs and Dr. Kim, I would like to thank you for been my committee in ORP and RPD. And I wish you all the best in the future.

Thirdly, I would like to thank Dr. Risen for being my reference. He is truly a nice professor to the chinese community in chemistry department. He phone interviewed me before I came to Brown and teached me advanced inorganic chemistry in my first year. You are truly missed, Bill.

Also, I want to thank Lynn, Ginni, Gen, Eric, Allen. Lynn, thank you for being so kind to me. Ginni, thank you for your help for all these five years. Gen, you are missed by the whole department.

Even though our group is not a rich group financially, and we haven't been to many different places for the conferences, but we have been to a few places many many times, and we had our fun as a team in sun valley, davenports, boss's house. Not many graduate students can really share a life with their advisors, we did and enjoyed it. Boss, to me, you are like a father. You are a person who always has a place in my

heart for as long as I live. I wish that you have a good health and great happiness in the future.

I wish all the students from Sweigart group best luck.

Finally, I would like to thank my mom and dad for being there with me whenever I need them. The only thing is, I missed them so much……

Abstract of "Synthesis and electrochemical study of aromatic manganese carbonyl complexes and applications in hydrogen storage & proton reduction catalysis" by Wei Dai, Ph.D., Brown University, May 2012.

The scope of understanding of aromatic manganese reductive electrochemistry was extended. Five internally connected projects will be introduced. My studies primarily focused on homogeneous and heterogeneous electrochemistry of organomanganese complexes and possible application in electrocatalysis, specifically, proton reduction catalysis.

The mechanism of homogeneous reductive electrochemistry of $[(\eta^6\text{-HMB})Mn(CO)_3]^+$ was investigated: it undergoes 1-electron irreversible reduction at room temperature and 2-electron reversible reduction at low temperature. And for the first time, we observed reversibility of 2-electron reduction at room temperature by altering the electrochemical environment.

An important reduction intermediate $[(\eta^6\text{-HMB})Mn(CO)_2]^-$ was believed to catalyze proton reduction in strong acidic condition. The proton coupled reduction mechanism was discussed, based on which, optimization of this new class of Mn-catalyst was also proposed. Followed by a different mechanism, polyarene analog, $(\eta^6\text{-naphthalene})\ Mn(CO)_3^+$ can be used to transfer and store electric energy to stable "metal hydride" complex and releases the hydrogen when needed.

A one-step synthetic method for direct synthesis of $(\eta^6$-aniline) manganese tricarbonyl cation and its analogs was discovered. The aniline complex is an important precursor for heterogeneous electrochemistry study. The purpose of heterogeneous electrochemistry study is to achieve the reductive electrochemical

reversibility by covalent attachment of electrode surface with arene manganese tricarbonyl moiety. Physical separation of manganese compound may stop the dimerization after one-electron reduction and result in reductive reversibility. One of my projects is focused on covalent attachment of arene manganese tricarbonyl using diazonium-base chemistry and collecting & analyzing e-chem signal from the surface functionalized electrode.

The η^6-aromatic manganese dicarbonyl anion is strong nucleophile. It would be interesting to check the reaction between the manganese anion with $[(\eta^6\text{-HMB})Re(CO)_3]PF_6$. We want to explore the possibility of forming the heterodinuclear dimmer with a novel core structure of Mn-Re metal-metal bond. There is no report about the study of Mn-Re metal-metal bond; furthermore, heterodinuclear complex has potential applications in molecular catalysis.

Table of contents

List of Figures

List of Schemes

List of Tables

List of Charts

List of Formula

Chapter 1

Synthesis and electrochemistry study of aromatic manganese carbonyl complexes and their applications in hydrogen storage, proton reduction catalysis:

General introduction

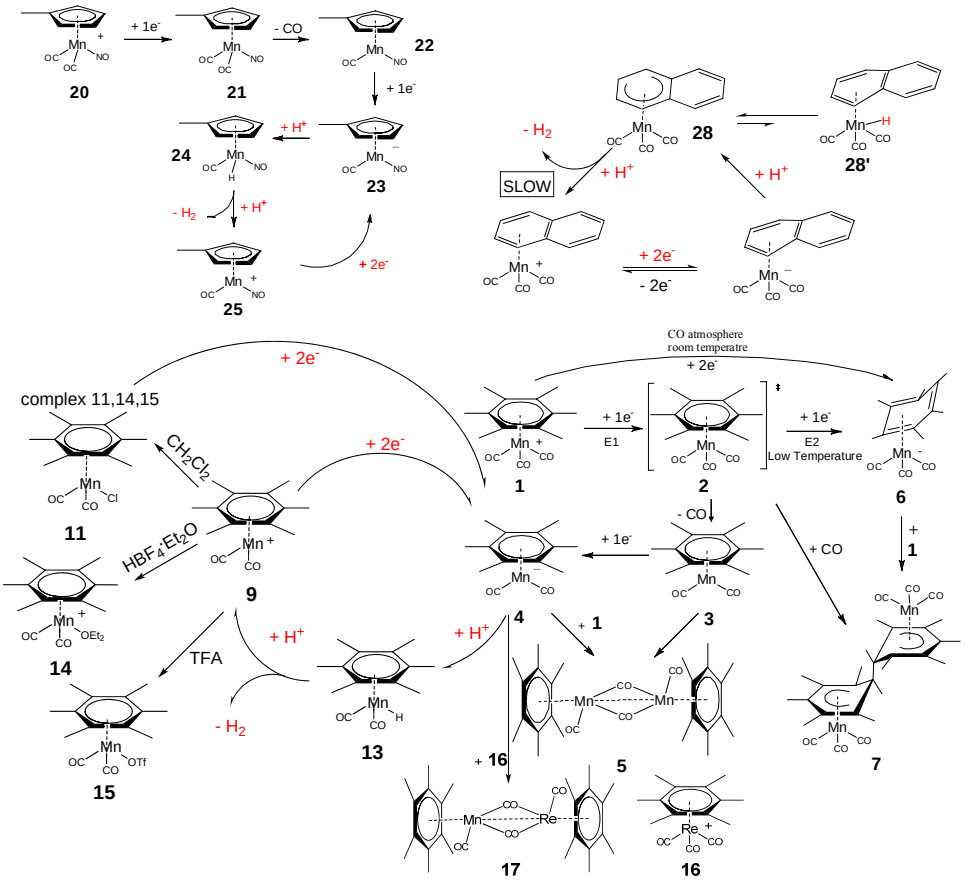

1.1 Overview

It is well known that the origins of organomanganese chemistry are found in the time of the discovery of ferrocene, and following development of organometallic chemistry has been in step with the rapid expansion of most other transition metals. However, the organometallic chemistry of manganese was only initiated in the late 1930s and early 1940s, and the first example is phenylmanganese species, of which the investigation was incomplete and unsubstantiated.

The development of the organomanganese chemistry dates essentially from 1954. Dimaganese decacarbonyl is the first fully characterized manganese compound. Methylcyclopentadienyl manganese tricarbonyl (MMT), which was marketed initially in 1958 as a supplement to the gasoline additive tetraethyl,[1] is the most wildly used organomanganese complex in the industry. Until late 1960s, the first η^6 arene manganese tricarbonyl was synthesized. Not surprisingly, due to the strong electron withdrawing ability, manganese tricarbonyl strongly changed the reactivity of the coordinated arene ring. For example, arene can readily undergo nucleophilic addition when coordinated to the manganese tricarbonyl moiety.[2a-g] This electrophilic activation leads to two important applications:

(1). Organic synthesis[3-4]: Manganese coordinated arene rings can be further functionalized by desired nucleophilic group.

(2). Remote activation: (A). C-C activation.[5-6] Cleavage of a strained C-C bond in the four-membered ring in biphenylene (BP) is enormously facilitated by coordination of the electrophilic fragment $Mn(CO)_3^+$ to one of the aromatic rings. (B). C-S

activation.[7-11] Coordination of $Mn(CO)_3^+$ to a carbocyclic ring of sterically congested thiophenes activates a C-S bond to regiospecific insertion of platinum. (C). C-O activation.[12]

In my group, the study of arene manganese tricarbonyl is not only one of the most important research areas, but also the most long lasting research topic. The past group members have thoroughly investigated synthetic scope[13] and chemical properties of monoarene and polyarene manganese tricarbonyl cations.[14] There is another important aspect deserves great attention, however not being well developed —— homogeneous and heterogenous electrochemistry of monoarene manganese tricarbonyl and its analogs, it will be discussed in chapter 3 and 6. Also, in chapter 4, the proton reduction catalyzed by aromatic manganese carbonyl complexes will be discussed. I also broaden the synthetic scope of aromatic manganese, and report the first direct synthesis method of (η^6-aniline) $Mn(CO)_3^+$ and its analogs (chapter 5).

1.2 Electrochemistry of aromatic manganese carbonyl complex and its analogs

The homogeneous electrochemistry of monoarene manganese tricarbonyl and dicarbonyl was investigated: Compared with the far greater reactivity of the polyarene manganese tricarbonyl cations,[14] monoarene manganese tricarbonyl complex $[(\eta^6\text{-HMB})Mn(CO)_3]PF_6$ and its analogs exhibit quite stable properties. It is reduced irreversibly by one electron at much more negative potential to give $19e^-$ unstable radical at room temperature, the free radicals will dissociate one carbonyl from the

$Mn(CO)_3^+$ moiety followed by dimerization to afford a green color bimetallic compound with a metal-metal bond.[15] However, when the temperature is low enough, the reduction is 2-electron chemically reversible with η^4-HMB $Mn(CO)_3^-$ as the product. Slow heterogeneous charge transfer accompanies the formation of the ring-slippage contribute to the large peak separation in the cyclic voltammogram. The electrochemical properties of other analogs, such as HMB $Re(CO)_3^+$ PF_6^- was also studied via combining CV, bulk electrolysis and in-situ optic IR techniques together.

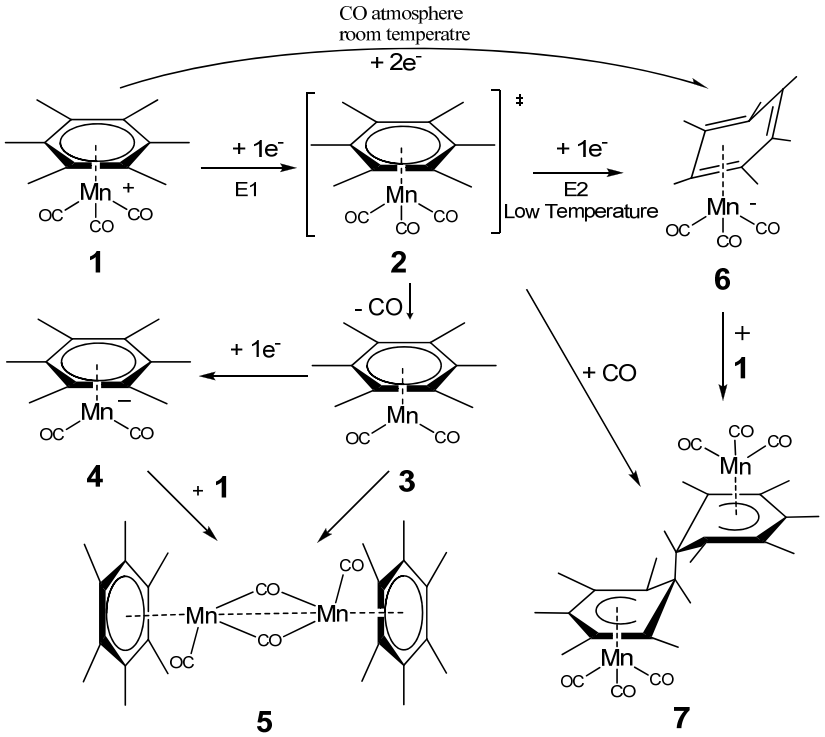

Scheme 1-1. Mechanism of (η6-HMB)$Mn(CO)_3^+$ reduction electrochemistry.

Interestingly, under the protection of carbon monoxide, the same compound $[(HMB)Mn(CO)_3]PF_6$ exhibits chemically reversible cyclic voltammetry curve at room temperature. It is common to observe ring-slipped polyarene manganese tricarbonyl anions at room temperature which have already been synthesized and

characterized by x-ray[16-17]. It is the first time to observe the formation of ring slippage monoarene manganese tricarbonyl anion at such a high temperature. Chemical reduction carried out under CO might afford isolable compound **6** (η^4-HMB) $Mn(CO)_3^-$ anion. The structure information might be interesting.

1.3 Proton reduction catalyzed by aromatic manganese carbonyl complexes

Hexamethylbenzene manganese tricarbonyl cation $[(\eta^6\text{-HMB})Mn(CO)_3]PF_6$ is very stable towards acid. However it is not after it is reduced. Since its reduction intermediate ($(\eta^6\text{-HMB})Mn(CO)_2^-$) would react with proton to generate ($(\eta^6\text{-HMB})Mn(CO)_2H$), which is also reactive towards acid. This metal hydride $[(\eta^6\text{-HMB})Mn(CO)_2H]$ complex would be protonated to afford hydrogen and $[(\eta^6\text{-HMB})Mn(CO)_2L]$ (L is the solvent or counter anion of the acid). The stability and reactivity of the complex $[(\eta^6\text{-HMB})Mn(CO)_2H]$ has been previously studied by Eyman.[18] The $[(\eta^6\text{-HMB})Mn(CO)_2L]$ can be reduced by two electrons and react with proton to finish the catalytic cycle. It has been proved that, $(\eta^6\text{-HMB})Mn(CO)_2^+$ does catalyze the proton reduction reaction after it is reduced in dichloromethane with HBF_4 presents. Inspired by it, we synthesized another aromatic manganese carbonyl cation: methylcyclopentadienyl manganese dicarbonyl nitrosyl $[methylcyclopentadienylMn(CO)_2NO^+]$, which can be reduced at more positive reduction potential compared with $[(\eta^6\text{-HMB})Mn(CO)_3^+]$. Not surprisingly, it does show similar proton coupled reductive electrochemistry at -0.3V (Vs Ag/AgCl).

Herein, we want to report the first proton reduction catalyzed by aromatic manganese carbonyl complex based on metal hydride mechanism. These aromatic manganese derivatives are promising catalysts for proton reduction. We are working on optimizing the efficiency of this class of catalyst.

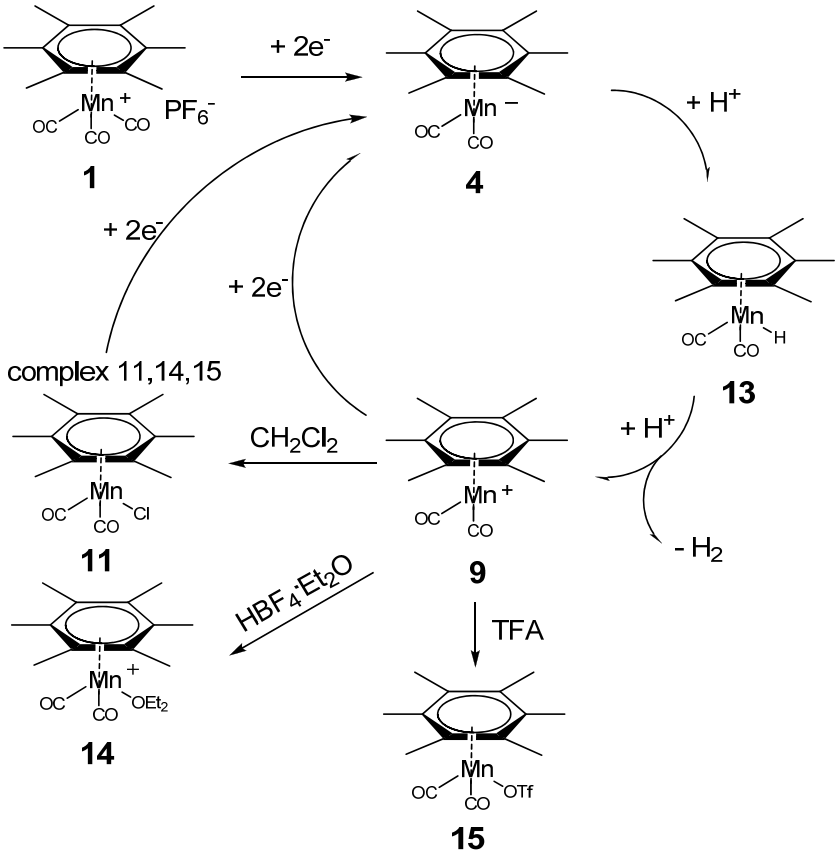

Scheme 1-2. Proposed mechanism of proton reduction catalyzed by (η^6-hexamethylbenzene) manganese dicarbonyl anion.

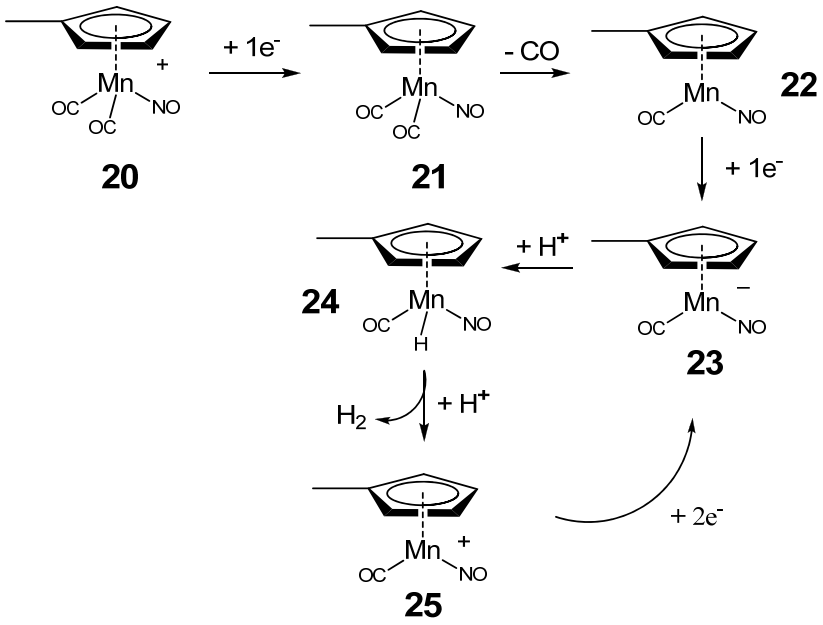

Scheme 1-3. Proposed mechanism of proton reduction catalyzed by [(η^5-methylcyclopentadienyl)Mn(CO)$_2$NO]BF$_4$

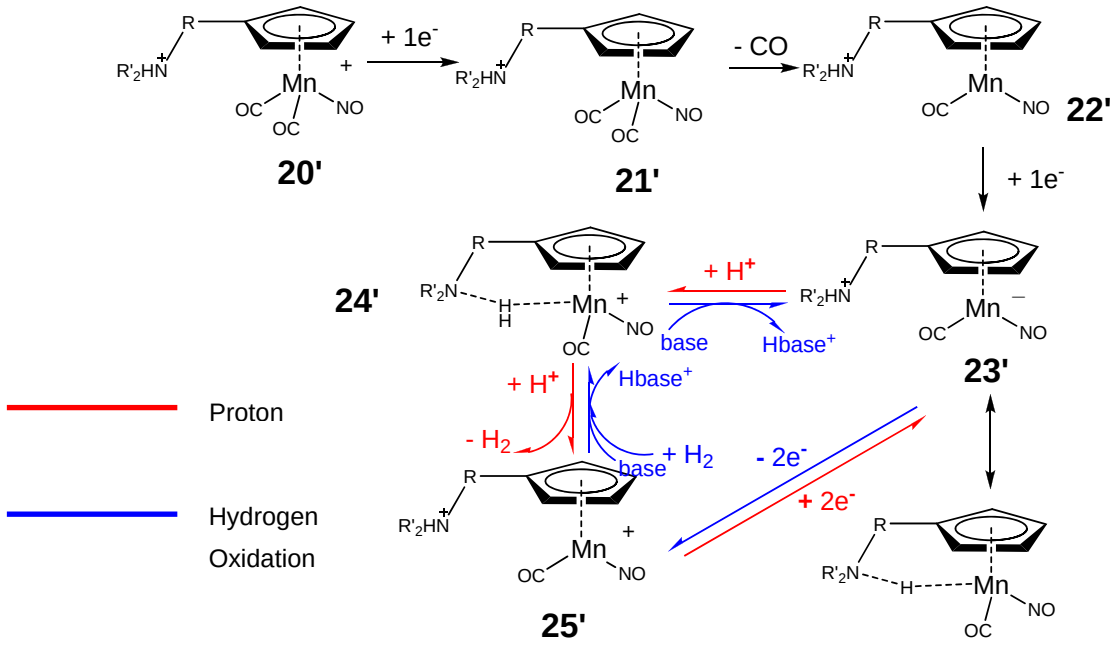

Scheme 1-4. Optimization of (η^5-Cp)Mn(CO)$_2$NO$^+$ procatalyst.

Moreover, η5-hydronaphthalene complex, such as polyarene (η^5- $C_{10}H_9$) $Mn(CO)_3$ or monoarene (η^5- C_6H_7) $Mn(CO)_3$, could react with proton to liberate dihydrogen gas and generate (η^6-naphthalene) $Mn(CO)_3^+$ cation. Specifically,

(η^6-naphthalene) $Mn(CO)_3^+$ can be used to transfer and store electric energy to stable "metal hydride" complex and releases the hydrogen when needed.

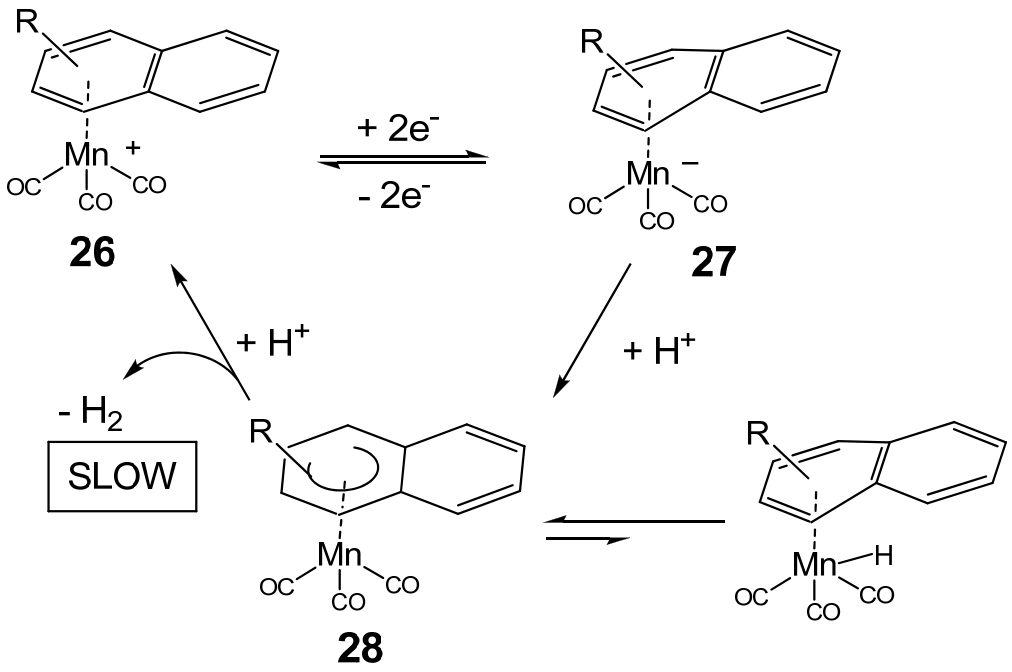

Scheme 1-5. Polyarene manganese tricarbonyl mediated proton coupled electron storage ("hydride" storage) and hydrogen slow release.

1.4 Direct synthesis of (η^6-aniline) manganese tricarbonyl cation and its analogs

Arene manganese tricarbonyl is one of the most useful compounds in organomanganese chemistry. Four methods have been applied to the synthesis of arene manganese complexes, but the direct synthesis of (η^6-aniline) manganese tricarbonyl complex remains challenging[13] because of the basicity of amine group. Traditionally, manganese complexes of this kind could only be obtained through

nucleophilic substitution of chloroarene manganese tricarbonyl by primary or secondary amines,[19] which involves side reactions and usually in an overall low yield. Herein we report a direct synthetic method of making (η^6-aniline) manganese tricarbonyl complexes in moderate to high yield. The synthesis follows the mechanism shown below: one equivalent of manganese (MTT) links to three equivalents of amine to yield 29, which reacts with a second MTT to produce 30. Complex 30 spontaneously cleavages to the desired product 31. The X-ray structure of 31 (R = H, m-NH_2) was determined. The objective of direct synthesis of π-bonded aniline mangaeses complex is two folds: (1) synthesis of aniline analogs with desired functional group (2) precursor of heterogeneous electrochemistry using diazonium attachment (see chapter 6).

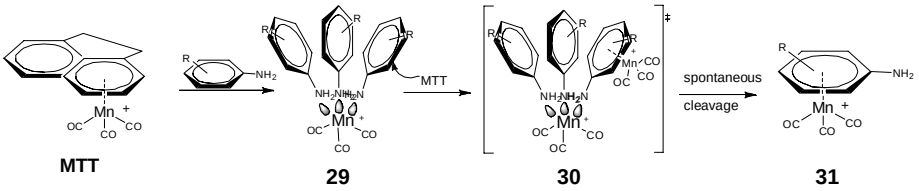

Scheme 1-6. Mechanism of direct synthesis of (η^6-aniline) $Mn(CO)_3^+$ and its analogs (R = alkyl, or m-NH_2 group)

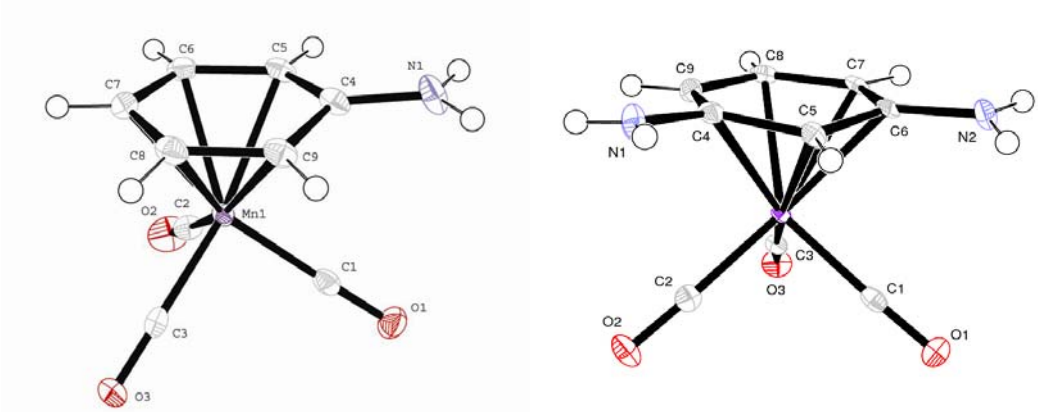

31 (R = H) 31 (R = m-NH_2)

Figure 1-1. Crystal structure of compound **31**

Direct synthesis method of (η^6-aniline) $Mn(CO)_3^+$ was discovered, which provided us a new and much simplified synthetic route toward activation of aniline and organic synthesis of aniline analogs with desirable functional groups. Furthermore, (η^6-aniline) $Mn(CO)_3^+$ is an important precursor for surface modification of the electrode using diazonium attachment.

1.5 Surface electrochemistry of aromatic manganese tricarbonyl complexes using diazonium attachment and physical attachment.

The purpose of heterogeneous electrochemistry study is to achieve the electrochemical reductive reversibility by covalent attachment of arene manganese tricarbonyl using diazonium-base chemistry or simply physical adsorption attachment. Physical separation of manganese compound may stop the dimerization after one-electron reduction and result in reductive reversibility. Organometallic electrode[20] is a new concept in the area of heterogeneous electrochemistry. One of my projects is focused on covalent attachment of arene manganese tricarbonyl using

diazonium-base chemistry and collecting and analyzing e-chem signal from the surface functionalized electrode.[21]

Not being alike aniline by itself, manganese tricarbonyl functionalized aniline complex (η^6-aniline) $Mn(CO)_3^+$ could not be diazotized by nitrite. So we change its hapticity from eta6 to eta5 to make the π system more electron rich. (η^5-aminocyclohexadienyl) manganese tricarbonyl was synthesized and diazotized to afford (η^5-cyclohexadienyldiazonium) manganese tricarbonyl complex. This cyclohexadienyl manganese tricarbonyl diazonium complex can be reduced to liberate nitrogen and form a bond between the cyclohexadienyl group and electrode surface. The substituted hydrogen could be removed by treating with CPh_3^+ or strong acid thereafter. Herein, we want to report a unique method for surface modification of electrode by (η^6-aromatic) manganese tricarbonyl cation. We want to compare its reductive electrochemistry before and after electrode surface modification, and we expect to see that the chemical reversibility shows up. No preliminary data has been acquired yet. We are still working on the purification and characterization of the intermediates. (η^6-$C_6H_5NHC_6H_4NH_2$)$Mn(CO)_3^+$ was synthesized from nucleophilic substitution of (η^6-C_6H_5Cl)$Mn(CO)_3^+$ by p-phenylenediamine, then it was diazotized to afford (η^6-$C_6H_5NHC_6H_4N_2$)$Mn(CO)_3^{2+}$. We can see partial reversibility shows up in the CV time scale.

In the meanwhile, taking advantage of the solubility of arene manganese tricarbonyl complex, we have done their heterogeneous electrochemistry by physical attachment.

(η^5-aminocyclohexadienyl) manganese tricarbonyl mediated slow hydrogen release is the side reaction when it is treated with acid. Other (η^5-hydrocyclohexadienyl) manganese tricarbonyl analogs show similar properties of hydrogen release. The amine group of $(\eta^5\text{-}C_6H_6NH_2)Mn(CO)_3$ facilitates the hydrogen release reaction.

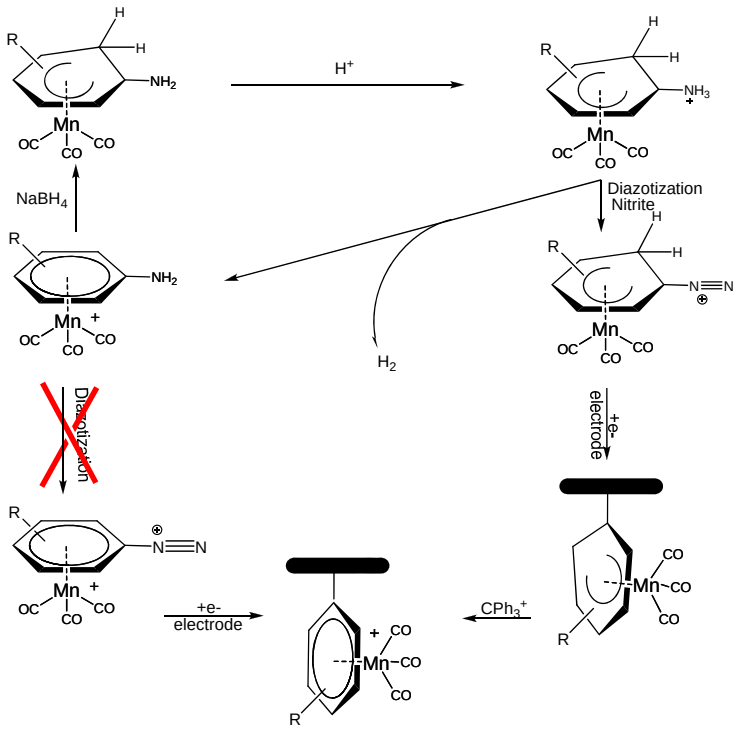

Scheme 1-7. Surface modification of electrode by aromatic manganese tricarbonyl cation through diazonium attachment & slow hydrogen release as side reaction.

1.6 Synthesis and characterization of heterodinuclear complex with the core structure of Mn-Re metal-metal bond.

The η^6-aromatic manganese dicarbonyl anion is strong nucleophile, it was proposed to be the important intermediate which catalyzed the proton reduction

reaction (chapter 4). By introducing the dicarbonyl anion with the tricarbonyl cation stoichiometrically, Eyman reported the formation of an aromatic homodinuclear manganese complex with a Mn-Mn bond and bridged carbonyl ligands.[18] It would be interesting to check the reaction between the same manganese anion with $[(\eta^6\text{-HMB})Re(CO)_3]PF_6$. We want to explore the possibility of forming the heterodinuclear dimmer with a novel core structure of Mn-Re metal-metal bond. There is no report about the study of Mn-Re metal-metal bond; furthermore, heterodinuclear complex has potential applications in molecular catalysis.

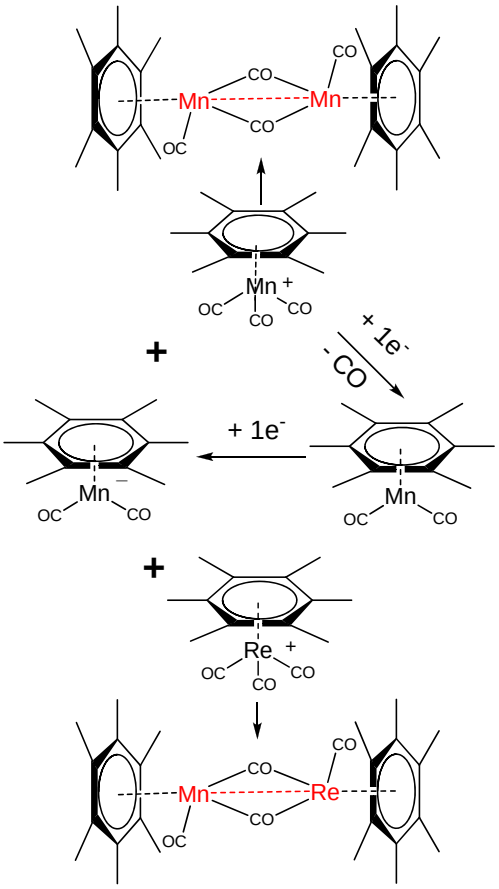

Scheme 1-8. Proposed scheme of formation of Mn-Re metal metal bond

1.7 References

1. Information about Methylcyclopentadienyl manganese tricarbonyl, please refer to wikipedia at http://en.wikipedia.org/wiki/Methylcyclopentadienyl_manganese_tricarbonyl
2. (a) Rose-Munch, F.; Rose, E. Eur. J. *Inorg. Chem.* **2002**, 1269. (b) Auffrant, A.; Prim, D.; Rose-Munch, F.; Rose, E.; Schouteeten, S.; Vaissermann, J. *Organometallics* **2003**, 22, 1898. (c) Prim, D.; Andrioletti, B.; Rose-Munch, F.; Rose, E.; Couty, F. *Tetrahedron 2004*, 60, 3325. (d) Ku¨ndig, E. P.; Pape, A. Top. *Organomet. Chem.* **2004**, 7, 71. (e) Sweigart, D. A.; Reingold, J. A.; Son, S. U. *Comprehensive Organometallic Chemistry III*; Crabtree, R. H., Mingos, D. M. P., Eds.; Elsevier: Oxford, U.K., **2006**; Vol. 5, Chapter 10, pp 761-814. (f) Jacques, B.; Chavarot, M.; Rose-Munch, F.; Rose, E. *Angew. Chem., Int. Ed.* **2006**, 45, 3481. (g) Jacques, B.; Chanaewa, A.; Chavarot-Kerlidou, M.; Rose-Munch, F.; Rose, E.; Ge´rard, H. *Organometallics* **2008**, 27, 626.
3. Anthony J. Pearson* and Paul R. Bruhn *J. Org. Chem.* **1991**. 56, 70927097
4. Pearson, A. J and Shin, H. *Tetrahedron* **1992** 48, 7527-7538
5. X. Zhang, G. B. Carpenter and D. A. Sweigart, *Organometallics*, **1999,**18, 4887
6. M. Oh, K. Yu, H. Li, E. J. Watson, G. B. Carpenter and D. A. Sweigart, A*dv. Synth. Catal.*, **2003** 345, 1.
7. K. Yu, H. Li, E. J. Watson, K. L. Virkaitis, G. B. Carpenter and D. A. Sweigart, *Organometallics*, **2001** 20, 3550
8. C. A. Dullaghan, X. Zhang, D. L. Greene, G. B. Carpenter, D. A. Sweigart, C.

Camiletti and E. Rajaseelan, *Organometallics*, **1998** 17, 3316.

9. X. Zhang, C. A. Dullaghan, E. J. Watson, G. B. Carpenter and D. A. Sweigart, *Organometallics*, **1998,** 17, 2067.
10. C. A. Dullaghan, X. Zhang, D. Walther, G. B. Carpenter and D. A. Sweigart, *Organometallics*, **1997** 16, 5604.
11. C. A. Dullaghan, S. Sun, G. B. Carpenter, B. Weldon, and D. A. Sweigart, *Angew. Chem. Int. Ed. Engl.*, **1996,** 35, 212.
12. X. Zhang, E. J. Watson, C. A. Dullaghan, S. M. Gorun and D. A. Sweigart, *Angew. Chem. Int. Ed. Engl*., **1999** 38, 2206.
13. J. Derek Jackson, Sharon J. Villa, Deborah S. Bacon, and Robert D. Pike* *Organometallics* **1994,** *13,* 3972-3980
14. Reingold, J. A.; Virkaitis, K. L.; Carpenter, G. B.; Sun, S.; Sweigart, D. A.; Czech, P. T.; Overly, K. R. *J. Am. Chem. Soc.* **2005***, 127*, 11146.
15. Neto, C. C.; Baer, C. D.; Chung, Y. K.; Sweigart, D. A. *Chem. Commun*. **1993**, 816.
16. Jacqueline M. Veauthier, Albert Chow, Gideon Fraenkel, Steven J. Geib and N. John Cooper* *Organometallics* **2000**, 19, 3942-3947
17. Jacqueline M. Veauthier, Albert Chow, Gideon Fraenkel Steven J. Geib and N. John Cooper* *Organometallics 2000*, 19, 661-671
18. Peter J. Schlom, Ann M. Morken, Darrell P. Eyman,' Norman C. Baenziger, and Steven J. Schauer *Organometallics* **1993**,12, 3461-3467
19. Peter L. Pauson and John A. Segal, *J.C.S. Dalton* **1975** 1677-1682

20. Jannie C. Swarts, Derek Laws, and William E. Geiger* *Organometallics* **2005,** *24,* 341-343

21. Derek R. Laws, John Sheats, Arnold L. Rheingold and William E. Geiger*, *Langmuir* **2010**, 26(18), 15010–15021

Chapter 2

General experiments

2.1 Inert atmosphere work

1. Nitrogen gas

Nitrogen is the most inexpensive and wildly used inert gas applied to the protection and synthesis of air and moisture sensitive organometallics complex. The nitrogen gas was passed through a drierite ($CaSO_4$ 97% and $CoCl_2$ 3%). The apparatus is basically a T-type connection with one end connected to the nitrogen valve and an exit containing a gas bubbler to monitor the flow rate of the dried nitrogen gas and to balance the pressure in the protected system. In some cases which require more inert atmosphere; nitrogen will be replaced by argon (99.998%).

2. Air-free technique

1). Schlenk techniques

The two most common types of air-free technique involve the use of a glovebox and a Schlenk line. The two methods share one similarity: glassware is pre-dried in ovens prior to use. After the connectivity to the schlenk line, they should be flame-dried to remove adsorbed water.

2). Glove box and Glove bag

Glove box provides direct inner atmosphere under argon’s protection. It has a copper made catalyst to remove oxygen, and molecular sieves to remove water by adsorbing it in the molecular sieves' pores. According to the needs of the chemist, the atmosphere can be nitrogen and vacuum. You can put equipments inside of the glove

box, such as balance.

Glove bag is a much simplified glove box, it has the advantage of much cheaper but is usually a poorer substitute because it is more difficult to purge, and less well sealed.

3). Schlenk line.

The Schlenk line is the most commonly-used air free technique developed by Wilhelm Schlenk. It consists of a dual manifold with several ports. One manifold is connected to a source of purified inert gas, usually nitrogen, while the other is connected to a high-vacuum pump. Special stopcocks allow chemist to select vacuum or inert gas without placing the sample on a separate line. The high vacuum is often used to remove the last traces of solvent from a sample. Vacuum gas manifolds often have many ports and lines, and with care it is possible for several reactions to be run in the same time.

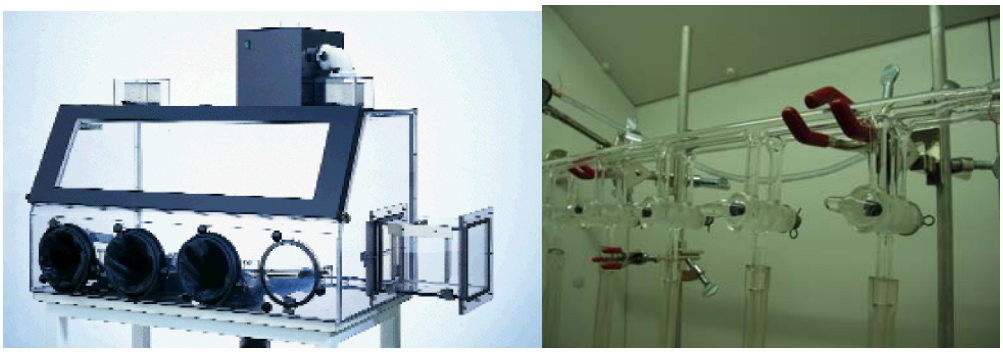

Fiture 2-1. Glove box (left) and schlenk line (right).

3. Compound Storage

In the case of air sensitive chemicals, we usually seal it with parafilm and keep it in the nitrogen box with drierite inside. Light sensitive compound will be wrapped with aluminum foil. For longer storage, compounds could be stored in vacuum desiccators.

2.2 Instruments and measurements

1. Liquid infrared spectroscopy measurement

The instrument is an ATI Mattson Infinity Series FT-IR spectrophotometer (Mattson Instruments, Madison, Wisconsin). The data was recorded and analyzed with Winfirst Version 3.2 software. We use liquid infrared cell for the measurement of sample in the solution. The cell is made of two CaF_2 (International Crystal, Inc., Garfield, New Jersey) crystal plates. The sample was dissolved in proper solvent at relatively low concentration, and was transferred into the liquid cell. Make sure there is no bubble in the test window of the cell. Sample was run at room temperature using 16 scans. After testing each sample, the cell will be thoroughly rinsed by acetone and dried by passing nitrogen through. We have many choices of solvents: acetone, acetonitrile, dichloromethane, ether, hexane…… Different solvents have different cut-off lines; the choice of solvent is limited by solubility of the sample and the cut-off line. In our group, since carbonyl peak (2100~1700 cm^{-1}) is the characteristic of the manganese carbonyl complex and most solvents don't have any overlap in 2100~1700 cm^{-1} area, so there is no disturbance from the solvent we use.

Figure 2-2. Liquid infrared cell

2. Solid infrared spectroscopy measurement

The same instrument was used in solid infrared measurement; however, KBr pellet of the sample was made instead of dissolving sample into the solvent. Mortars and pestles are the ideal tool for grinding a matrix of a solid sample with KBr powder in preparation for making a transparent pellet free from absorption peaks. We mixed small amount of sample together with the proper amount of KBr (purchased from Aldrich, FT-IR grade, and used as is), grinded them into fine uniform powder. We put one bolt on the bottom of the barrel and added proper amount of grinded powder, screwed another bolt on the top by hand initially and later on by ratchet. Hold the ratchet tight for one minute, and then we removed both bolts, leaving the pellet in the middle of the barrel. Ideally, the pellet should be one piece and transparent. 128 scans were used for the IR data collection.

Figure 2-3. Bolt, barrel, mortar and pestle for solid IR[1]

3. In-situ Infrared (IR) optic probe

The equipment used for in-situ IR spectroscopic measurements was manufactured by the Remspec Corporation[2] and consists of three primary components used in conjunction with a Matteson Infinity Series FTIR. The first part is the probe itself, which was immersed into the sample solution for direct IR measurements during the reaction. The second portion is an external detector to collect information returned from the probe tip. The final portion is the launch module, which is attached to the outside of the FTIR spectrometer and directs the input signal to the probe tip. The three components are connected by 7 fiber optic cables, which are bundled together and sheathed in a flexible steel housing.

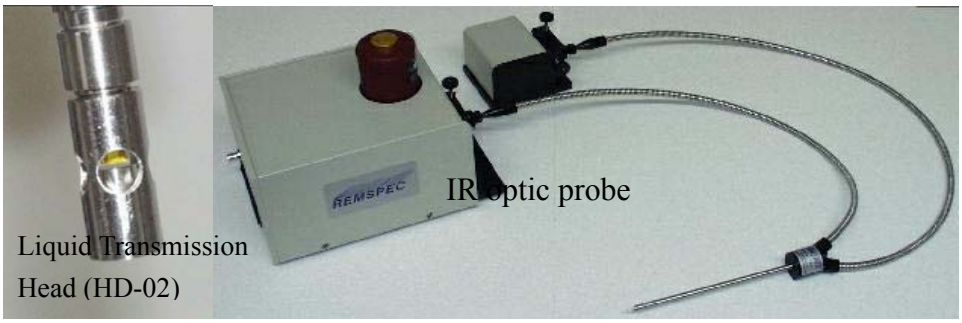

Figure 2-4. In-situ IR probe with external detector and its tip[2]

The probe tip itself is fitted with a low temperature head to protect the fiber optic cables from damage due to thermal expansion and contraction when changing temperature. The low temperature head allows for real time in-situ measurements to temperature as low as -90C. The fiber optic cable bundle is butted up against the low temperature head, which consists of a ZnSe crystal and Meldin sheath. Below the end of the ZnSe crystal is a mirror that reflects the signal back through the crystal and eventually to the detector. The path length can be adjusted by screwing in or out the mirror to increase the gap between the crystal tip and the mirror.

4. Mass Spectroscopy

Mass spec. was recorded on the Kratos MS-80 spectrometer[3] ref 3 by Dr. Shen in chemistry department. ESI was used to test the molecular weight of manganese cation, since most our manganese cations are plus one charged, so there is no need of ionization. For the most cases, ESI mode works very well. Different solvents are available: H_2O, acetone, acetonitrile and dichloromethane.

5. Nuclear Magnetic Resonance (NMR)

The Chemistry Department currently has four Bruker high field NMR spectrometers: two 300 Megahertz (MHz) instruments and two 400 MHz instruments.[4] Approximately 3ml deuterated solvent is needed for a standard sample. For 1D proton NMR, the concentration of the sample should be higher than 0.1mM; For COSY - Proton-proton correlation experiment, the recommend concentration

should be higher than 10mM; For 1D ^{13}C NMR experiment, the recommend concentration is 100mM. For 1D phosphorus NMR experiment, the recommend concentration. The NMR tube was used as it was in the lab.

2.3 Electrochemical method

1. Electrolyte

Electrolyte is a substance containing free ions that behaves as an electrically conductive medium. For most of the experiments we use tetrabutylammonium hexaflourophosphate ($TBAPF_6$), because it is inert to most compounds, and pretty stable over a wide potential range, furthermore, it is still soluble at relatively low temperature(-60/℃). It was reported by Geiger that, in low polarity solvent (dichloromethane, THF), large anions such as $B(C_6F_5)_4^-$ (TFAB)and $B(C_6H_3(CF_3)_2)_4^-$, will significantly reduce the error in cyclic voltammetry by enhanced conductivity and expanded scan rate range. Typically, the concentration of the electrolyte is 0.1M.

2. Synthesis of electrolyte $TBAPF_6$ and $\{NBu_4[B(C6F5)_4]\}$

32.6g tetrabutylammonium bromide was dissolved in 1L erlenmeyer flask with 450ml distilled water. 21.0 ml 60% hexafluorophosphoric acid was slowly added to the above solution, and a large amount of white precipitate formed instantaneously. Keep stirring for 30mins after all the acid was added. Then the white slurry was filtered through a big 500ml coarse fritted filter using vacuum filtration. The white product was completely dissolved in minimal amount of hot ethanol and allowed to cool down at room temperature and thereafter put into a freezer for further

recrystallization. The crystal was collected by filtration and the above procedure was repeated twice more to ensure the purity of the electrolyte.

Synthesis of electrolyte $\{NBu_4[B(C6F5)_4]\}$[5-6] ref 5-6, tetrabutylammonium tetrakis (pentafluoro -phenyl) borate: One to one equivalent of an aqueous solution of Li[B(C6F5)4]·nEt2O(n =2-3) and a solution of tetrbutylammonium bromide in methanol were combined, white precipitate formed instantaneously. The precipitate was washed with water and dried under vacuum, and recrystallized three times from dichloromethane/Ether.

3 Test the purity of the electrolyte

To make sure the synthesized electrolyte is pure. Simply run a cyclic voltammetry of arene chromium tricarbonyl (purchased from aldrich) in dichloromethane (HPLC grade, purchased from Fisher). If nice reversibility was observed at around +0.5V, you can use the electrolyte. The mechanism is, after the oxidation of the chromium complex, it generates a $17e^-$ intermediate which would react rapidly with any impurities in the solution.

4. Solvent

The solvent typically used for cyclic voltammetry is HPLC grade methylenechloride (CH_2Cl_2) purchased from Fisher Chemical. CH_2Cl_2 is the primary solvent because it will not tend to coordinate to the metal like MeCN and it is fairly inert to most compounds we synthesized.

5. Preparation of reference electrode[1]

Ag/AgCl electrode and a glass salt bridge were needed. Firmly attach the

salt bridge to the open end of the Ag/AgCl electrode and seal the attachment with parafirm. Invert the electrode and fill the glass salt bridge with 0.1 M $TBAClO_4$ in dichloromethane. The tip of the salt bridge is sealed by Teflon shrink wrap with a porous vycor tip. The electrode system will need at overnight to fully settle down and if the solution level changes, more 0.1 M $TBAClO_4$ should be added and the seal should be strengthened. The new reference electrode should be stored in a 0.1 M $TBAClO_4$ dichloromethane solution saturated with LiCl[1].

6. Work Station and three-electrode system

Our cyclic voltammetry experiments are carried out by the PGSTAT100[7] ref 7 work station which is a high voltage potentiostat/ galvanostat with a standard three electrode working system. The reference electrode (RE) is an electrode with stable potential and Ag/AgCl reference electrode is the one we are using. The counter electrode (CE, made of Pt) is used to make sure that current doesn't go through the reference electrode (the passage of current will affect the potential of the reference E and will also affect the measured potential because of iRs drop, in which Rs is the solution resistance between RE and WE); Working electrode is where the reaction of interest is occurring.

Three-electrode system:
Working E; Reference E;
Counter E

Working E:
GC;Au;Pt

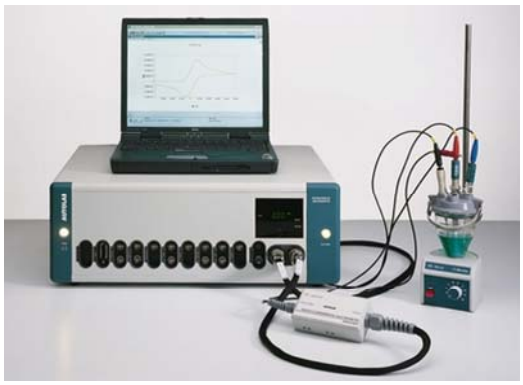

Reference E
Ag/AgCl

Counter E
Pt

Figure 2-5. PGSTAT100 potentiostat/ galvanostat with a standard three electrode working system

7. Hardware installation and instruction

For cyclic voltammetry, only three plus one connections are needed. Working electrode connection is labeled by “WE” and it is red color. Reference electrode connection is labeled by “RE” and it is blue color. Counter electrode connection is label by “CE” and it is black color. And one more connection is ground connection and it should be connected to the ground all the time to protect the work station and the people working on the station. The ground connection is green color. After each electrode is connected, you will need to press the “on/off” button once, so the work station is powered on. Then press “cell on/off” button, then the electrochemical cell is powered on.

8. Software installation and instruction

Simply put the CD (from Metrohm Autolab, version 4.9.007) into the CD player, and follow the instruction displayed to install the software. After you finish, you will see folder “autolab software” from all programs. Click the “autolab software”, you will see four icons: GPES, Interface, Diagnostics, Hardware.

9. Conduct cyclic voltammetry at room temperature

A schlenk tube was filled 2/3 with the solvent used in the cyclic voltammetry. Nitrogen gas was bubbled through the solvent from the top of the schlenk tube and exited from the side arm to the three electrode cell. The schlenk tube should be put into a beaker filled with water. The water level should be higher than the solvent level inside the schlenk tube. The above procedure is extremely important for maintaining the consistency of cyclic voltammetry at room temperature. The nitrogen gas saturated with the solvent will maintain the concentration of the solution inside the e-chem cell. Without the protection of the bubbling system, the solvent inside the e-chem cell would evaporate quickly, and the current shown in the cyclic voltammetry will keep increasing as the time going on.

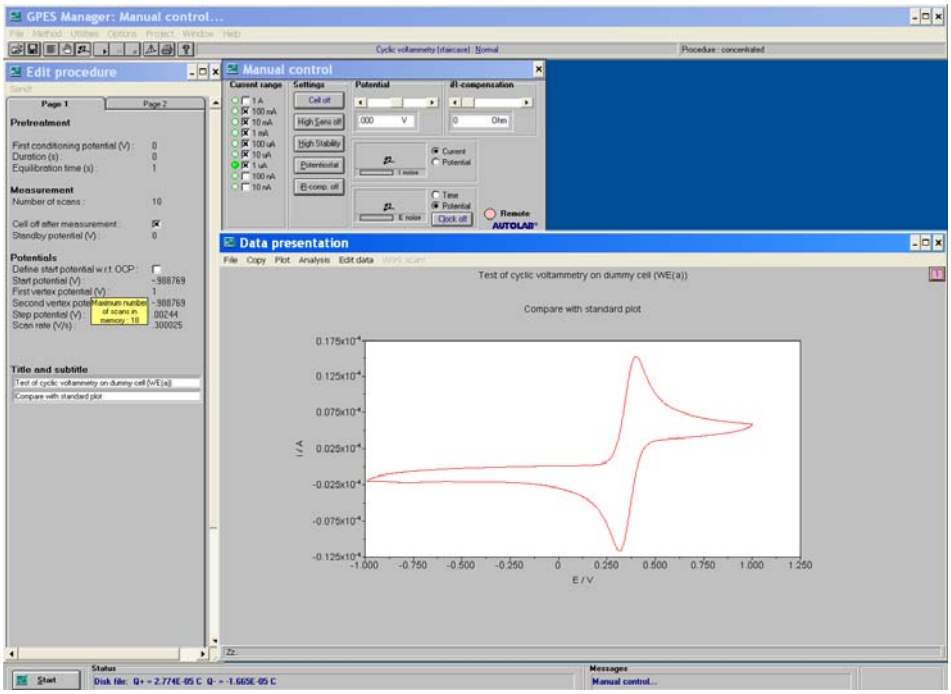

Figure 2-6. GPES software, which controls the PGSTAT100 potentiostat/ galvanostat.

After the four connections were made and power button was turned on, click the "interface" icon, after 10s, computer should tell you that the interface was connected. Click the "Gpes" icon, you will see the following page, which was made of four important parts: "GPES Manager", "Manual control", "Edit procedure", "Data presentation". From "GPES Manager", select "method", choose "cyclic voltammetry". From "Edit procedure", select desired scans numbers, scan range, scan rates. "Manual control" provided a way to manually reduce the experimental error. After clicking the "start" button at the left bottom, an in time cyclic voltammetry will show in the "Data presentation"window. You can run as many scans as you want to. After finished, only the last scan was shown in the window.

Both the data and picture file of the CV could be saved after the experiment. For data file, select "file"→ "save scan as" from the "GPES manager"; for picture file, select

"copy"→ "copy to" from the "Data presentation" window.

10. Conduct cyclic voltammetry at low temperature

Usually, dry ice/acetone bath was made as low temperature bath for low temperature CV experiments. By carefully and slowly adding different amount of dry ice to the acetone bath, the temperature of the bath could be controlled. The e-chem cell with three electrodes and a thermometer was kept in the dry ice/acetone bath. The thermometer will indicate the temperature simultaneously. The bubbling system was no longer needed when the temperature was lower than 0 ℃.

11. Interpretation of the cyclic voltammetry

In a cyclic voltammetry experiment, a voltage is applied to a working electrode in solution and current flowing at the working electrode is plotted versus the applied voltage to give the cyclic voltammogram (Figure 2). Cyclic voltammetry can be used to study the electrochemical properties of species in solution as well as at the electrode/electrolyte interface. Because any change of the components in the solution is limited in the diffusion layer.

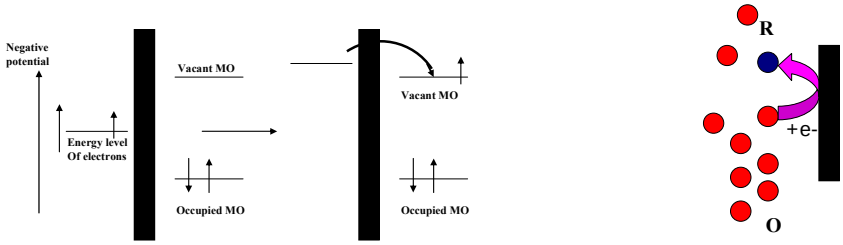

Figure 2-7. Representation of reduction of an electrochemical active species in the solution.

By driving the electrode to more negative potentials, the energy of the

electrons is raised, and they will eventually reach a level high enough to occupy vacant states on the species in the electrolyte, it is a process of reduction (Figure 3); Meanwhile, if you apply more positive potentials to the electrode, the energy of the electrons will be lowered, finally, when the energy gets lower enough, electrons from the occupied MO(molecular orbital) of the surface redox active molecule will jump to the electrode, it's a process of oxidation

12. The mechanism of the cyclic voltammogram (Scheme 2-1)**:**

1). For a given bulk solution containing only O: at potentials well positive of the redox potential, there is no net conversion of O to R. (O is oxidant; R is reductant)

2). When redox potential is almost approached, there is a net cathodic current, which increases exponentially with potential due to the exponential potential dependence of the rate of heterogeneous electron transfer. Shown in **A**

3). When the redox potential is reached at **B**, and the surface concentrations of O and R are equal at this potential. In the meanwhile, the product R tends to diffuse away from the electrode surface, the O will diffuse towards the electrode.

4). After passing the (cathodic) peak potential **C**, the current decays as a result of the decrease of O in the interfacial region. The rate of electrolysis (and hence the current) now depends on the rate diffusion of O from the bulk solution to the electrode surface; so the time dependence is $t^{-½}$. The peak is therefore asymmetric.

5).Then reversing of the direction of the potential scan, the current continues to decay **D** with $t^{-½}$ until the potential gets close to the redox potential **E**, at which point there begins a net reoxidation of R to O which causes an anodic current.

6). After the peak potential, the anodic current will decrease as a result of the depletion of R in the interfacial region, just like repeating the reversal process of 4…….

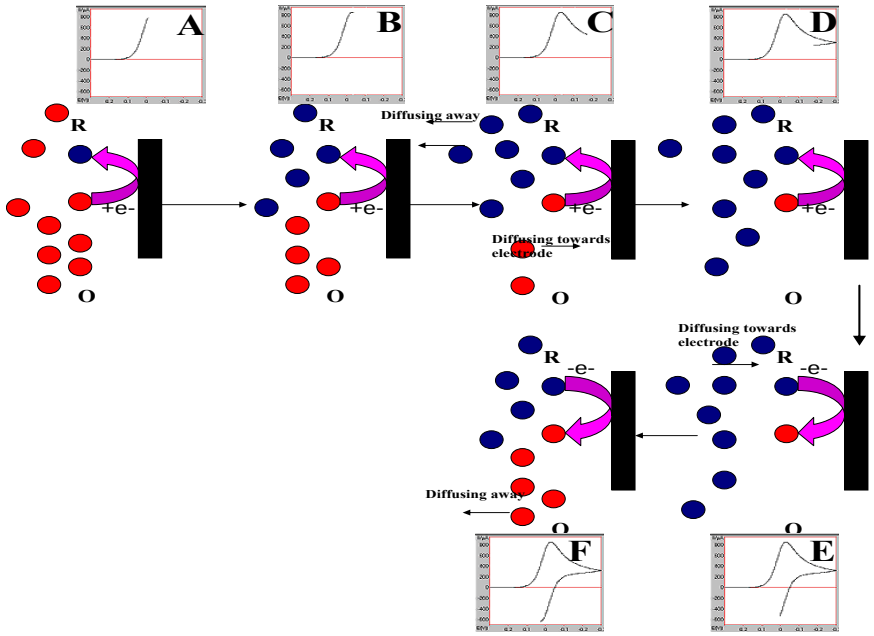

Scheme 2-1. Simplified scheme of cyclic voltammogram.

Bulk electrolysis is to electrochemically reduce or oxidize the redox active species in the solution in bulk amount with basket-like working and counter electrode. It's different from the cyclic voltammetry. Firstly, it has much larger surface area of working and counter electrode; secondly, it will keep potential at fixed value, not back and forth like the sweeping potential applied in cyclic voltammetry; finally, you have to stir the solution to destroy the diffusion layer, to make sure that all the solution is mixed evenly.

One great advantage of our research is: we can use the CO on the moiety of metal-tricarbonyl as a labeling ligand because of its characteristic IR frequency; IR can be easily applied to monitor the change in the bulk solution. Meanwhile, due to

the previous tremendous work on Mn and other metal-tricarbonyl complexes, our lab has accumulated large amount of IR data. In-situ optic IR probe is used to detect the characteristic IR frequencies due to the electrochemical reaction. On the other hand, you can simply insert its tip to the solution and the measurement can be done under an atmosphere of N_2, CO without exposure to the air from room temperature to as low as -90°C. The minimum interval between each spectrum is 30s. So we can easily combine bulk electrolysis techniques (electrochemistry) and in-situ optic IR (Spectroscopy) together by simply inserting the tip of the probe into the bulk solution.

13. Digital simulation of cyclic voltammgram[8]

Digisim 3.0 from BASi was installed and used for digital simulation of cyclic voltammetry. A dongle from the company was needed when using the digisim software for secure connectivity.

14. Bulk electrolysis

Bulk electrolysis is a potential controlled coulometry, which uses three electrode system controlled by potentiostat. During the process of electrolysis, a potential is hold at certain value, the current is monitored all the time, so the overall coulomb can be easily calculated. As the oxidation or reduction going to finish, the current gets smaller, and becomes zero when all the starting material is consumed.

Working and counter electrode: the working and counter electrode used for bulk electrolysis are bulky basket electrodes made of platinum.

Cell design: The cell for bulk electrolysis is shown below. The working and

reference electrode were kept in the left cell; the counter electrode was kept in the other side, there was a salt bridge between them.

Figure 2-8. Cell design for bulk electrolysis.

During the process of electrolysis, in order to make the solution homogeneous, a medium size stirring bar was needed, and kept stirring during the whole process.

If the bulk electrolysis was conducted at room temperature, a similar bubbling system was needed to maintain the concentration of the solution. If the bulk electrolysis was done at low temperature, the dry ice/acetone bath should be used to control the temperature. The bubbling system wasn't needed.

2.4 References

1. Dr. Jeffery. A. Reingold thesis.
2. Remspec Corporation website http://www.remspec.com/
3. Brown University Chemistry department mass spectrometry facility webpage. http://www.chem.brown.edu/facilities/mass_spec/mass_spec.html
4. Brown University Chemistry department NMR facility webpage. http://www.chem.brown.edu/facilities/NMR/nmr.html
5. Robert J. LeSuer, Catherine Buttolph, and William E. Geiger Anal. Chem., 2004, 76
6. Robert J. LeSuer and William E. Geiger* Angew. Chem. Int. Ed. 2000, 39, No. 1
7. Parameters for Metrohm Autolab PGSTAT100, please go to autolab website at: http://www.nlab.pl/pgstat100_en.html.
8. More information about digisim program, please refer to its webpage at: http://www.basinc.com/products/ec/digisim/

Chapter 3

Electrochemical Study of Manganese and Rhenium Arene Complexes $(C_6R_6)M(CO)_3^+$ (R = Me, Et)

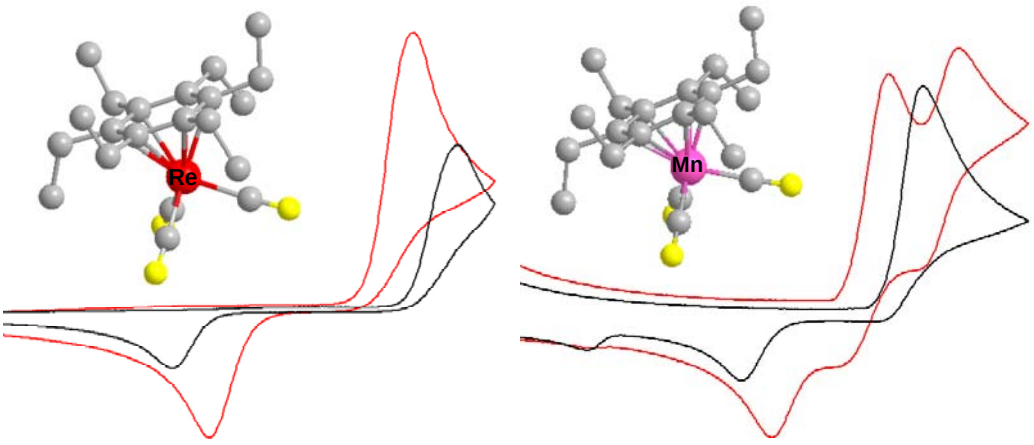

3.1 Introduction

Electrochemical methods have been widely used to study the reactivity of 17- and 19-electron organometallic radicals generated from stable 18-electron precursors.[1,2] Electron-transfer-induced ligand dissociation, addition, and substitution reactions, as well as structural rearrangements and catalysis, have been probed by using transient voltammetry, bulk electrolysis, and chemical redox reagents. Variable temperature studies have been especially valuable for understanding the chemical reactions that occur subsequent to electron transfer.

The reductive electrochemistry of monocyclic arene and polycyclic arene complexes has been studied in considerable depth.[3-7] In some cases, especially with the heavier transition metals, an overall two-electron reduction occurs that is accompanied by arene ring slippage from η^6 to η^4 bonding. It is thought that the first electron addition (E_1^o) generates a 19-electron complex and that ring slippage occurs in concert with addition of the second electron (E_2^o) to afford an 18-electron η^4-bonded arene product. The nuclear reorganization associated with the η^6 to η^4 slippage manifests in two important ways: (1) E_2^o is near or even positive (anodic) of E_1^o, with the separation ΔE being significantly temperature dependent and (2) the heterogeneous charge-transfer rate constant for the second electron addition, $k_s(2)$, is much smaller than that for the first addition, $k_s(1)$.

This paper is concerned with the reductive electrochemistry of (η^6-arene)$M(CO)_3^+$ (M = Mn, Re) complexes. A preliminary report of selected monocyclic arene systems has appeared.[6] Recently, a complete electrochemical

study of naphthalene-based polycyclic arene complexes (arene)$Mn(CO)_3^+$ has been published.[7] Cooper and coworkers have shown previously that the generic complex (η^6-benzene)$Mn(CO)_3^+$ can be reduced chemically at low temperature to afford the nucleophilic (η^4-benzene)$Mn(CO)_3^-$ anion, which undergoes an impressive variety of reactions with electrophilic reagents.[5]

We report herein a description of the monocyclic arene complexes (η^6-C_6R_6)$M(CO)_3^+$ (R = Me, Et; M = Mn, Re). The purpose of this study was to determine the influence of the metal and steric congestion on the nature and stability of the reactants and their reduction products. It is shown that the two rhenium systems, which differ greatly in their reactivity as 18-electron cations, are cleanly reduced to the anionic η^4-arene complexes on the voltammetric time scale regardless of solvent or temperature. With manganese, however, the situation is less straightforward, with the reduction products depending on solvent, temperature and steric congestion (R). As indicated in **Chart 3-1**, reduction of **1** can lead to the anion **3**, the ring-coupled product **5**, or the dimeric complex **6**. The last complex, which was first reported by Eyman and coworkers,[8] is produced by CO dissociation from the neutral 19-electron radical (η^6-C_6R_6)$Mn(CO)_3$. While the cation (η^6-C_6Me_6)$Mn(CO)_3^+$ is generally more reactive than (η^6-C_6Et_6)$Mn(CO)_3^+$, a primary conclusion from the present work is that the transient neutral 19-electron radical displays the opposite reactivity, (η^6-C_6Et_6)$Mn(CO)_3$ >> (η^6-C_6Me_6)$Mn(CO)_3$. It is also concluded that in general the (η^6-C_6R_6)$M(CO)_3$ radicals follow the chemical reactivity order Mn >> Re, which is opposite to the reactivity order found for the

$(\eta^6\text{-}C_6R_6)M(CO)_3^+$ precursors (Re >> Mn).

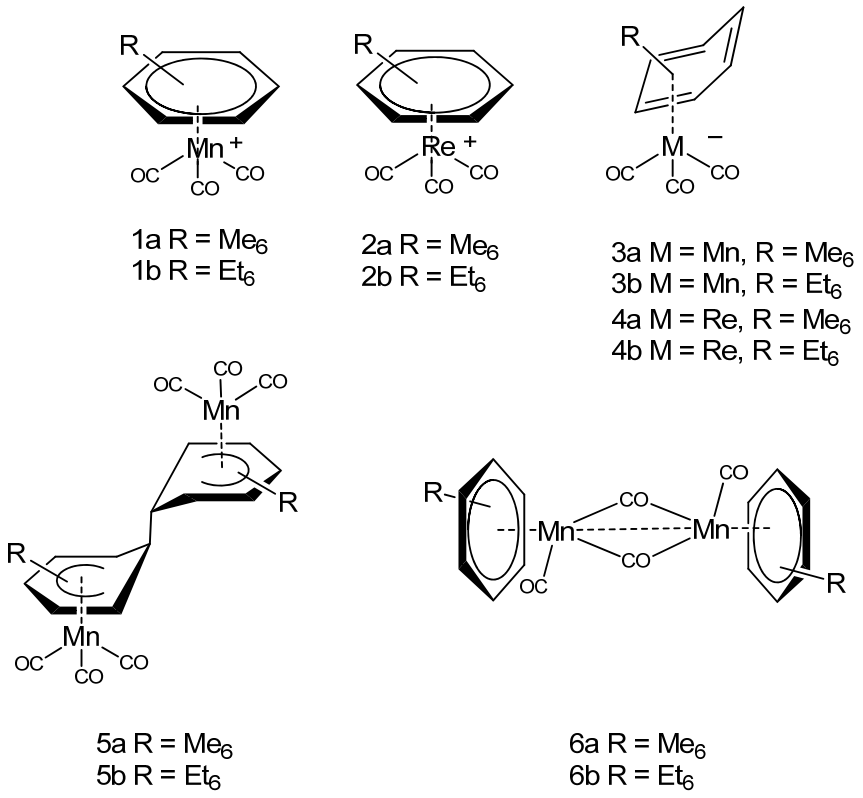

Chart 3-1. Complexes relevant to this study.

3.2 Experimental Section

1. Solvents

Solvents were purchased from commercial sources as HPLC grade. Methylene chloride and acetonitrile solvents were stored and opened under nitrogen. The hexamethylbenzene complexes [**1a**]BF_4 and [**2a**]PF_6 were prepared by literature methods.[9] The hexaethylbenzene analogues [**1b**]BF_4 and [**2b**]PF_6 were synthesized by similar procedures.

2. Synthesis

[(η^6-Hexaethylbenzene)$Mn(CO)_3$]BF_4 Acenaphthene manganese tricarbonyl tetrafluoroborate (0.600 g, 1.58 mmol) and hexaethylbenzene (0.581 g, 2.37 mmol) were combined with 17 ml methylene chloride (Fisher Scientific Co.) in a 20 ml pressure tube under nitrogen. The tube was sealed, wrapped in aluminum foil, and placed in a 75 ^oC oil bath for 2 hrs. The solvent was then removed and the yellow solid residue was washed with diethyl ether to afford the product in 71% yield (0.529 g). A crystal suitable for X-ray analysis was obtained by diethyl ether diffusion into a methylene chloride solution at room temperature Anal. Calcd for $C_{21}H_{30}O_3MnBF_4$: C, 53.42; H, 6.40. Found: C, 52.86; H, 6.22. IR (CH_2Cl_2, cm^{-1}): 2060, 2003. ^1H NMR (CD_2Cl_2, 300 MHz, room temperature, δ ppm): 2.66 (q, J = 7.5 Hz, 2H), 1.40 (t, J = 7.5 Hz, 3H).

[(η^6-Hexaethylbenzene)$Re(CO)_3$]PF_6. $Re(CO)_5Br$ (0.400 g, 0.98 mmol), hexaethylbenzene (1.210 g, 4.92 mmol) and $AlCl_3$ (0.390 g, 2.95 mmol) were mixed in a 50 ml round bottle flask with 25 ml of degassed decane. The mixture was heated at 150 ^oC for 1 hour. After cooling down, the decane layer was removed. The orange-red solid residue was washed with cyclohexane three times. Then 20 ml of ice water was added, and any residue remaining undissolved after ca. 30 s of shaking was removed by filtration. NH_4PF_6 (0.19 g, 1.2 mmol) was added to the aqueous solution to precipitate the pale white product. Recystallization was effected twice by dissolving the product in a minimum amount of methylene chloride, and slowly adding diethyl ether. The yield was 65%. A sample suitable for single crystal X-ray crystallographic analysis was obtained by diethyl ether diffusion into a

methylene chloride solution at -20 °C. IR (CH_2Cl_2, cm^{-1}): 2064, 1993. ^1H NMR (CD_2Cl_2, 400 MHz, room temperature, δ ppm): 2.66 (q, J = 7.5 Hz, 2H), 1.39 (t, J = 7.5 Hz, 3H).

3. Electrochemistry

1). Cyclic voltammetry

Voltammetric data were collected under a blanket of nitrogen that was saturated with solvent. The electrolyte was 0.10 M Bu_4NPF_6, which was synthesized by the metathesis of Bu_4NBr and HPF_6, recrystallized from hot ethanol, and dried under vacuum. The solvents were HPLC grade CH_2Cl_2 and CH_3CN. Additional purification was not required. Voltammetry at low temperatures utilized a simple slush bath; with a thermocouple probe inserted to monitor the temperature.[10] Cyclic voltammetry data were measured with Eco Chemie AUTOLAB potentiostatic instrumentation. A standard three-electrode system was used. The working electrode was a 2 mm diameter platinum disk, and the counter electrode was a platinum wire. The reference was a Metrohm Ag/AgCl electrode filled with CH_2Cl_2/0.10 M Bu_4NPF_6 and saturated with LiCl. The reference electrode was separated from the test solution by a salt bridge containing 0.10 M Bu_4NPF_6 in the solvent in use. Ferrocene was generally added as an internal potential standard. Bulk electrolyses, performed with an EG&G 175 potentiostat and a 179 digital coulometer under an atmosphere of nitrogen, utilized a platinum-basket working electrode and a platinum-mesh counter electrode, which were separated from the test solution by a salt bridge. IR spectra of solutions undergoing electrolysis or chemical

reduction were recorded at variable temperatures with a Remspec fiber optic probe. Digital simulation of the proposed mechanisms were performed with Digisim.[11]

The cyclic voltammetry of $(\eta^6\text{-}C_6Me_6)Mn(CO)_3^+$ (**1a**) in the solid state was probed by dissolving [**1a**]BF_4 in acetone and then adding several drops of the solution to the working area of a 3 mm glassy carbon disk electrode. After complete evaporation of the acetone, the electrode was placed in water containing 1.0 *M* KCl, with connection to an aqueous Ag/AgCl reference electrode in 3.0 *M* KCl. The two electrodes were connected with a salt bridge containing 3.0 *M* KCl in water.

2). Bulk electrolysis

Bulk electrolysis is to electrochemically reduce or oxidize the redox active species in the solution in bulk amount with basket-like working and counter electrode. It's different from the cyclic voltammetry. Firstly, it has much larger surface area of working and counter electrode; secondly, it will keep potential at fixed value, not back and forth like the sweeping potential applied in cyclic voltammetry; finally, you have to stir the solution to destroy the diffusion layer, to make sure that all the solution is mixed evenly.

4. Crystallography

X-ray data collection for [**1b**]BF_4 and [**2b**]PF_6 was carried out using a Bruker single-crystal diffractometer equipped with an APEX CCD area detector and controlled by SMART version 5.0. Data were collected at room temperature. Data reduction was performed by SAINT version 6.0 and absorption corrections were applied by SADABS version 2.0. The structures were determined by direct methods

and refined on F squared by use of programs in SHELXTL. Most hydrogen atoms appeared in a difference map, or they were inserted in ideal positions, riding on the atoms to which they are attached.

3.3 Results and Discussion

1. Manganese Complexes

1). Cyclic voltammetry

Cyclic voltammetry of the hexamethylbenzene complex **1a** at a Pt electrode was studied as a function of temperature in CH_2Cl_2 and in CH_3CN

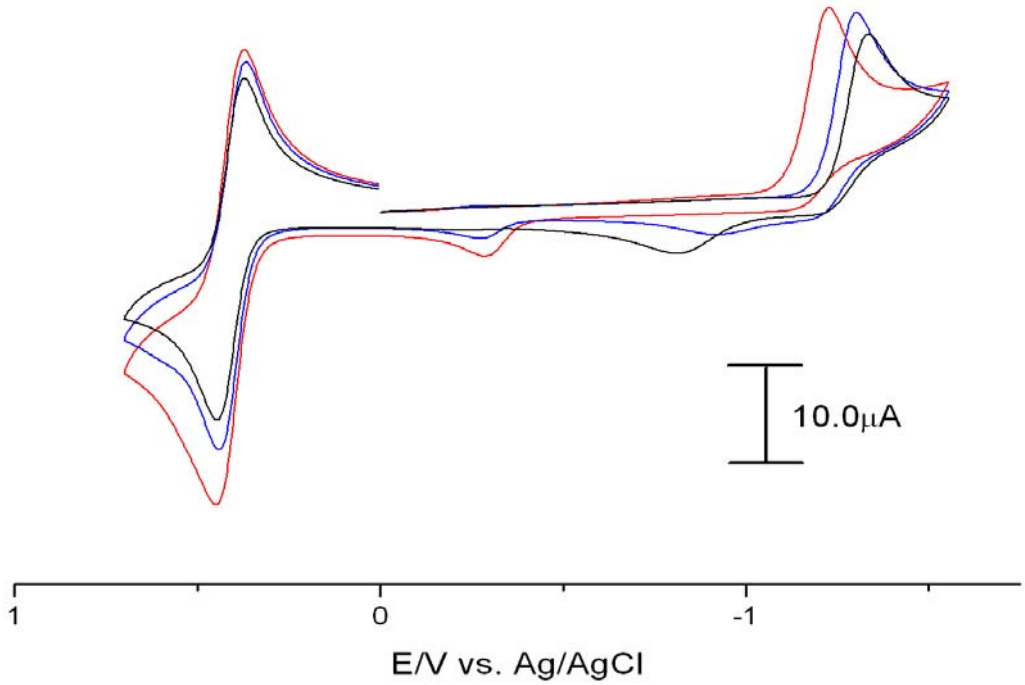

Figure 3-1. CVs of 1.0 mM $[(\eta^6\text{-}C_6Me_6)Mn(CO)_3]BF_4$ (**1a**) at +14 °C (red), -20 °C (blue) and -40 °C (black) in CH_2Cl_2/0.10 M Bu_4NPF_6 under N_2. The working electrode was a 2.0 mm diameter platinum disk, and the scan rate was 0.50 V s^{-1}. A ferrocene internal standard was added (left).

Figure 3-1 illustrates the results in CH_2Cl_2 at two temperatures. The

reversible couple on the left of Figure 3-1 is due to the ferrocene added to the cell as an internal reference standard. At +14 ^{o}C, the system shows a 1-electron reduction that is chemically irreversible. The product of the reduction is known to be the dimer **6a**, as established by the potential of the associated oxidation (-0.29 V).[6] We found similar behavior at a Pt electrode in CH_3CN solvent.[12] As the temperature is lowered, the wave attributable to dimer **6a** vanishes and evidence of chemical reversibility appears. Curiously, the reduction peak current does not decrease much with temperature (compare to the ferrocene oxidation current) until about -40 ^{o}C, below which the current drops off as may be expected. Our interpretation is that dissociation of CO from the initial reduction product, $(\eta^6\text{-}C_6Me_6)Mn(CO)_3$, becomes relatively slow and a second reduction to the slipped η^4-arene complex **3a** becomes prominent as the temperature is lowered, which explains why the peak current does not drop off as anticipated.

2). Bulk electrolysis (BE)

Bulk electrolysis results are consistent with the CV results. BE of **1a** in CH_3CN at room temperature produced the green dimer **6a** (ν_{CO} = 1849, 1680 cm^{-1}), which slowly decomposed. BE in CH_2Cl_2 at room temperature also produced **6a**, which is stable in this solvent. Interestingly, BE in CH_2Cl_2 at -60 ^{o}C did not lead to any **6a**. Rather, a mixture of **3a** and **5a** was produced. It was further observed that at low temperature with no applied potential the η^4-**3a** complex reacted with the starting material η^6-**1a** to yield the η^5-dimer **5a**. This reaction was previously observed[5d] during chemical reduction of $(\eta^6\text{-benzene})Mn(CO)_3^+$.

On the cyclic voltammetric time scale at low temperature it is likely that the only product is the 2-electron reduced complex **3a**. Digital simulations agree well with the interpretation that electrochemical reduction of **1a** is a 1-electron process at room temperature to give **6a** but a 2-electron process at low temperatures to give **3a**. The simulations quantitatively reproduce the observed peak potentials and current ratios provided $\Delta E = E_2^o - E_1^o$ is zero or slightly positive at room temperature and more positive (ca. 250 mV) at low temperature. Additionally, it is required that the heterogeneous charge-transfer rate constant $k_s(2)$ be much smaller than $k_s(1)$. This order of charge transfer rates is unsurprising in view of the ring slippage that occurs in the second electron reduction step, which exhibits electrochemical irreversibility by virtue of its very slow heterogeneous electron-transfer rate constant. That ΔE becomes more positive as the temperature is lowered was observed with analogous manganese naphthalene complexes and is predictable from consideration of the relative entropy changes that accompany the two reduction steps.[7]

The peak reduction current shown in Figure 3-1 shifts negative with decreasing temperature. This represents the combined effect of a positive kinetic shift at +14 ^oC due to chemical irreversibility and a negative shift at -40 ^oC due to a very small value of $k_s(2)$ (estimated as 1×10^{-3} cm/s at +14 ^oC and 2×10^{-5} cm/s at -40 ^oC). Simulations indicate that E_1^o does not change with temperature (-1.35 V) and that E_2^o increases from -1.25 to -1.10 V, so that $\Delta E = E_2^o - E_1^o$ increases with temperature, as expected.

The hexaethylbenzene manganese complex **1b** undergoes reduction reactions

that are significantly different in comparison to the hexamethylbenzene complex **1a**. Because **1b** and the rhenium analogue **2b** are new, their X-ray structures were determined. As shown in Figure 3-2, the ethyl substituents point alternatively up and down as may be expected. The result is that the $M(CO)_3^+$ moiety is shielded from nucleophilic attack and the cations **1b** and **2b** are unusually stable for this reason when compared to other (monoarene)$M(CO)_3^+$ complexes. This stabilization is especially remarkable for the rhenium complexes (vide infra).

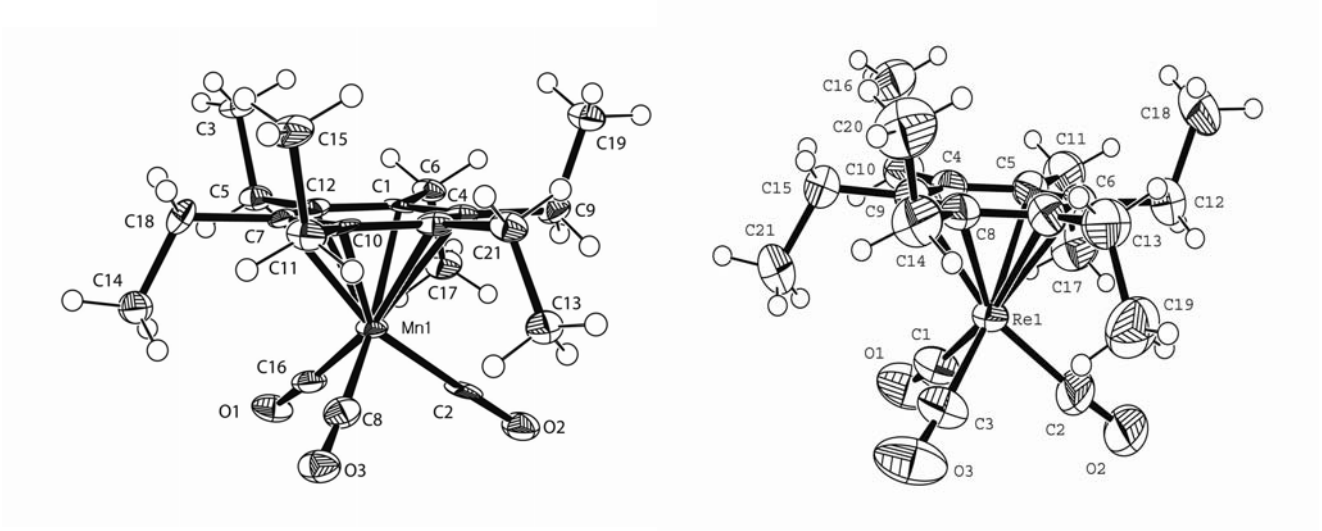

Figure 3-2. X-ray structures of $[(C_6Et_6)Mn(CO)_3]BF_4$ (**1b**) and $[(C_6Et_6)Re(CO)_3]PF_6$ (**2b**). The average M-C(arene) bond length is 2.22(1) A for Mn and 2.35(1) A for Re.

Complex **1b** undergoes reduction in CH_2Cl_2 at room temperature in a chemically irreversible manner to give unknown products. The dimeric product **6b**, resulting from CO dissociation from the neutral radical, was not observed. At low temperatures in CH_2Cl_2, however, chemical reversibility is seen, but with especially

slow charge transfer (e.g., $k_s(2)$ is simulated to be 3 x 10^{-6} cm/s at -40 ^oC). The electrochemical behavior of **1b** in CH_3CN solvent is easier to interpret, and significant chemical reversibility was observed at all temperatures. Relevant results are given in Figure 3-3. The room temperature voltammogram features two waves, which at -30 ^oC merge into one wave. The CVs at low temperatures also show a hint of product **6b**. Digital simulations indicate that $k_s(2)$ at -40 ^oC for **1b** in CH_3CN is 4 x 10^{-6} cm/s, which is about 100 times smaller than that found with **1a**. Two waves are seen at room temperature with **1b** even though E_2^o is simulated to be slightly *positive* of E_1^o; this is due to the small value of $k_s(2)$ (ca. 4 x 10^{-5} cm/s).

BE experiments with **1b** were very informative. BE in CH_3CN gave the dark green dimer **6b** at both room temperature and at -40 ^oC. The dimer slowly decomposes at room temperature and all CO bands fade away. In CH_2Cl_2, BE at room temperature gives only CO bands assigned to $(C_6Et_6)Mn(CO)_2Cl$. At -55 ^oC in CH_2Cl_2, BE led to a mixture of dimer **6b** and anion **3b**, both of which decompose upon heating to -30 ^oC. That dimer **6b** is formed during BE of **1b** but not **1a** in CH_2Cl_2 at low temperature suggests that the 19-electron radical follows the order $(\eta^6\text{-}C_6Et_6)Mn(CO)_3 > (\eta^6\text{-}C_6Me_6)Mn(CO)_3$ for the rate of CO dissociation. Indeed, **6b** can even be seen in trace amounts in the CVs of **1b** at low temperatures. Ligand dissociation is enhanced by steric effects is what one would expect.

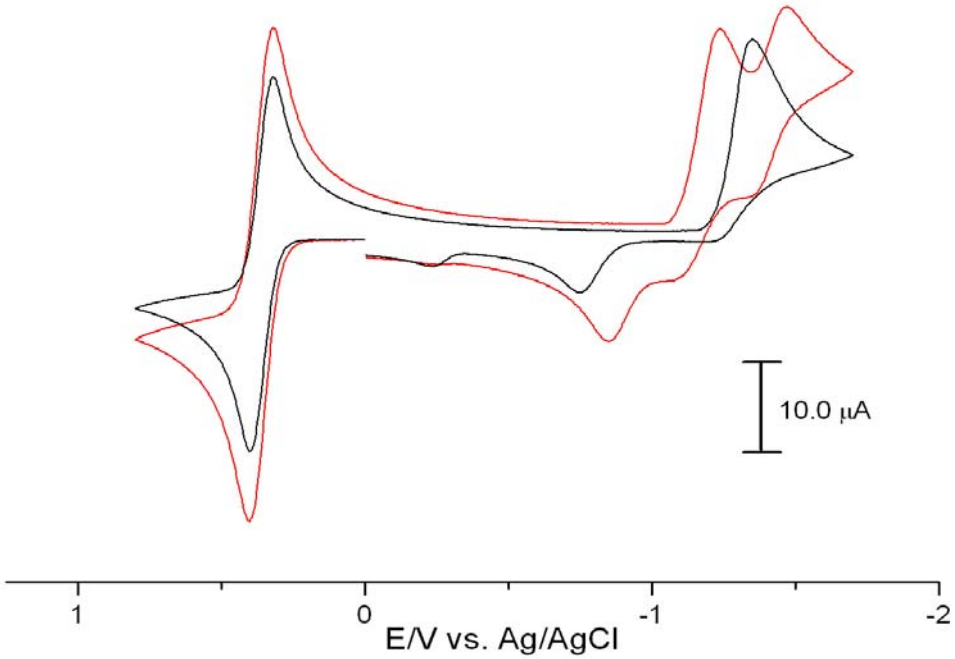

Figure 3-3. CVs of 1.0 mM $[(\eta^6\text{-}C_6Et_6)Mn(CO)_3]BF_4$ (**1b**) at +20 ^oC (red) and -30 ^oC (black) in CH_3CN/0.10 M Bu_4NPF_6 under N_2. The working electrode was a 2.0 mm diameter platinum disk, and the scan rate was 0.50 V s^{-1}. A ferrocene internal standard was added (left).

Of course, the steric congestion can influence all chemical reactions of $(\eta^6\text{-}C_6R_6)Mn(CO)_3^+$ including CO dissociation, ring coupling to afford **5**, and $\eta^6 \rightarrow \eta^4$ ring slippage to accompany a second electron addition when **1** is reduced. Comparison of the present work to published results[7] with $(\eta^6\text{-naphthalene})Mn(CO)_3^+$ reduction leads to the conclusion that the rate of second electron addition to $(\eta^6\text{-arene})Mn(CO)_3^+$ as measured by $k_s(2)$ is in the order: naphthalene >> C_6Me_6 >> C_6Et_6. This order seems to be reasonable for the relative order of ring slippage. The

small $k_s(2)$ for the monoarenes in effect provides extra time for the $(\eta^6\text{-}C_6R_6)Mn(CO)_3$ radical to react by pathways other than electron addition, in accordance with the CV and BE results presented herein. The "extra time" is not available to $(\eta^6\text{-naphthalene})Mn(CO)_3^+$ and this complex is reduced in a chemically reversible 2-electron manner at all temperatures.

The $\eta^6 \rightarrow \eta^4$ ring slippage is more facile for the naphthalene complex because the diminishment of its resonance energy upon ring slippage is less severe. This effect manifests as a larger $k_s(2)$ and a more positive $\Delta E = E_2^o - E_1^o$. The electron transfer rate is indeed larger for polycyclic arenes than for monocyclic arenes. Curiously, however, the thermodynamics as reflected by $\Delta E = E_2^o - E_1^o$ do not follow this order. Rather, ΔE is surprisingly constant (200 – 300 m*V*) at low temperatures for all three arene manganese complexes (naphthalene, C_6Me_6, C_6Et_6). This observation may mean that the activation barrier for the second electron addition reflects slippage that is not directly in concert with the bending of the arene ring, which is known[5] to be 37° in $(\eta^4\text{-naphthalene})Mn(CO)_3^-$. Alternatively, it is possible that the actual ring bending is significantly less with the manganese monocyclic arene complexes.

3). Manganese dicarbonyl complexes

[$(\eta^6\text{-}C_6Me_6)Mn(CO)_2THF]^+$ and $(\eta^6\text{-}C_6Me_6)Mn(CO)_2Cl$ was synthesized and discovered that their reductive electrochemistry is mimicking the one of **[**$(\eta^6\text{-}C_6Me_6)Mn(CO)_3]^+$.

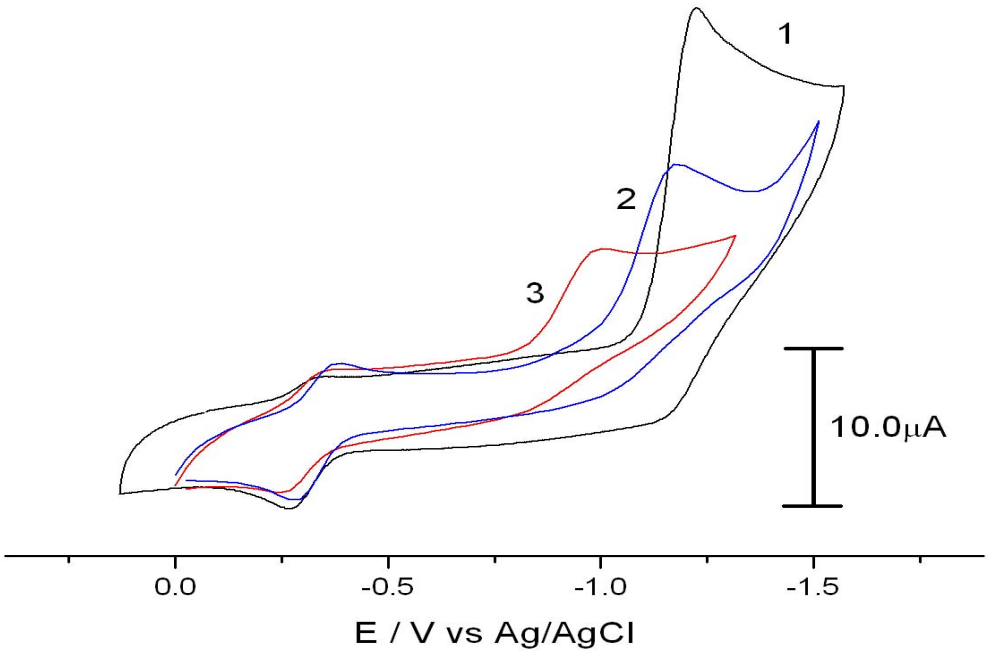

Figure 3-4. Electrochemistry of **[**$(\eta^6\text{-}C_6Me_6)Mn(CO)_2THF]BF_4$ and $(\eta^6\text{-}C_6Me_6)Mn(CO)_2Cl$. The CV of both complexes was conducted in 0.1M $TBAPF_6$ dichloromethane solution at room temperature, and scan rate was 0.5V/s. Glassy carbon electrode was used. (1) CV in black is 1mM **[**$(\eta^6\text{-}C_6Me_6)Mn(CO)_3]BF_4$. (2) CV in blue is **[**$(\eta^6\text{-}C_6Me_6)Mn(CO)_2THF]BF_4$ with unknown concentration. (3) CV in red is $(\eta^6\text{-}C_6Me_6)Mn(CO)_2Cl$ with unknown concentration.

After comparing CVs between manganese tricarbonyl complex [**1a**]BF_4 and dicarbonyl complexes, we conclude that, the reductive electrochemistry of all above three compound is the same. They all undergo 1-electron reduction and then ligand cleavage (CO, Cl^- or THF) followed by dimerization. Their reduction potential differs from each other because of different electron density of each molecule. However from figure 3-4, it is obvious that they share the very same reduction product **6a**, which has the characteristic reversible redox peak located at aournd -0.25V. Manganese

dicarbonyl complexes have similar reductive electrochemical behavior at room tempterature. While at low temperature, their electrochemical properties haven't changed, still maintained 1-electron irreversible reduction with **6a** as the product.

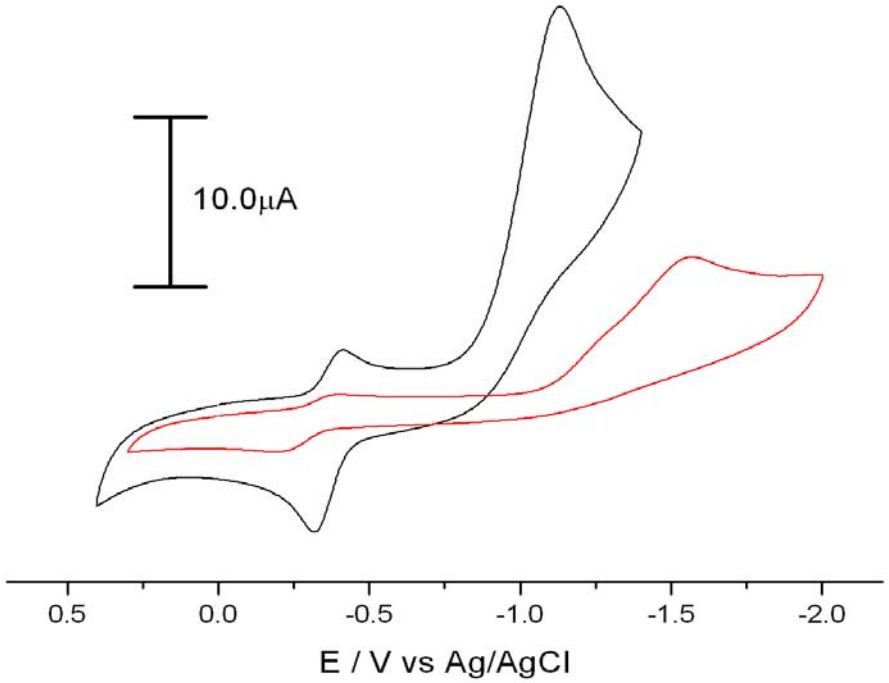

Figure 3-5. CVs of 1.0 mM $[(\eta^6\text{-}C_6Me_6)Mn(CO)_2THF]BF_4$ at +20 ^oC (black) and -60 ^oC (red) in CH_2Cl_2/0.10 M Bu_4NPF_6 under N_2. The working electrode was a 2.0 mm diameter platinum disk, and the scan rate was 0.50 V s^{-1}.

CV of $[(\eta^6\text{-}C_6Me_6)Mn(CO)_2THF]BF_4$ at both room temperature and low temperature gave characteristic redox peak corresponding to the dimer **6a** (figure 3-5). It indicates a much weaker bond between THF and Mn center compared with the bond between CO and Mn, which explains the irreversible electrochemistry of the dicarbonyl complex even at low temperature.

4). Reversibility of $[(\eta^6\text{-}C_6Me_6)Mn(CO)_3]BF_4$

Electrochemist prefers reversibility not only because that it indicates the

stability under reduction or oxidation, but also the potential application as an electrocatalyst. If the decomposition, in another word, dimerization of the complex **1a** could be stopped, the electrochemistry could very possibly be chemically reversible. Enabling the reversibility of complex 1 would widen the scope of our view of electrochemistry of monoarene manganese complex. A redox active complex would be more attractive, might have potential applications in catalysis and sensor. In order to achieve chemical reversibility of **1a**, we need to retain the chemical structure unchanged after reduction, thus, stop the cleavage of carbonyl group from Mn center. Excess carbon monoxide was bubbled through the dichloromethane solution of 1a. CV was taken with saturated CO presence (figure 3-6).

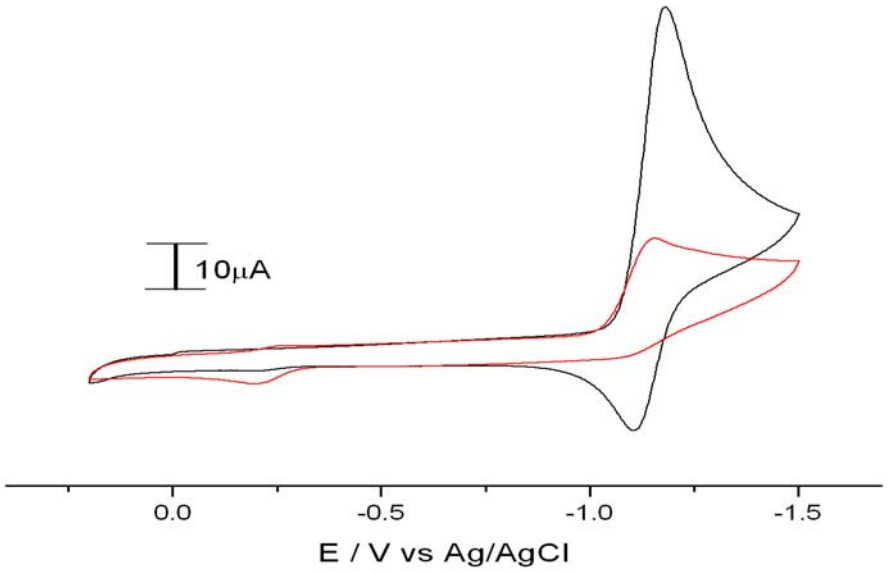

Figure 3-6. Cyclic voltammetry of 1mM **1a** in 0.1M $TBAPF_6$ dichloromethane solution with the protection gas of (1) CO (2) N_2 on glassy carbon electrode at room temperature. Scan rate is 0.50V/s.

Under nitrogen protection, after 1-electron irreversible reduction, peak corresponding to the dimer **6a** was observed, however, under the protection of carbon

monoxide, reduction became partially 2-electron reversible reduction, and the peak corresponding to the dimer completely vanished. Under 1atm, excess CO prevents the CO ligand from leaving the manganese center, thus the re-association rate of CO is faster compared with the dissociation

The partial reversibility comes from the reaction between 2-electron reduction product **3a** and starting material **1a**. Since cyclic voltammetry only changes the component of the tiny area on the electrode surface, after 2-electron reduction, **3a** will be the only component close to the surface area after reduction, however, in the bulky solution, the only component is **1a**. As the generation and diffusion of 3a, ring couple reaction was initiated and resulted in loss of reversibility. Peak current jump indicates that the number of electrons transferred has changed, which was confirmed by the diminish peak current corresponding to the dimer. The importance of this reversibility generation is: it is for the first time ever that, we observe the formation of ring slippaged form of monoarene manganese tricarbonyl anion at such a high temperature. The formation of eta4 anion was only seen at low temperature before and could never be isolated. We are expecting to synthesize this anion by reducing the cation chemically under saturated CO atmosphere in dichloromethane solution.

2. Rhenium Complexes

$(Arene)Re(CO)_3^+$ complexes have long been known to be orders of magnitude more susceptible to nucleophilic attack at the metal than the corresponding manganese complexes.[9e] Arene displacement with CH_3CN according to eq 1 was examined for complexes **1** and **2**. As determined by IR spectrometry, the manganese

complexes **1a** and **1b** show no reactions after days in CH_3CN solvent at room temperature. However, eq 1 occurs smoothly with rhenium complex **2a**. At 20 ^oC in neat CH_3CN the half-life is 23 min. By comparison, the mesitylene analogue $(\eta^6\text{-}C_6H_3Me_3)Re(CO)_3^+$ has a half-life of 15 min. With the much more sterically encumbered complex **2b** (see Figure 3-2), there was no detectable reaction with neat CH_3CN after 5 hr, so that the reactivity must be in the order: $C_6H_3Me_3 > C_6Me_6 >>> C_6Et_6$. This pattern was anticipated, although the extreme inertness of **2b** to nucleophilic attack was surprising.

$$(\eta^6\text{-arene})Re(CO)_3^+ + 3\ CH_3CN \longrightarrow (CH_3CN)_3Re(CO)_3^+ + \text{arene} \qquad (1)$$

The CVs of **2a** and **2b** in CH_2Cl_2 were straightforward to interpret because the electron transfers are chemically reversible at all temperatures. Figure 3-7 reveals a typical result for **2b**. It can immediately be seen that the electron transfer reactions are very slow. The reduction peak corresponds to two electrons (vide infra) and simulations are consistent with a reduction potential separation $\Delta E = E_2^o - E_1^o$ at room temperature of 450 m*V* and 570 *V* for **2a** and **2b**, respectively. The charge transfer rate constants for the second electron addition at -40 ^oC were best simulated to be very slow: $k_s(2) = 4 \times 10^{-5}$ cm/s for **2a** and 6×10^{-6} cm/s for **2b**.

Bulk electrolysis in CH_2Cl_2 was performed only for complex **2a**. At -60 ^oC, the passage of two equivalents of electrons through the solution cleanly produced the η^4-anion **4a** (ν_{CO} = 1930, 1827, 1805 cm^{-1}). The addition of one equivalent electron at -60 ^oC gave a mixture of η^4-**4a** and η^6-**2a**, which reacted with each other above -10

°C to afford an η^5 complex (ν_{CO} = 2003, 1881 cm^{-1}) that is most likely the rhenium analogue of **5a**. BE at room temperature consumed 1.5 electrons and produced an observable mixture of η^4-**4a** and a η^5-species. Over time at room temperature the η^4-**4a** complex decomposed. Given these observations, it is virtually certain that *chemical* reaction of the 19-electron radical $(\eta^6\text{-}C_6R_6)Re(CO)_3$ to yield η^5-species is not significant on the CV time scale. Additionally, digital simulations were not influenced by incorporation of the thermodynamically favored disproportionation of $(\eta^6\text{-}C_6Me_6)Re(CO)_3$ to **2a** and **4a**.

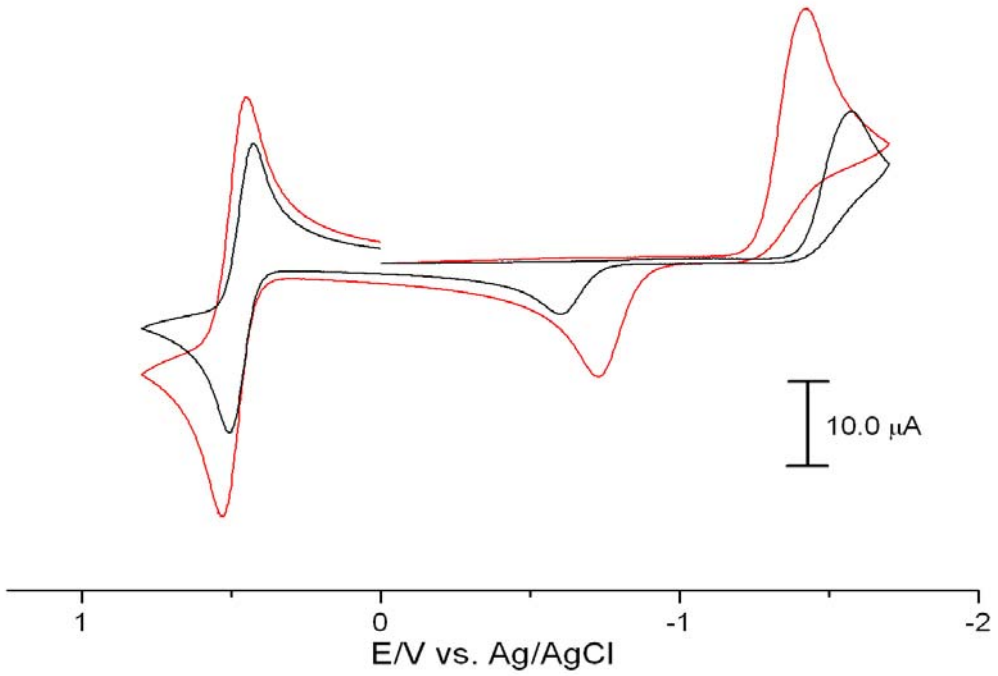

Figure 3-7. CVs of 1.0 mM $[(\eta^6\text{-}C_6Et_6)Re(CO)_3]PF_6$ (**2b**) at +20 °C (red) and -46 °C (black) in CH_2Cl_2/0.10 M Bu_4NPF_6 under N_2. The working electrode was a 2.0 mm diameter platinum disk, and the scan rate was 0.50 V s^{-1}. A ferrocene internal standard was added (left).

3.4 Conclusions

The complexes $(\eta^6\text{-}C_6R_6)M(CO)_3^+$ (M = Mn, Re; R = Me, Et) can be reduced electrochemically to give 19-electron radicals that can accept a second electron to yield ring-slipped $(\eta^4\text{-}C_6R_6)M(CO)_3^-$ complexes, or can react chemically by ring coupling to afford η^5-cyclohexadienyl dimeric species. Alternatively, the radicals can dissociate CO and couple to produce dimeric complexes **6**. Regardless of the metal or the R substituent, the second electron addition is characterized by very slow heterogeneous charge transfer and by an E_2^o value that is positive of E_1^o. With rhenium as the metal, only chemically reversible reduction is observed on the CV time scale. With manganese, however, the initial 1-electron reduction product can react chemically or, at low temperatures, undergo a second electron addition.

Consideration of all of the voltammetric and bulk electrolysis data leads to a number of interesting conclusions. In comparison to the hexamethylbenzene analogues, the effect of the ethyl substituents in **1b** and **2b** is to protect the metal from nucleophilic attack. As a result, the reactivity towards CH_3CN is in the order Me >> Et and Re >> Mn. In contrast, the 19-electron radicals obtained by 1-electron addition react by CO dissociation in the opposite order: Mn >> Re and C_6Et_6 >> C_6Me_6. Indeed, a key feature with the rhenium complexes is the great stability of the 19-electron radicals and the consequent reluctance to undergo any chemical reaction on the CV time scale. Similarly, the ring-slipped $(\eta^4\text{-}C_6R_6)M(CO)_3^-$ is more stable with rhenium, and can be directly observed via bulk electrolysis at room temperature.

The reductive electrochemistry of **1a** is illustrated in figure 3-8.

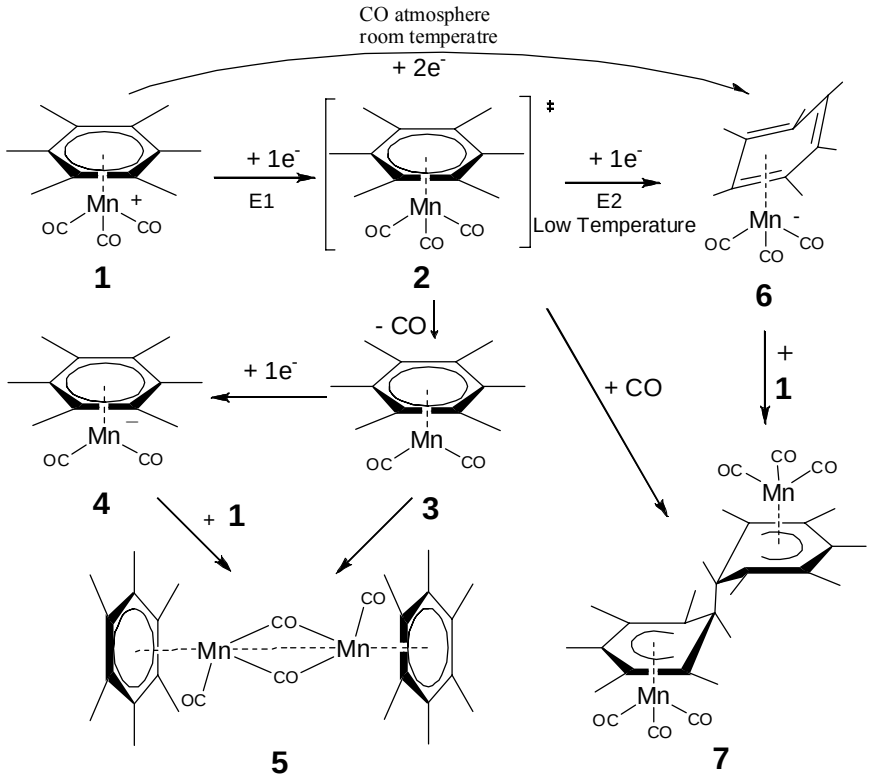

Figure 3-8. Reductive electrochemistry of **1a**

3.5 Supporting Information

1. Digital simulation

All digital simulations were completed using Digisim version 3.0 installed on a desktop. Simulations were done by comparison of ratios of the anodic and cathodic peaks measured from a common base line in both the CV and the simulation output. The simulation results were compared with the actual CV until the experimental result was mimicked as closely as possible. Ohmic polarization was not taken into account and was judged not in general of major importance by according to the behavior displayed by the internal ferrocene standard.

Metal	Temp	sol	E_1^o/V	k_{1s}	E_2^o/V	k_{2s}	α_2	E_3^o/V	10^5 D	Simulated (observed) E_p(V)
Re-HMB	RT	CH_2Cl_2	-1.43	0.1	-0.98	1.6E-3	-	-	1	E_p = -1.36 (-1.36), -0.85 (-0.86)
	-40 °C	CH_2Cl_2	-1.57	0.04	-0.97	4E-5	0.6	-	0.1	E_p = -1.50 (-1.49), -0.72 (-0.72)
Re-HEB	RT	CH_2Cl_2	-1.47	0.06	-0.90	7E-4	-	-	1	E_p = -1.41 (-1.41), -0.73 (-0.73)
	-46 °C	CH_2Cl_2	-1.57	0.01	-0.94	6E-6	0.6	-	0.1	E_p = -1.56 (-1.56), -0.60 (-0.60)
Mn-HMB	RT	CH_2Cl_2	-1.35	1	-1.25	1E-3	-	-0.315	1	E_p = -1.225 (-1.22), -0.29 (-0.29)
	-40 °C	CH_2Cl_2	-1.35	0.1	-1.1	2E-5	0.6	-	0.1	E_p = -1.34 (-1.33), -0.81 (-0.81)
	RT	MeCN	-1.35	1	-1.1	3E-3	-	-0.31	1	E_p = -1.23 (-1.25), -1.01 (-1.01)
	-40 °C	MeCN	-1.44	0.1	-1.04	3E-4	0.6	-	0.1	E_p = -1.35 (-1.35), -0.89 (-0.89)
Mn-HEB	-40 °C	CH_2Cl_2	-1.3	0.01	-1.1	3E-6	0.6	-0.31	0.1	E_p = -1.30 (-1.29), -1.46 (-1.44), -0.70 (-0.70)
	RT	MeCN	-1.2	0.1	-1.15	4E-5	-	-0.31	1	E_p = -1.235 (-1.22), -1.485 (-1.47), -0.82 (-0.85)
	-40 °C	MeCN	-1.38	0.1	-1.1	4E-6	0.6	-0.31	0.1	E_p = -1.38 (-1.38), -0.72 (-0.73)

Table 3-s1. Simulation data based on actual CV of each compound (unit of k_{1s}, k_{2s} is cm/s; unit of D is cm^2/s).

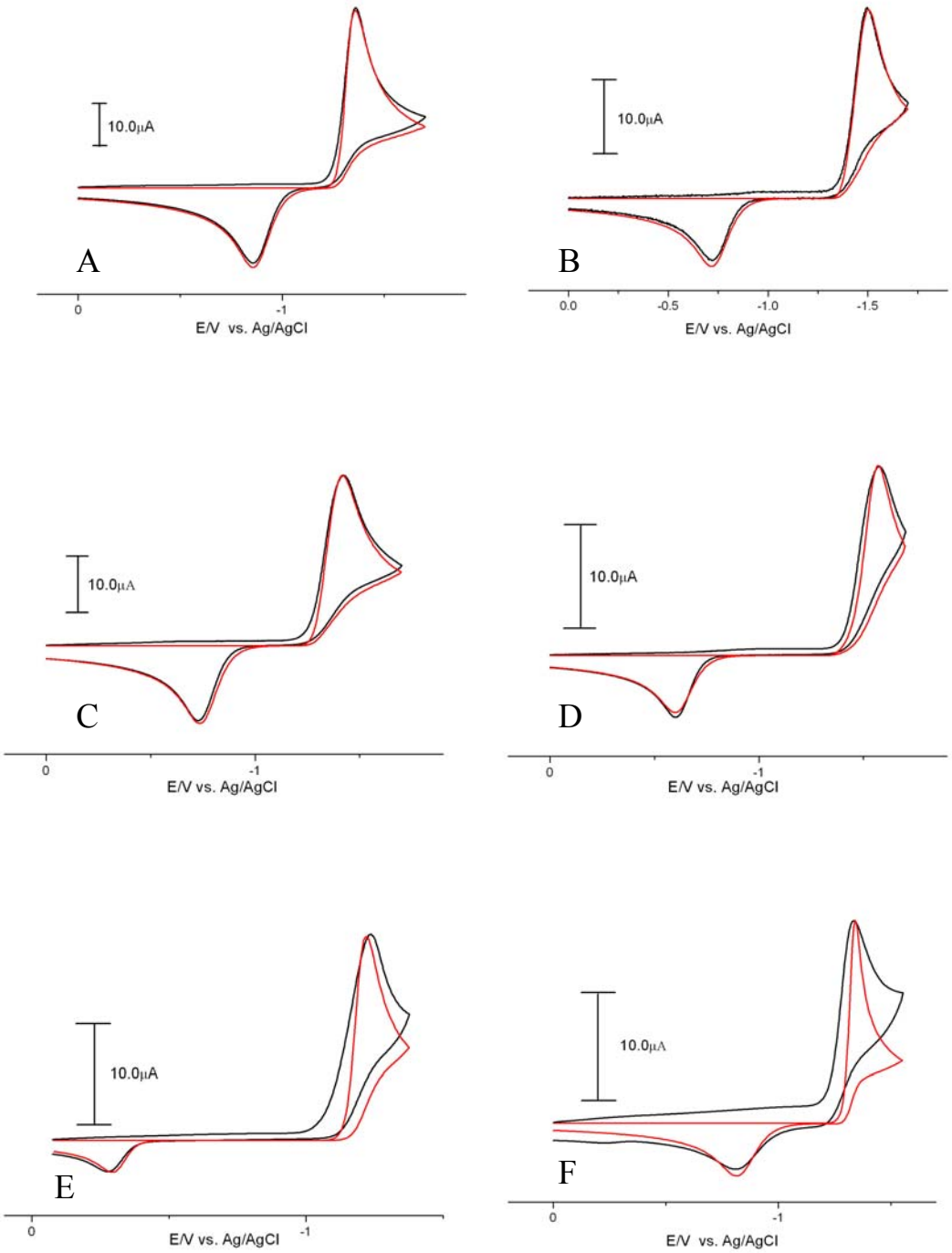

Figure 3-s1. Simulations A). **2a** in CH_2Cl_2 at R.T. ; B). **2a** in CH_2Cl_2 at -40 °C ; C). **2b** in CH_2Cl_2 at R.T. ; D). **2b** in CH_2Cl_2 at -46 °C ; E). **1a** in CH_2Cl_2 at R.T. ; F). **1a** in

CH_2Cl_2 at -40 °C. Pt was used as the electrode. Scan rate was 0.5V/s. The concentration of each compound is 1mM/ 0.1M Bu_4NPF_6. Red line is simulated CV, black line is actual CV.

2. In-situ IR Spectroscopy and Bulk Electrolysis

At room temperature, we fixed the applied potential at -1.2V for 15min, the light yellow color solution of **1a** got greener and greener, the in-situ optic IR spectra suggested that, the band which corresponded to the **6a** got stronger and stronger (Figure s2A), there was barely anything else (though we got slight amount of the byproduct (HMB) $Mn(CO)_2Cl$)). The CV shown in Figure s2B agrees with the conclusion. When we used CH_3CN as the solvent, the result stayed the same.

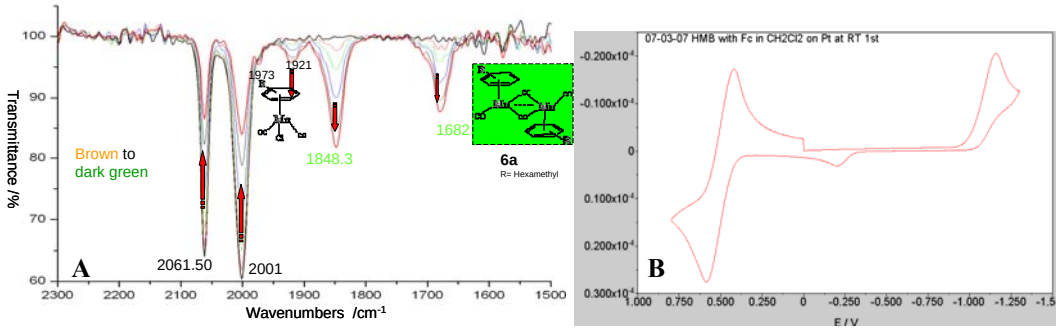

Figure 3-s2. A). In-situ IR spectra for the bulk electrolysis process of [**1a**]BF_4 in CH_2Cl_2 with 0.1M Bu_4NPF_6 under N_2 at R.T. Applied potentical -1.2V : Changes are labeled by red arrows. B). corresponding CV of 1mM [**1a**]BF_4 and 1mM ferrocene (left) in CH_2Cl_2 with 0.1M Bu_4NPF_6 under N_2 at R.T.

When we lowered the temperature to -60 °C, and applied potential at -1.4V for 25min to the system, the light yellow color (**1a**) got deeper. In-situ IR suggested to have the ring slippage η^4-**3a** species (1910, 1817, 1786 cm^{-1}) and η^5-**5a** (1990, 1910

cm^{-1}) as products.

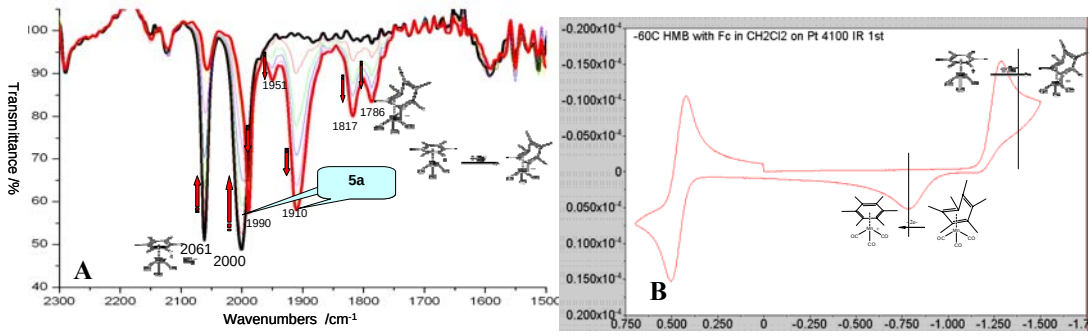

Figure 3-s3. A). In-situ IR spectra for the bulk electrolysis process of [**1a**]BF_4 in CH_2Cl_2 with 0.1M Bu_4NPF_6 under N_2 at -60 ^oC. Applied potential -1.4V : Changes are labeled by red arrows. B). corresponding CV of 1mM [**1a**]BF_4 and 1mM ferrocene (left) in CH_2Cl_2 with 0.1M Bu_4NPF_6 under N_2 at -60 ^oC

Keeping the above solution at -60 ^oC, +0.1V was applied to the system. It was found that all the η^4-**3a** went back to the starting material, shown in Figure s4, which confirmed that at low temperature, the reduction was chemically reversible.

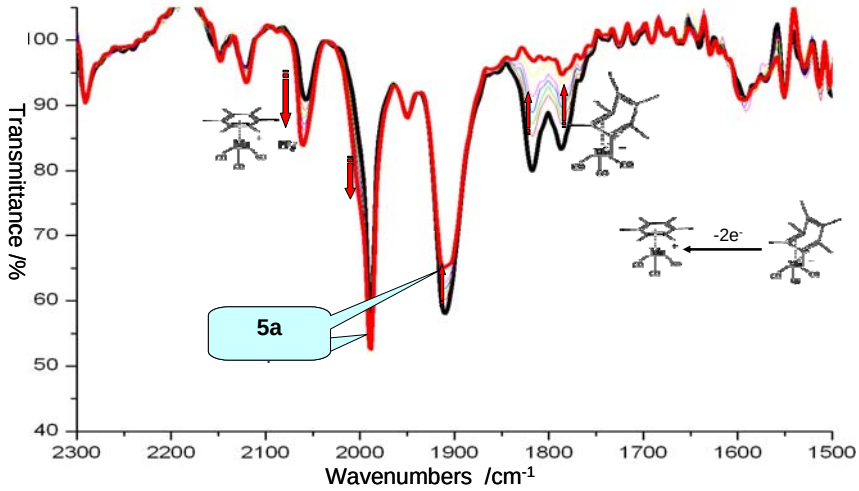

Figure 3-s4. In-situ IR spectra for the bulk electrolysis process of [**1a**]BF_4 in CH_2Cl_2 with 0.1M Bu_4NPF_6 under N_2 at -60 ^oC. Applied potential +0.1V: Changes are labeled by red arrows.

In a control experiment, when the starting material was still present and the transmittance of IR bands for the starting material η^6-**1a**, η^5-**5a** and the η^4-**3a** was almost equal to each other, we stopped applying potensital to the solution and kept the temperature at -60 °C for 20mins. We could clearly see that, the starting material and the η^4 reductant were disappearing; in the meanwhile, the IR bands of η^5-**5a** were getting stronger. Thus, it is reasonable to believe that the starting material and the η^4 reductant react to afford η^5-**5a**.

As the η^4 species was synthesized electrochemically from the surface of the bulky working electrode, it diffused away to the bulk solution. Since it has negative charge, it's easy for it to react with the positive charged starting compound, they can dimerize together to give η^5 neutral species **5a**.

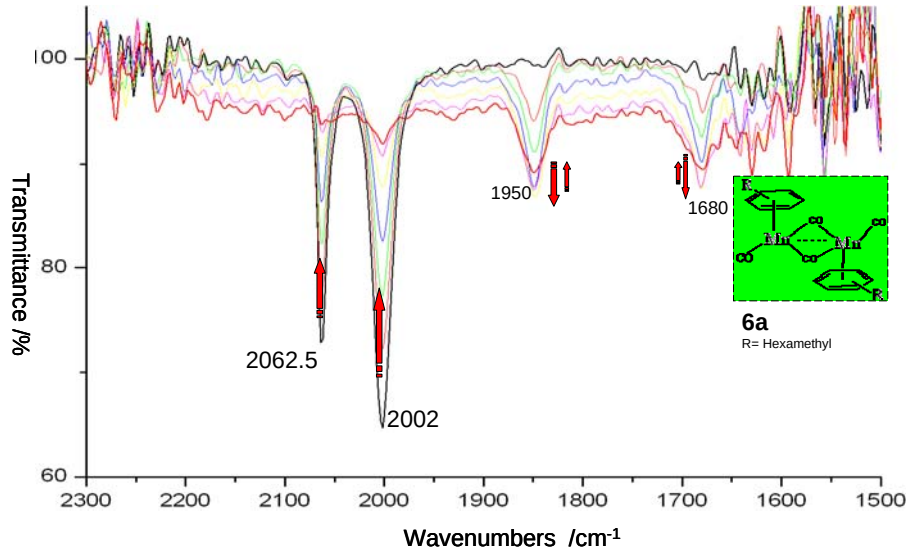

Figure 3-s5. Bulk electrolysis [**1a**]BF_4 in CH_3CN + 0.1M Bu_4NPF_6 under N_2 at RT. Apply -1.2V for about 15 mins.

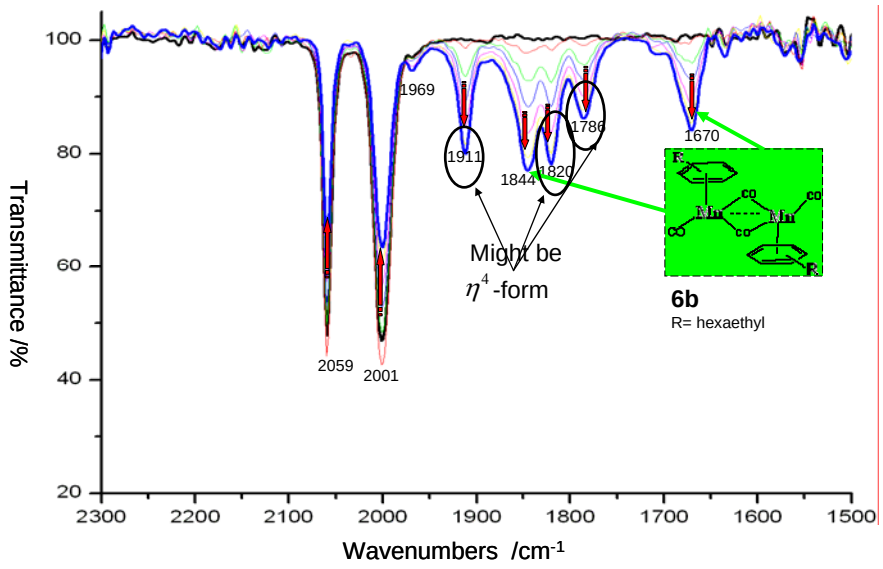

Figure 3-s6. In-situ IR spectra for the bulk electrolysis process of [**1b**]BF_4 in CH_2Cl_2 with 0.1M Bu_4NPF_6 under N_2 at -60 °C. Applied potential -1.5V: Changes are labeled by red arrows.

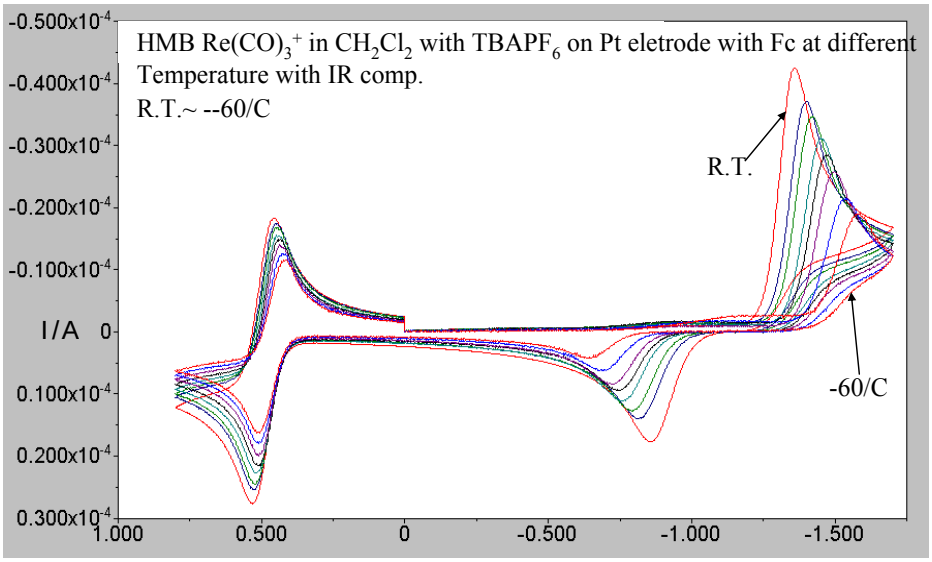

Figure 3-s7. Overlapped CV of 1mM [**2a**]PF_6 and 1mM ferrocene (left) in CH_2Cl_2 with 0.1M Bu_4NPF_6 under N_2 from room temperature to -60 °C. Pt was used as working electrode.

3.6 X-ray crystal structure data

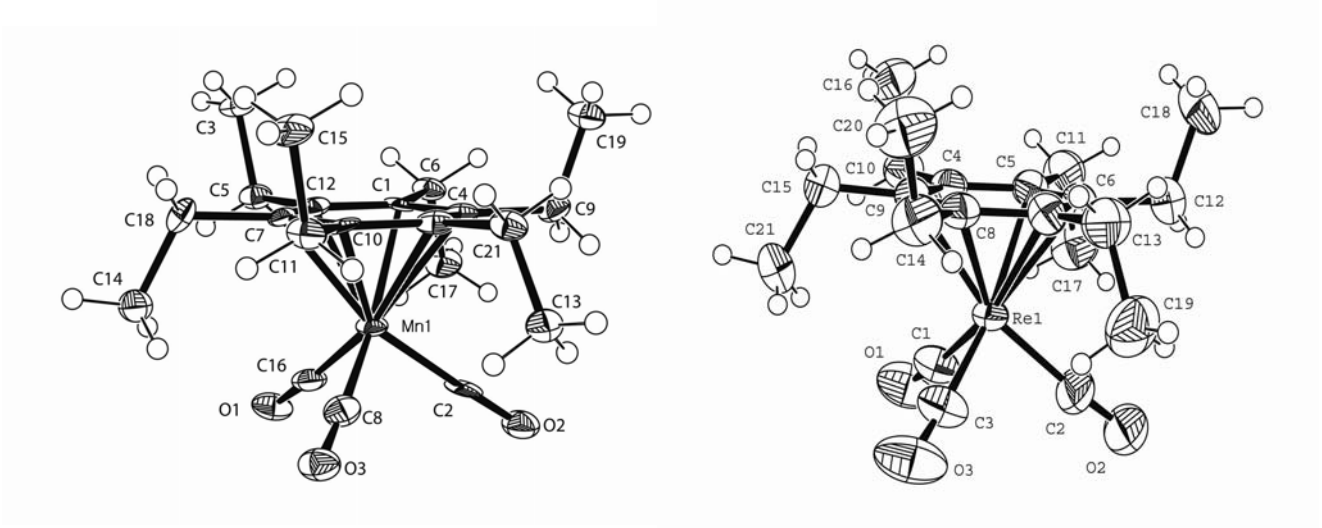

X-ray structures of $[(C_6Et_6)Mn(CO)_3]BF_4$ (**1b**) and $[(C_6Et_6)Re(CO)_3]PF_6$ (**2b**). The average M-C(arene) bond length is 2.22(1) A for Mn and 2.35(1) A for Re.

Table 3-C1-1. Crystal data and structure refinement for [1b]BF_4.

Identification code	[1b]BF_4
Empirical formula	C21 H30 B1 F4 Mn1 O3
Formula weight	553.48
Temperature	293(2) K
Wavelength	0.71073 A
Crystal system, space group	Orthorhombic, P2(1)2(1)2(1)
Unit cell dimensions	a = 8.9357(18) A alpha = 90 deg. b = 14.007(3) A beta = 90 deg. c = 17.480(4) A gamma = 90 deg.
Volume	2187.8(8) A^3
Z, Calculated density	4, 1.680 Mg/m^3
Absorption coefficient	1.215 mm^-1
F(000)	1112
Crystal size	1 x 1 x 1 mm
Theta range for data collection	1.86 to 28.31 deg.
Limiting indices	-11<=h<=11, -18<=k<=18, -23<=l<=22
Reflections collected / unique	18886 / 5297 [R(int) = 0.0701]
Completeness to theta = 28.31	98.6 %
Absorption correction	done
Refinement method	Full-matrix least-squares on F^2
Data / restraints / parameters	5297 / 0 / 277
Goodness-of-fit on F^2	1.024
Final R indices [I>2sigma(I)]	R1 = 0.0442, wR2 = 0.0954
R indices (all data)	R1 = 0.0559, wR2 = 0.1000
Absolute structure parameter	0.157(17)
Largest diff. peak and hole	0.668 and -0.269 e.A^-3

Table 3-C1-2. Atomic coordinates (x 10^4) and equivalent isotropic displacement parameters (A^2 x 10^3) for [1b]BF_4. U(eq) is defined as one third of the trace of the orthogonalized Uij tensor.

	x	y	z	U(eq)
F(1)	6620(2)	5712(1)	7527(1)	45(1)
Mn(1)	3479(1)	5094(1)	403(1)	16(1)
C(1)	1321(3)	4684(2)	958(1)	16(1)
O(3)	6585(2)	5777(1)	162(1)	27(1)
C(2)	2763(3)	5808(2)	-390(1)	19(1)
C(3)	1420(3)	2567(2)	1810(1)	22(1)
C(4)	1565(3)	5681(2)	1057(1)	15(1)
C(5)	2172(3)	2963(2)	1084(1)	19(1)
O(2)	2260(2)	6257(2)	-871(1)	30(1)
C(6)	-181(3)	4335(2)	651(1)	19(1)
C(7)	3805(3)	4355(2)	1517(1)	17(1)
C(8)	5375(3)	5521(2)	223(1)	20(1)
C(9)	350(3)	6384(2)	828(1)	18(1)
C(10)	4027(3)	5352(2)	1622(1)	17(1)
O(1)	3884(2)	3440(2)	-633(1)	30(1)
C(11)	5437(3)	5701(2)	2010(1)	20(1)
C(12)	2451(3)	4028(2)	1180(1)	17(1)
C(13)	3835(3)	7662(2)	927(2)	25(1)
C(14)	6142(3)	3338(2)	1196(2)	25(1)
C(15)	5208(3)	5735(2)	2881(1)	28(1)
C(16)	3754(3)	4095(2)	-251(1)	22(1)
C(17)	-303(3)	4246(2)	-219(1)	25(1)
C(18)	4979(3)	3639(2)	1793(1)	21(1)
C(19)	-726(3)	6550(2)	1498(1)	22(1)
C(20)	2906(3)	6019(2)	1403(1)	17(1)
C(21)	3100(3)	7084(2)	1564(1)	19(1)
F(3)	6323(2)	4796(1)	8592(1)	38(1)
F(2)	5395(2)	6304(1)	8566(1)	29(1)
F(4)	4323(2)	5141(2)	7839(1)	51(1)
B(1)	5654(4)	5487(2)	8130(2)	28(1)

Table 3-C1-3. Bond lengths [A] and angles [deg] for [1b]BF_4.

F(1)-B(1)	1.398(4)	C(4)-C(9)	1.519(3)
Mn(1)-C(8)	1.824(3)	C(5)-C(12)	1.522(3)
Mn(1)-C(16)	1.824(3)	C(6)-C(17)	1.529(3)
Mn(1)-C(2)	1.825(3)	C(7)-C(12)	1.422(4)
Mn(1)-C(10)	2.216(2)	C(7)-C(10)	1.422(4)
Mn(1)-C(4)	2.216(3)	C(7)-C(18)	1.530(3)
Mn(1)-C(12)	2.219(3)	C(9)-C(19)	1.531(3)
Mn(1)-C(7)	2.225(2)	C(10)-C(20)	1.422(4)
Mn(1)-C(1)	2.235(2)	C(10)-C(11)	1.512(4)
Mn(1)-C(20)	2.235(3)	O(1)-C(16)	1.139(3)
C(1)-C(12)	1.419(3)	C(11)-C(15)	1.537(3)
C(1)-C(4)	1.424(3)	C(13)-C(21)	1.525(3)
C(1)-C(6)	1.526(3)	C(14)-C(18)	1.532(4)
O(3)-C(8)	1.144(3)	C(20)-C(21)	1.529(4)
C(2)-O(2)	1.142(3)	F(3)-B(1)	1.394(4)
C(3)-C(5)	1.539(3)	F(2)-B(1)	1.395(4)
C(4)-C(20)	1.423(4)	F(4)-B(1)	1.382(4)

C(8)-Mn(1)-C(16)	91.05(12)
C(8)-Mn(1)-C(2)	90.89(11)
C(16)-Mn(1)-C(2)	89.51(12)
C(8)-Mn(1)-C(10)	84.68(10)
C(16)-Mn(1)-C(10)	134.27(11)
C(2)-Mn(1)-C(10)	135.94(11)
C(8)-Mn(1)-C(4)	133.21(11)
C(16)-Mn(1)-C(4)	135.40(11)
C(2)-Mn(1)-C(4)	85.31(10)
C(10)-Mn(1)-C(4)	67.28(9)
C(8)-Mn(1)-C(12)	135.32(11)
C(16)-Mn(1)-C(12)	85.57(10)
C(2)-Mn(1)-C(12)	133.52(11)
C(10)-Mn(1)-C(12)	67.20(9)
C(4)-Mn(1)-C(12)	67.28(9)
C(8)-Mn(1)-C(7)	100.49(10)
C(16)-Mn(1)-C(7)	100.02(10)
C(2)-Mn(1)-C(7)	164.94(10)
C(10)-Mn(1)-C(7)	37.36(9)
C(4)-Mn(1)-C(7)	79.71(9)
C(12)-Mn(1)-C(7)	37.32(9)
C(8)-Mn(1)-C(1)	163.95(9)
C(16)-Mn(1)-C(1)	101.02(10)

C(2)-Mn(1)-C(1)	99.68(10)
C(10)-Mn(1)-C(1)	79.33(9)
C(4)-Mn(1)-C(1)	37.32(9)
C(12)-Mn(1)-C(1)	37.17(9)
C(7)-Mn(1)-C(1)	67.21(9)
C(8)-Mn(1)-C(20)	99.10(10)
C(16)-Mn(1)-C(20)	164.96(10)
C(2)-Mn(1)-C(20)	101.32(10)
C(10)-Mn(1)-C(20)	37.27(9)
C(4)-Mn(1)-C(20)	37.28(9)
C(12)-Mn(1)-C(20)	79.41(9)
C(7)-Mn(1)-C(20)	67.35(9)
C(1)-Mn(1)-C(20)	67.12(9)
C(12)-C(1)-C(4)	119.6(2)
C(12)-C(1)-C(6)	120.9(2)
C(4)-C(1)-C(6)	119.5(2)
C(12)-C(1)-Mn(1)	70.81(14)
C(4)-C(1)-Mn(1)	70.64(15)
C(6)-C(1)-Mn(1)	133.49(15)
O(2)-C(2)-Mn(1)	177.2(2)
C(20)-C(4)-C(1)	120.4(2)
C(20)-C(4)-C(9)	119.9(2)
C(1)-C(4)-C(9)	119.6(2)
C(20)-C(4)-Mn(1)	72.08(15)
C(1)-C(4)-Mn(1)	72.04(15)
C(9)-C(4)-Mn(1)	131.00(15)
C(12)-C(5)-C(3)	109.4(2)
C(1)-C(6)-C(17)	116.0(2)
C(12)-C(7)-C(10)	119.3(2)
C(12)-C(7)-C(18)	120.2(2)
C(10)-C(7)-C(18)	120.5(2)
C(12)-C(7)-Mn(1)	71.08(14)
C(10)-C(7)-Mn(1)	70.95(14)
C(18)-C(7)-Mn(1)	132.11(17)
O(3)-C(8)-Mn(1)	175.2(2)
C(4)-C(9)-C(19)	110.2(2)
C(20)-C(10)-C(7)	120.8(2)
C(20)-C(10)-C(11)	119.7(2)
C(7)-C(10)-C(11)	119.5(2)
C(20)-C(10)-Mn(1)	72.09(14)
C(7)-C(10)-Mn(1)	71.69(14)
C(11)-C(10)-Mn(1)	131.97(17)
C(10)-C(11)-C(15)	110.1(2)
C(1)-C(12)-C(7)	120.6(2)

C(1)-C(12)-C(5)	119.2(2)
C(7)-C(12)-C(5)	120.1(2)
C(1)-C(12)-Mn(1)	72.02(14)
C(7)-C(12)-Mn(1)	71.60(14)
C(5)-C(12)-Mn(1)	131.32(17)
O(1)-C(16)-Mn(1)	176.3(2)
C(7)-C(18)-C(14)	115.5(2)
C(10)-C(20)-C(4)	119.3(2)
C(10)-C(20)-C(21)	120.8(2)
C(4)-C(20)-C(21)	119.9(2)
C(10)-C(20)-Mn(1)	70.63(14)
C(4)-C(20)-Mn(1)	70.64(14)
C(21)-C(20)-Mn(1)	133.13(17)
C(13)-C(21)-C(20)	115.6(2)
F(4)-B(1)-F(3)	109.8(3)
F(4)-B(1)-F(2)	110.2(3)
F(3)-B(1)-F(2)	108.9(2)
F(4)-B(1)-F(1)	109.4(2)
F(3)-B(1)-F(1)	109.2(3)
F(2)-B(1)-F(1)	109.3(3)

Symmetry transformations used to generate equivalent atoms:

Table 3-C1-4. Anisotropic displacement parameters (A^2 x 10^3) for [1b]BF_4. The anisotropic displacement factor exponent takes the form: -2 pi^2 [h^2 a*^2 U11 + ... + 2 h k a* b* U12]

	U11	U22	U33	U23	U13	U12
F(1)	50(1)	47(1)	39(1)	5(1)	25(1)	8(1)
Mn(1)	15(1)	19(1)	14(1)	0(1)	1(1)	0(1)
C(1)	17(1)	21(1)	11(1)	0(1)	3(1)	-1(1)
O(3)	19(1)	38(1)	25(1)	2(1)	1(1)	-5(1)
C(2)	16(1)	26(2)	16(1)	-1(1)	6(1)	3(1)
C(3)	24(1)	19(1)	23(1)	2(1)	3(1)	-4(1)
C(4)	17(1)	17(1)	13(1)	0(1)	1(1)	0(1)
C(5)	18(1)	17(1)	21(1)	1(1)	-1(1)	-2(1)
O(2)	25(1)	40(1)	23(1)	7(1)	3(1)	6(1)
C(6)	17(1)	20(1)	19(1)	-3(1)	-1(1)	-2(1)
C(7)	18(1)	17(1)	15(1)	1(1)	2(1)	2(1)
C(8)	20(1)	25(2)	16(1)	0(1)	0(1)	3(1)
C(9)	17(1)	16(1)	19(1)	0(1)	0(1)	0(1)
C(10)	16(1)	22(2)	12(1)	2(1)	2(1)	0(1)
O(1)	35(1)	28(1)	28(1)	-7(1)	10(1)	-3(1)
C(11)	17(1)	22(2)	20(1)	1(1)	-2(1)	-3(1)
C(12)	18(1)	19(1)	13(1)	0(1)	3(1)	1(1)
C(13)	26(2)	19(2)	30(1)	3(1)	1(1)	-3(1)
C(14)	19(1)	23(2)	33(1)	1(1)	3(1)	5(1)
C(15)	31(2)	34(2)	18(1)	-1(1)	-5(1)	-3(1)
C(16)	23(2)	24(2)	21(1)	2(1)	4(1)	-3(1)
C(17)	24(1)	28(2)	21(1)	-5(1)	-5(1)	0(1)
C(18)	20(1)	18(1)	24(1)	3(1)	-5(1)	2(1)
C(19)	18(1)	26(2)	24(1)	-3(1)	2(1)	1(1)
C(20)	17(1)	21(2)	14(1)	3(1)	2(1)	-3(1)
C(21)	20(1)	18(1)	20(1)	-3(1)	-1(1)	-2(1)
F(3)	52(1)	26(1)	37(1)	3(1)	3(1)	8(1)
F(2)	30(1)	24(1)	34(1)	-3(1)	6(1)	2(1)
F(4)	39(1)	62(2)	53(1)	-22(1)	-9(1)	-7(1)
B(1)	32(2)	26(2)	25(2)	-2(1)	7(1)	0(2)

Table 3-C1-5. Hydrogen coordinates (x 10^4) and isotropic displacement parameters (A^2 x 10^3) for [1b]BF_4.

	x	y	z	U(eq)
H(3A)	2058	2678	2243	33
H(3B)	1254	1894	1752	33
H(3C)	479	2884	1888	33
H(5A)	3113	2635	996	22
H(5B)	1530	2854	645	22
H(6A)	-954	4769	826	23
H(6B)	-388	3714	874	23
H(9A)	-200	6136	393	21
H(9B)	802	6985	679	21
H(11A)	5687	6334	1824	24
H(11B)	6261	5277	1889	24
H(13A)	4829	7426	838	37
H(13B)	3884	8321	1075	37
H(13C)	3256	7602	467	37
H(14A)	5643	3057	764	37
H(14B)	6814	2880	1417	37
H(14C)	6697	3887	1031	37
H(15A)	4455	6199	3003	41
H(15B)	6132	5908	3125	41
H(15C)	4895	5118	3060	41
H(17A)	-125	4858	-449	37
H(17B)	-1287	4029	-353	37
H(17C)	427	3797	-401	37
H(18A)	4467	3071	1973	25
H(18B)	5502	3914	2227	25
H(19A)	-1102	5948	1675	33
H(19B)	-1545	6942	1331	33
H(19C)	-204	6865	1906	33
H(21A)	2122	7356	1667	23
H(21B)	3695	7155	2024	23

Table 3-C2-1. Crystal data and structure refinement for [**2b**]PF_6.

Identification code	[**2b**]PF_6
Empirical formula	C42 H60 F12 O6 P2 Re2
Formula weight	1323.24
Temperature	296(2) K
Wavelength	0.71073 A
Crystal system, space group	?, ?
Unit cell dimensions	a = 19.922(5) A alpha = 90 deg.
	b = 23.118(5) A beta = 130.666(5) deg.
	c = 13.913(5) A gamma = 90 deg.
Volume	4860(2) A^3
Z, Calculated density	4, 1.808 Mg/m^3
Absorption coefficient	5.132 mm^-1
F(000)	2592
Crystal size	0.20 x 0.20 x 0.10 mm
Theta range for data collection	1.61 to 30.32 deg.
Limiting indices	-28<=h<=27, -32<=k<=32, -19<=l<=15
Reflections collected / unique	45814 / 6864 [R(int) = 0.0290]
Completeness to theta = 30.32	94.1 %
Max. and min. transmission	0.6279 and 0.4268
Refinement method	Full-matrix least-squares on F^2
Data / restraints / parameters	6864 / 42 / 295
Goodness-of-fit on F^2	1.165
Final R indices [I>2sigma(I)]	R1 = 0.0633, wR2 = 0.1875
R indices (all data)	R1 = 0.0768, wR2 = 0.1970
Largest diff. peak and hole	5.841 and -1.671 e.A^-3

Table 3-C2-2. Atomic coordinates (x 10^4) and equivalent isotropic displacement parameters (A^2 x 10^3) for [**2b**]PF_6. U(eq) is defined as one third of the trace of the orthogonalized Uij tensor.

	x	y	z	U(eq)
Re(1)	2439(1)	569(1)	7362(1)	37(1)
O(1)	1611(7)	-196(4)	5041(9)	78(3)
O(2)	4081(6)	-204(4)	8917(13)	118(5)
O(3)	1522(8)	-206(4)	7999(10)	89(3)
C(1)	1928(8)	58(4)	5912(10)	52(2)
C(2)	3461(8)	63(5)	8361(14)	77(4)
C(3)	1880(8)	65(4)	7779(10)	53(2)
C(4)	1962(6)	1366(4)	6012(8)	40(2)
C(5)	2912(6)	1374(4)	6904(9)	44(2)
C(6)	3367(6)	1383(4)	8230(9)	44(2)
C(7)	2902(6)	1381(4)	8688(9)	48(2)
C(8)	1956(6)	1377(4)	7787(9)	42(2)
C(9)	1484(5)	1375(4)	6468(8)	39(2)
C(10)	1473(7)	1375(4)	4610(9)	51(2)
C(11)	3426(8)	1409(5)	6441(12)	61(3)
C(12)	4377(7)	1422(5)	9182(11)	60(3)
C(13)	3405(8)	1442(5)	10102(10)	60(3)
C(14)	1445(8)	1403(5)	8258(11)	56(2)
C(15)	481(6)	1407(4)	5511(10)	50(2)
C(16)	1297(9)	1990(5)	4111(12)	69(3)
C(17)	3674(9)	822(6)	6263(14)	73(3)
C(18)	4666(9)	2063(6)	9425(15)	85(4)
C(19)	3681(10)	844(7)	10798(12)	79(4)
C(20)	1261(11)	2001(6)	8392(15)	77(4)
C(21)	12(7)	831(6)	5078(15)	81(4)
P(1)	2404(1)	3296(1)	7510(2)	29(1)
F(1)	3282(10)	3301(8)	7720(20)	293(11)
F(2)	2934(17)	3039(14)	8827(17)	360(14)
F(3)	1578(9)	3311(8)	7342(18)	187(6)
F(4)	2594(12)	3904(7)	8000(30)	303(11)
F(5)	2157(12)	2725(7)	6850(20)	267(9)
F(6)	1924(14)	3600(12)	6295(18)	292(10)

Table 3-C2-3. Bond lengths [A] and angles [deg] for [**2b**]PF_6.

Re(1)-C(2)	1.939(11)
Re(1)-C(3)	1.944(10)
Re(1)-C(1)	1.957(10)
Re(1)-C(4)	2.345(8)
Re(1)-C(8)	2.346(9)
Re(1)-C(6)	2.346(9)
Re(1)-C(5)	2.354(9)
Re(1)-C(9)	2.355(8)
Re(1)-C(7)	2.358(10)
O(1)-C(1)	1.102(13)
O(2)-C(2)	1.123(14)
O(3)-C(3)	1.133(13)
C(4)-C(5)	1.436(12)
C(4)-C(9)	1.447(12)
C(4)-C(10)	1.510(13)
C(5)-C(6)	1.431(13)
C(5)-C(11)	1.524(14)
C(6)-C(7)	1.427(14)
C(6)-C(12)	1.528(13)
C(7)-C(8)	1.430(13)
C(7)-C(13)	1.524(14)
C(8)-C(9)	1.416(13)
C(8)-C(14)	1.529(13)
C(9)-C(15)	1.518(12)
C(10)-C(16)	1.519(15)
C(10)-H(10A)	0.9700
C(10)-H(10B)	0.9700
C(11)-C(17)	1.518(17)
C(11)-H(11A)	0.9700
C(11)-H(11B)	0.9700
C(12)-C(18)	1.546(16)
C(12)-H(12A)	0.9700
C(12)-H(12B)	0.9700
C(13)-C(19)	1.567(17)
C(13)-H(13A)	0.9700
C(13)-H(13B)	0.9700
C(14)-C(20)	1.475(16)
C(14)-H(14A)	0.9700
C(14)-H(14B)	0.9700
C(15)-C(21)	1.509(15)

C(15)-H(15A)	0.9700
C(15)-H(15B)	0.9700
C(16)-H(16A)	0.9600
C(16)-H(16B)	0.9600
C(16)-H(16C)	0.9600
C(17)-H(17A)	0.9600
C(17)-H(17B)	0.9600
C(17)-H(17C)	0.9600
C(18)-H(18A)	0.9600
C(18)-H(18B)	0.9600
C(18)-H(18C)	0.9600
C(19)-H(19A)	0.9600
C(19)-H(19B)	0.9600
C(19)-H(19C)	0.9600
C(20)-H(20A)	0.9600
C(20)-H(20B)	0.9600
C(20)-H(20C)	0.9600
C(21)-H(21A)	0.9600
C(21)-H(21B)	0.9600
C(21)-H(21C)	0.9600
P(1)-F(6)	1.470(11)
P(1)-F(5)	1.495(10)
P(1)-F(4)	1.501(11)
P(1)-F(3)	1.505(10)
P(1)-F(2)	1.517(11)
P(1)-F(1)	1.577(10)

C(2)-Re(1)-C(3)	87.8(6)
C(2)-Re(1)-C(1)	88.4(5)
C(3)-Re(1)-C(1)	86.1(4)
C(2)-Re(1)-C(4)	137.5(5)
C(3)-Re(1)-C(4)	134.3(4)
C(1)-Re(1)-C(4)	89.0(4)
C(2)-Re(1)-C(8)	135.4(5)
C(3)-Re(1)-C(8)	89.6(4)
C(1)-Re(1)-C(8)	135.9(4)
C(4)-Re(1)-C(8)	63.8(3)
C(2)-Re(1)-C(6)	90.5(4)
C(3)-Re(1)-C(6)	137.7(4)
C(1)-Re(1)-C(6)	136.1(4)
C(4)-Re(1)-C(6)	63.6(3)
C(8)-Re(1)-C(6)	63.1(3)
C(2)-Re(1)-C(5)	104.7(5)
C(3)-Re(1)-C(5)	164.5(4)
C(1)-Re(1)-C(5)	103.3(4)
C(4)-Re(1)-C(5)	35.6(3)
C(8)-Re(1)-C(5)	75.0(3)
C(6)-Re(1)-C(5)	35.5(3)
C(2)-Re(1)-C(9)	164.9(4)
C(3)-Re(1)-C(9)	102.1(4)
C(1)-Re(1)-C(9)	103.6(4)
C(4)-Re(1)-C(9)	35.9(3)
C(8)-Re(1)-C(9)	35.1(3)
C(6)-Re(1)-C(9)	74.5(3)
C(5)-Re(1)-C(9)	63.9(3)
C(2)-Re(1)-C(7)	103.2(5)
C(3)-Re(1)-C(7)	104.6(4)
C(1)-Re(1)-C(7)	164.4(4)
C(4)-Re(1)-C(7)	75.5(3)
C(8)-Re(1)-C(7)	35.4(3)
C(6)-Re(1)-C(7)	35.3(3)
C(5)-Re(1)-C(7)	64.0(3)
C(9)-Re(1)-C(7)	63.5(3)
O(1)-C(1)-Re(1)	174.9(11)
O(2)-C(2)-Re(1)	174.8(15)
O(3)-C(3)-Re(1)	176.4(11)
C(5)-C(4)-C(9)	119.6(8)
C(5)-C(4)-C(10)	119.6(8)
C(9)-C(4)-C(10)	120.8(8)
C(5)-C(4)-Re(1)	72.5(5)
C(9)-C(4)-Re(1)	72.5(5)

C(10)-C(4)-Re(1)	129.0(6)
C(6)-C(5)-C(4)	119.0(8)
C(6)-C(5)-C(11)	120.5(9)
C(4)-C(5)-C(11)	120.4(9)
C(6)-C(5)-Re(1)	72.0(5)
C(4)-C(5)-Re(1)	71.9(5)
C(11)-C(5)-Re(1)	130.8(7)
C(7)-C(6)-C(5)	121.7(8)
C(7)-C(6)-C(12)	119.0(9)
C(5)-C(6)-C(12)	119.2(9)
C(7)-C(6)-Re(1)	72.8(5)
C(5)-C(6)-Re(1)	72.6(5)
C(12)-C(6)-Re(1)	130.1(7)
C(6)-C(7)-C(8)	118.5(9)
C(6)-C(7)-C(13)	120.3(9)
C(8)-C(7)-C(13)	121.0(10)
C(6)-C(7)-Re(1)	71.9(6)
C(8)-C(7)-Re(1)	71.8(5)
C(13)-C(7)-Re(1)	132.5(7)
C(9)-C(8)-C(7)	121.3(9)
C(9)-C(8)-C(14)	119.4(8)
C(7)-C(8)-C(14)	119.3(9)
C(9)-C(8)-Re(1)	72.8(5)
C(7)-C(8)-Re(1)	72.8(5)
C(14)-C(8)-Re(1)	129.5(7)
C(8)-C(9)-C(4)	119.9(8)
C(8)-C(9)-C(15)	121.3(8)
C(4)-C(9)-C(15)	118.8(8)
C(8)-C(9)-Re(1)	72.1(5)
C(4)-C(9)-Re(1)	71.7(5)
C(15)-C(9)-Re(1)	130.6(6)
C(4)-C(10)-C(16)	111.4(9)
C(4)-C(10)-H(10A)	109.3
C(16)-C(10)-H(10A)	109.3
C(4)-C(10)-H(10B)	109.3
C(16)-C(10)-H(10B)	109.3
H(10A)-C(10)-H(10B)	108.0
C(17)-C(11)-C(5)	113.7(10)
C(17)-C(11)-H(11A)	108.8
C(5)-C(11)-H(11A)	108.8
C(17)-C(11)-H(11B)	108.8
C(5)-C(11)-H(11B)	108.8
H(11A)-C(11)-H(11B)	107.7
C(6)-C(12)-C(18)	109.8(9)

C(6)-C(12)-H(12A)	109.7
C(18)-C(12)-H(12A)	109.7
C(6)-C(12)-H(12B)	109.7
C(18)-C(12)-H(12B)	109.7
H(12A)-C(12)-H(12B)	108.2
C(7)-C(13)-C(19)	112.8(9)
C(7)-C(13)-H(13A)	109.0
C(19)-C(13)-H(13A)	109.0
C(7)-C(13)-H(13B)	109.0
C(19)-C(13)-H(13B)	109.0
H(13A)-C(13)-H(13B)	107.8
C(20)-C(14)-C(8)	112.4(9)
C(20)-C(14)-H(14A)	109.1
C(8)-C(14)-H(14A)	109.1
C(20)-C(14)-H(14B)	109.1
C(8)-C(14)-H(14B)	109.1
H(14A)-C(14)-H(14B)	107.9
C(21)-C(15)-C(9)	115.2(9)
C(21)-C(15)-H(15A)	108.5
C(9)-C(15)-H(15A)	108.5
C(21)-C(15)-H(15B)	108.5
C(9)-C(15)-H(15B)	108.5
H(15A)-C(15)-H(15B)	107.5
C(10)-C(16)-H(16A)	109.5
C(10)-C(16)-H(16B)	109.5
H(16A)-C(16)-H(16B)	109.5
C(10)-C(16)-H(16C)	109.5
H(16A)-C(16)-H(16C)	109.5
H(16B)-C(16)-H(16C)	109.5
C(11)-C(17)-H(17A)	109.5
C(11)-C(17)-H(17B)	109.5
H(17A)-C(17)-H(17B)	109.5
C(11)-C(17)-H(17C)	109.5
H(17A)-C(17)-H(17C)	109.5
H(17B)-C(17)-H(17C)	109.5
C(12)-C(18)-H(18A)	109.5
C(12)-C(18)-H(18B)	109.5
H(18A)-C(18)-H(18B)	109.5
C(12)-C(18)-H(18C)	109.5
H(18A)-C(18)-H(18C)	109.5
H(18B)-C(18)-H(18C)	109.5
C(13)-C(19)-H(19A)	109.5
C(13)-C(19)-H(19B)	109.5
H(19A)-C(19)-H(19B)	109.5

C(13)-C(19)-H(19C)	109.5
H(19A)-C(19)-H(19C)	109.5
H(19B)-C(19)-H(19C)	109.5
C(14)-C(20)-H(20A)	109.5
C(14)-C(20)-H(20B)	109.5
H(20A)-C(20)-H(20B)	109.5
C(14)-C(20)-H(20C)	109.5
H(20A)-C(20)-H(20C)	109.5
H(20B)-C(20)-H(20C)	109.5
C(15)-C(21)-H(21A)	109.5
C(15)-C(21)-H(21B)	109.5
H(21A)-C(21)-H(21B)	109.5
C(15)-C(21)-H(21C)	109.5
H(21A)-C(21)-H(21C)	109.5
H(21B)-C(21)-H(21C)	109.5
F(6)-P(1)-F(5)	90.5(16)
F(6)-P(1)-F(4)	81.9(16)
F(5)-P(1)-F(4)	172.4(17)
F(6)-P(1)-F(3)	89.1(11)
F(5)-P(1)-F(3)	92.1(10)
F(4)-P(1)-F(3)	88.5(10)
F(6)-P(1)-F(2)	174.3(17)
F(5)-P(1)-F(2)	95.1(16)
F(4)-P(1)-F(2)	92.5(17)
F(3)-P(1)-F(2)	91.5(11)
F(6)-P(1)-F(1)	91.1(8)
F(5)-P(1)-F(1)	90.1(7)
F(4)-P(1)-F(1)	89.4(7)
F(3)-P(1)-F(1)	177.9(10)
F(2)-P(1)-F(1)	88.1(8)

Symmetry transformations used to generate equivalent atoms:

Table 3-C2-4. Anisotropic displacement parameters (A^2 x 10^3) for [**2b**]PF_6. The anisotropic displacement factor exponent takes the form: -2 pi^2 [h^2 a*^2 U11 + ... + 2 h k a* b* U12]

	U11	U22	U33	U23	U13	U12
Re(1)	41(1)	25(1)	42(1)	0(1)	25(1)	-1(1)
O(1)	120(8)	57(5)	83(6)	-22(4)	77(6)	-19(5)
O(2)	58(5)	55(5)	152(11)	5(6)	30(6)	13(4)
O(3)	151(10)	61(5)	97(7)	-2(5)	100(8)	-20(6)
C(1)	70(6)	38(5)	61(6)	-8(4)	48(5)	-10(4)
C(2)	47(6)	45(6)	85(9)	-5(6)	20(6)	8(5)
C(3)	75(7)	42(5)	57(6)	-9(4)	49(6)	-13(5)
C(4)	45(4)	29(4)	43(4)	1(3)	28(4)	-2(3)
C(5)	41(4)	38(4)	52(5)	2(4)	31(4)	0(3)
C(6)	39(4)	36(4)	45(5)	-2(3)	22(4)	-1(3)
C(7)	44(4)	43(5)	45(5)	0(4)	23(4)	-5(4)
C(8)	46(4)	30(4)	48(5)	-3(3)	31(4)	0(3)
C(9)	37(4)	33(4)	44(4)	-1(3)	24(4)	1(3)
C(10)	57(5)	48(5)	45(5)	2(4)	31(5)	0(4)
C(11)	58(6)	65(7)	72(7)	6(5)	47(6)	0(5)
C(12)	39(5)	57(6)	62(6)	-2(5)	23(5)	-6(4)
C(13)	70(7)	55(6)	42(5)	-3(4)	30(5)	-3(5)
C(14)	64(6)	61(6)	63(6)	6(5)	49(6)	4(5)
C(15)	37(4)	46(5)	54(5)	5(4)	25(4)	3(4)
C(16)	80(8)	67(7)	57(6)	17(5)	43(6)	15(6)
C(17)	77(8)	76(8)	92(10)	10(7)	66(8)	14(7)
C(18)	56(7)	70(8)	91(10)	-4(7)	32(7)	-29(6)
C(19)	81(9)	85(9)	50(7)	9(6)	33(6)	9(7)
C(20)	94(10)	76(8)	90(10)	-1(7)	73(9)	14(7)
C(21)	42(5)	62(7)	104(10)	-2(7)	33(6)	-13(5)
P(1)	48(1)	16(1)	37(1)	-6(1)	34(1)	-8(1)
F(1)	166(12)	390(30)	430(30)	-110(20)	244(18)	-35(13)
F(2)	370(20)	580(30)	131(10)	179(14)	160(14)	300(30)
F(3)	131(9)	266(17)	237(16)	-42(13)	152(11)	-38(10)
F(4)	183(16)	162(12)	520(30)	-206(16)	207(18)	-81(10)
F(5)	213(16)	133(10)	357(19)	-139(12)	142(17)	-18(10)

F(6)	360(20)	348(19)	230(14)	203(14)	216(18)	150(20)

Table 3-C2-5. Hydrogen coordinates (x 10^4) and isotropic displacement parameters (A^2 x 10^3) for [2b]PF_6.

	x	y	z	U(eq)
H(10A)	915	1172	4159	61
H(10B)	1821	1174	4452	61
H(11A)	3071	1615	5641	73
H(11B)	3962	1631	7047	73
H(12A)	4617	1220	8852	72
H(12B)	4606	1239	9971	72
H(13A)	3036	1646	10217	72
H(13B)	3932	1673	10485	72
H(14A)	890	1196	7667	68
H(14B)	1786	1209	9072	68
H(15A)	284	1628	5880	60
H(15B)	304	1617	4773	60
H(16A)	869	2167	4127	104
H(16B)	1074	1983	3257	104
H(16C)	1838	2208	4634	104
H(17A)	4021	613	7049	110
H(17B)	4013	875	6002	110
H(17C)	3146	608	5627	110
H(18A)	4383	2254	8631	127
H(18B)	5296	2085	9939	127
H(18C)	4496	2249	9857	127
H(19A)	3169	601	10375	119
H(19B)	3934	904	11659	119
H(19C)	4108	663	10786	119
H(20A)	1807	2210	8962	116
H(20B)	962	1997	8722	116
H(20C)	892	2187	7578	116
H(21A)	292	575	4890	121
H(21B)	-596	885	4332	121
H(21C)	40	666	5738	121

3.7 References

(1) Geiger, W. E. *Organometallics* **2007,** *26*, 5738**.**

(2) Sun, S.; Sweigart, D. A. *Adv. Organomet. Chem.* **1996,** *40*, 171.

(3) (a) Pierce, D. T.; Geiger, W. E. *J. Am. Chem. Soc.* **1992,** *114*, 6063. (b) Bowyer, W. J.; Merkert, J. W.; Geiger, W. E.; Rheingold, A. L. *Organometallics* **1989,** *8*, 191. (c) Merkert, J.; Neilson, R. M.; Weaver, M. J.; Geiger, W. E. *J. Am. Chem. Soc.* **1989,** *111*, 7084.

(4) (a) Neilson, R. M.; Weaver, M. J. *Organometallics* **1989,** *8*, 1636. (b) Finke, R. G.; Voegell, R. H.; Laganis, E. D.; Boekelheide, V. *Organometallics* **1983,** *2*, 347. (c) Thompson, M. R.; Day, C. S.; Day, V. W.; Mink, R. I.; Muetterties, E. L. *J. Am. Chem.. Soc.* **1980,** *102*, 2979. (d) Rieke, R. D.; Henry, W. P.; Arney, J. S. *Inorg. Chem.* **1987,** *26*, 420. (e) Jonas, K.; Deffense, E.; Habermann, D. *Angew. Chem., Int. Ed. Engl.* **1983,** *22* 716. (f) Koelle, U.; Wang, M. H. *Organometallics* **1990,** *9*, 195. (g) Gusev, O. V.; Ievlev, M. A.; Peterleitner, M. G.; Peregudova, S. M.; Denisovich, L. I.; Petrovskii, P. V.; Ustynyuk, N. A. *J. Organomet. Chem.* **1997,** *534*, 57.

(5) (a) Thompson, R. L.; Lee, S.; Rheingold, A. L.; Cooper, N. J. *Organometallics* **1991,** *10*, 1657. (b) Thompson, R. L.; Geib, S. J.; Cooper, N. J. *J. Am. Chem. Soc.* **1991,** *113*, 8961. (c) Lee, S.; Geib, S. J.; Cooper, N. J. *J. Am. Chem. Soc.* **1995,** *117*, 9572. (d) Lee, S.; Lovelace, S. R.; Arford, D. J.; Geib, S. J.; Weber, S. G.; Cooper, N. J. *J. Am. Chem. Soc.* **1996,** *118*, 4190. (e) Veauthier, J. M.; Chow, A.; Fraenkel, G.; Geib, S. J.; Cooper, N. J. *Organometallics* **2000,** *19*, 661.

(f) Veauthier, J. M.; Chow, A.; Fraenkel, G.; Geib, S. J.; Cooper, N. J. *Organometallics* **2000**, *19*, 3942. (g) Shao, L.; Geib, S. J.; Cooper, N. J. *Organometallics* **2003**, *22*, 4361.

(6) Neto, C. C.; Baer, C. D.; Chung, Y. K.; Sweigart, D. A. *Chem. Commun*. **1993**, 816.

(7) Reingold, J. A.; Virkaitis, K. L.; Carpenter, G. B.; Sun, S.; Sweigart, D. A.; Czech, P. T.; Overly, K. R. *J. Am. Chem. Soc.* **2005**, *127*, 11146.

(8) Morken, A. M.; Eyman, D. P.; Wolff, M. A.; Schauer, S. J. *Organometallics* **1993**, *12*, 725.

(9) (a) Winkhaus, G.; Singer, H. *Z. Naturforsch* **1963**, *B18*, 418. (b) Jackson, J. D.; Villa, S. J.; Bacon, D. S.; Pike, R. D. *Organometallics* **1994**, *13*, 3972. (c) Sun, S.; Yeung, L. K.; Sweigart, D. A.; Lee, T.-Y.; Lee, S. S.; Chung, Y. K.; Switzer, S. R.; Pike, R. D. *Organometallics* **1995**, *14*, 2613. (d) Sweigart, D. A.; Alavosus, T. J.; Chung, Y. K.; Halpin, W. A.; Honig, E. D.; Williams, J. C. "Metal Carbonyl Cations with Cyclic π -Hydrocarbon Ligands," in *Organometallic Syntheses*, Volume 4, R. B. King and J. J. Eisch (eds.), Elsevier, 1988, pp 108-120. (e) Kane-Maguire, L. A. P.; Sweigart, D. A. *Inorg. Chem.* **1979**, *18*, 700.

(10) Stone, N. J.; Sweigart, D. A.; Bond, A. M. *Organometallics* **1986**, *5*, 2553.

(11) DigiSim is a registered trademark of Bioanalytical Systems, Inc., West Lafayette, IN.

(12) It has been reported[5d] that reduction of (benzene)$Mn(CO)_3^+$ in CH_3CN at -15°C is a 2-electron chemically reversible and electrochemically quasi-reversible process at a hanging mercury drop electrode. We have been unable to verify this result.

Chapter 4

Proton reduction catalyzed by aromatic manganese carbonyl complexes

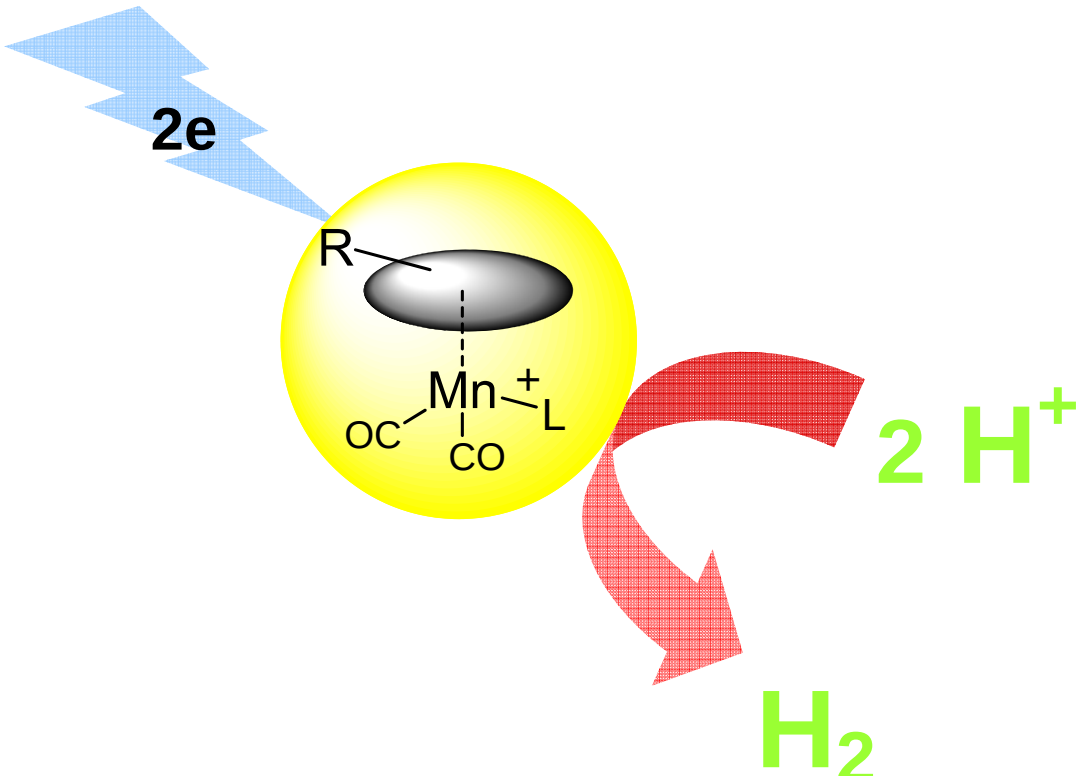

4.1 Introduction

Hydrogen is considered as a promising fuel alternative. Solar, wind power can be indirectly stored as hydrogen gas. The production of hydrogen from proton reduction is the simplest fuel generation reaction. Platinum is a great catalyst for this reaction and its reverse; however the high price and low abundance limits its usage in industry. Cheap metal catalyst is always the primary alternative. In the nature, the well known hydrogenase iron sulfur clusters, ferredoxin does a gread job on hydrogen production and oxidation. These biological catalysts can accept or discharge electrons. The core structure is iron atoms with the oxidation states switched between +2 and +3.[1] One proposed structure in which azadithiolate promotes the bonding and heterolytic cleavage of hydrogen is illustrated in figure 2.[2,3]

Transition metal hydride complexes are attracting a lot of attention due to their intimate relationship to the dihydrogen oxidation and production. Early transition metal complexes mimic of these enzymes have been investigated extensively by a number of chemists.

$$2H^+ + 2e^- \rightleftharpoons H_2$$

Figure 4-1. Reaction equilibrium of proton reduction and hydrogen oxidation.

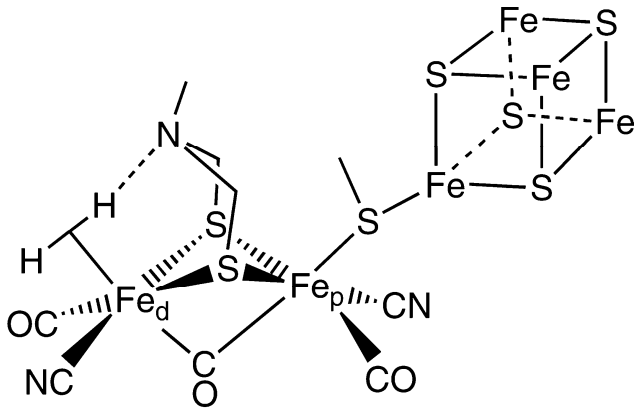

Figure 4-2. Proposed hydrogen bonding and hyterolytic cleavage via an Fe2S2 ferredoxin

Hydrogenase mimics, nickel $[Ni(P^{R}_{2}N^{R'}_{2})_{2}]^{2+}$ (R = Ph, Cy; R'= Ph, Bz) [3]and cobalt phosphine systems [4] designed by Dubois group were proved to catalyze proton reduction at relative low overpotential[5] based on the following mechanism shown in scheme 4-1 .

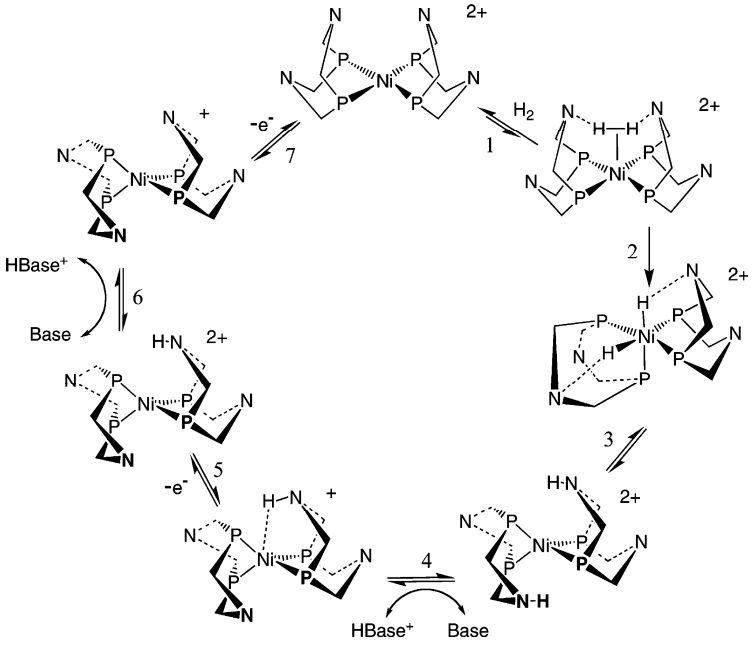

Scheme 4-1. The mechanism of hydrogen oxidation and production catalyzed by $[Ni(P^{R}_{2}N^{R'}_{2})_{2}]^{2+}$. Mechanism for proton reduction is shown anticlockwisely; Mechanism for hydrogen is shown clockwisely.

Dubois concluded that two positioned pendant bases are superior to complexes having two bases that are not positioned near the metal center. This pendant bases priorities were also supported by computational studies for the nickel complexes.[6] Also Peters group found similar result using their aryl-substituted tetraimine cobalt complexes [7,8] (a). Similar research was conducted on $[(\eta^5\text{-}C_5H_5)Fe(CO)_2]_2$ [9], which is a procatalyst of the proton reduction catalyzed by $(\eta^5\text{-}C_5H_5)Fe(CO)_2^-$ anion.

Organomanganese compound wasn't recognized as a good candidate for catalysis, the most wildly used manganese complex in the industry is methylcyclopentadienyl manganese tricarbonyl (MMT, which is used to increase the fuel's octane rating). Thus, there are very few examples of its catalytic properties. Ustynyuk [10]reported the unprecedented observation of a catalytic electrochemical proton reduction based on metallocumulene complexes: manganese diphenylallenylidene $(\eta^5\text{-}C_5H_5)$ $(CO)_2Mn=C=C=CPh_2$ is shown to catalyze the reduction of protons from HBF_4 to H_2 at -0.84 V (in acetonitrile) vs. Fc/Fc^+. The scheme is shown as following.

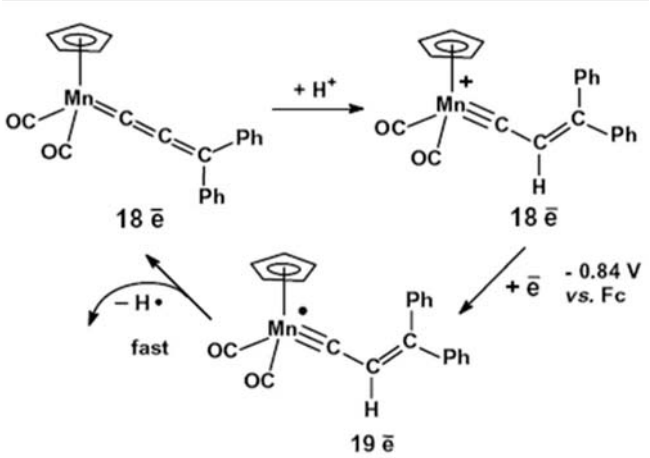

Scheme 4-2. Proposed mechanism of proton reduction catalyzed by (η^5-C_5H_5)$(CO)_2Mn{=}C{=}C{=}CPh_2$

Ustynyuk [10] proposed an uncommon mechanism for dihydrogen production, which is the formation of hydrogen radicals followed by their recombination into H_2 gas. He tentatively proposed that the driving force might be the reformation of the stable 18 electrons configuration. The real intermediate hydrogen species remains unclear.

No matter what metal was used, the general reaction pathway of dihydrogen production was suggested to go through two parallel routes[11]: (1) bimolecular reductive elimination of dihydrogen from two metal hydrides; (2) dihydrogen generation from protonation of metal hydride complex

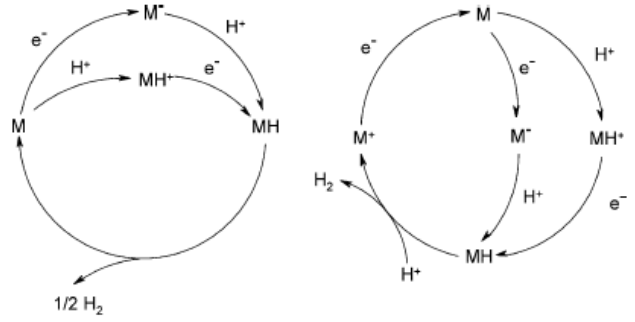

Scheme 4-3. Homolytic (left) and heterolytic (right) mechanism for proton reduction catalyzed by a organometallic compound.[12]

In chapter 3, the mechanistic insight of the reductive electrochemistry of $(\eta^6\text{-HMB})Mn(CO)_3^+$ was introduced[13] (scheme 4-4). There are several intermediates generated from the reduction of the starting material, one of them is $(\eta^6\text{-HMB})Mn(CO)_2^-$ anion which was chemically synthesized by Eyman[14,15] This dicarbonyl anion is 18 electrons, but very reactive because of the negative charge on the manganese. It is "extremely air and moisture sensity"[16] And it reacts with the starting material stoichiometrically to afford the known green color $[(\eta^6\text{-HMB})Mn(CO)_2]_2$ dimer[16], which perfectly matches the cyclic voltammetry of the $(\eta^6\text{-HMB})Mn(CO)_3^+$. Most importantly, compound **4** reacts with strong acid to liberate dihydrogen. Compound **1** is a great procatalyst for this proton reduction reaction; it can survive in strong acid. The molecular structure was modified, another Mn (I) analog, $(\eta^5\text{-}C_5H_5)Mn(CO)_2NO^+$ which can be reduced at -0.8V vs Fc/Fc^+ caught our attention. Not surprisingly, the potential of proton reduction shifted around 1V towards the positive side, which was a big improvement.

Herein, we want to report the first example of proton reduction catalyzed by

aromatic manganese carbonyl complex based on metal hydride mechanism. These aromatic manganese derivatives are promising catalysts for proton reduction. The proton catalytic reduction can be achieved at -1.7V vs Fc/Fc^+ when $[(\eta^6\text{-HMB})Mn(CO)_3]PF_6$ is used as procatalyst while -0.8V vs Fc/Fc^+ when $[(\eta^5\text{-}C_5H_5)Mn(CO)_2NO]BF_4$ is used. The efficiency of both is not high. We are working on optimizing the molecular structure to improve the efficiency of this class of catalyst.

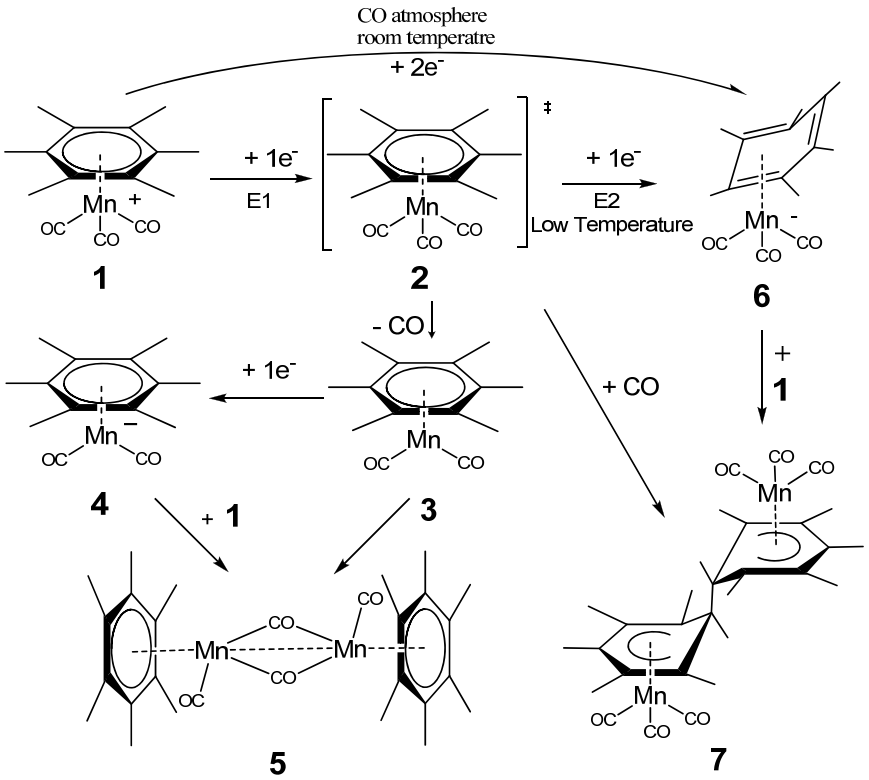

Scheme 4-4. Mechanism of $(\eta^6\text{-HMB})Mn(CO)_3^+$ reduction electrochemistry

Moreover, (η^5-hydroarene) manganese tricarbonyl complex, such as polyarene (η^5- hydronaphthalene) $Mn(CO)_3$ or monoarene (η^5- hydrobenzene) $Mn(CO)_3$, could react with proton gradually to liberate dihydrogen gas and re-generate (η^6-arene) $Mn(CO)_3^+$ cation. Especially, (η^6-naphthalene) $Mn(CO)_3^+$ can

be electrochemically reduced at -1V vs Fc/Fc^+ and form (η^5-hydronaphthalene) $Mn(CO)_3$ complex in the presence of proton. Since the protonation of (η^5-hydronaphthalene) $Mn(CO)_3$ is slow process (takes overnight), (eta6- polyarene) manganese tricarbonyl cations have potential usage to transfer and store electric energy to stable "metal-hydride" complex and releases the hydrogen gas when needed, and the resulting manganese complex can be reused.

4.2 Experiments

1. Synthesis

Solvents were purchased from commercial sources as HPLC grade. Methylene chloride and acetonitrile solvents were stored and opened under nitrogen.

[(η^6-hexamethylbenzene)$Mn(CO)_3$]BF_4. Acenaphthene manganese tricarbonyl tetrafluoroborate (0.760 g, 2.00 mmol) and hexamethylbenzene (0.504 g, 4.00 mmol) were combined with 17 ml methylene chloride (Fisher Scientific Co.) in a 20 ml pressure tube under nitrogen. The tube was sealed, wrapped in aluminum foil, and placed in a 75 ^oC oil bath for 2 hrs. The solvent was then removed and the yellow solid residue was washed with diethyl ether to afford the product in 75% yield (0.528 g). A crystal suitable for X-ray analysis was obtained by diethyl ether diffusion into a methylene chloride solution at room temperature. IR (CH_2Cl_2, cm^{-1}): 2060, 2000.

(η^6-hexamethylbenzene)$Mn(CO)_2I$, (η^6-hexamethylbenzene)$Mn(CO)_2H$ and [(η^6-hexamethylbenzene)$Mn(CO)_2$]Li. All above three compounds were synthesized via published literature method.[16] (η^6-hexamethylbenzene)$Mn(CO)_2I$ was

synthesized from [(η^6-hexamethylbenzene)$Mn(CO)_3$]$^+$ with 1 equivalent of Me_3NO and TBAI, and was purified by running through a silica gel column, dichloromethane was used as eluent. Then (η^6-hexamethylbenzene)$Mn(CO)_2I$ was treated with 1 equivalent of $TBABH_4$ in THF to affoard (η^6-hexamethylbenzene)$Mn(CO)_2H$, which was purified via washing with hexane. [(η^6-hexamethylbenzene)$Mn(CO)_2$]Li was synthesized from deprotonation of (η^6-hexamethylbenzene)$Mn(CO)_2H$ using t-butyl lithium. Since [(η^6-hexamethylbenzene)$Mn(CO)_2$]Li is very reactive, it was used as made.

[(η^5-methylcyclopentadienyl)$Mn(CO)_2NO$]BF_4.

(η^5-Methylcyclopentadienyl)$Mn(CO)_3$ was purchased from Aldrich and used as it was. 2ml (2.760g, 12.67mmol) of (η^5-Methylcyclopentadienyl)$Mn(CO)_3$ and nitrosyl tetrafluoroborate $NOBF_4$ (1.776g, 15.20mmol) were combined with 15ml acetone in 50ml round bottom flask. The flask was cooled in the ice bath. There was a lot of gas bubbling inside the flask while acetone was added. The color of the solution changed from light yellow to dark brown. After 10mins, IR indicated that all starting material was gone and the reaction completed. Then acetone was removed by blowing nitrogen into the solution. Diethyl ether was added to wash the solid several times. The product was recrystallized by diffusing ether into its acetone solution, and the yield is 90% (3.450g, 11.40mmol). IR (CH_2Cl_2, cm^{-1}): 2118, 2076 for CO; 1840 for NO.

[(η^6-naphthalene)$Mn(CO)_3$]BF_4. Manganese pentacarbonyl bromide (1.280g, 4.65mmol) and silver tetrafluoroborate (1.000g, 5.14mmol) were combined

with 50ml dichloromethane in a 100ml round bottom flask under nitrogen. The mixture was stirred and heated to reflux for 2 hours. 2equivlent of naphthalene (1.317g, 10.28mmol) was added to the solution and heated to reflux for 8 hours. The product was recrystallized by diffusing ether into its dichloromethane solution, and the yield is 70% (1.153g, 3.26mmol) IR in dichloromethane 2077, 2019 cm^{-1}

(η^5-hydronaphthalene)Mn(CO)$_3$ [(η^6-naphthalene)Mn(CO)$_3$]BF_4 (0.354g, 1mmol) and tetrabutylammonium borohydride (0.283g, 1.1mmol) were combined with 20ml dichloromethane in a 50ml round bottom flask in ice bath. The reaction mixture was stirred for 30mins in ice bath and then 30mins at room temperature. The product was purified by running through the silica gel column using dichloromethane as eluent. IR in dichloromethane 2009, 1929 cm^{-1}. IR in hexane 2017, 1943 and 1931cm^{-1}

2. Protonation of (η^5-hydronaphthalene)Mn(CO)$_3$

(η^5-hydronaphthalene)- Mn(CO)$_3$ was dissolved in diethyl ether, excess $HBF_4 \cdot Et_2O$ was added. The solution was stirred and after 5mins, yellow solid precipitated out, which turned out to be [(η^6-naphthalene)Mn(CO)$_3$]BF_4.

3. Electrochemistry

Electrochemical instrumentation and the source and treatment of solvents and supporting electrolytes have been reported earlier, in chapter 3. All potentials are reported vs the potential of the silver chloride reference electrode. The voltammetric experiments were conducted at room temperature, 298 K.

4. Further Experiments

This research project is still undergoing, only preliminary data is demonstrated in chapter 4. There are further experiments to be done. (1) Bulk electrolysis and in-situ IR will be incorporated to a dichloromethane solution of $[(\eta^6\text{-HMB})Mn(CO)_3]BF_4$ and excess $HBF_4 \cdot Et_2O$ to detect proposed reduction intermediate $(\eta^6\text{-HMB})Mn(CO)_2H$ and $(\eta^6\text{-HMB})Mn(CO)_2Cl$ or $[(\eta^6\text{-HMB})Mn(CO)_2Et_2O]^+$. (2) Bulk electrolysis and in-situ IR will be incorporated to a dichloromethane solution of $[(\eta^5\text{-cyclopentadienyl})Mn(CO)_2NO]BF_4$ to investigate its electrochemical reduction mechanism, which was proposed to mimic the one of $[(\eta^6\text{-HMB})Mn(CO)_3]BF_4$. (3) After understanding $[(\eta^5\text{-cyclopenta-dienyl})Mn(CO)_2NO]BF_4$, the reductive electrochemistry of $[(\eta^5\text{-cyclopentadienyl})Mn(CO)_2NO]BF_4$, bulk electrolysis will be applied to CH_2Cl_2 solution of $[(\eta^5\text{-cyclopentadienyl})Mn(CO)_2NO]BF_4$ and excess $HBF_4 \cdot Et_2O$ as proton source. GC will be used to confirm the existence of dihydrogen. (4) Further optimization was proposed in the result and discussion section.

4.3 Result and discussion

1. Aromatic manganese dicarbonyl

Compound **4**, the reduction intermediate of procatalyst **1**, can be easily oxidized and protonated[16] when proton source presents, to afford a neutral manganese hydride complex $(\eta^6\text{-HMB})Mn(CO)_2H$, which can be further protonated to liberate dihydrogen and $[(\eta^6\text{-HMB})Mn(CO)_2L^+]$ (L is solvent). $[(\eta^6\text{-HMB})Mn(CO)_2^+]$ is a

16-electron species, which was never isolated by itself. [(η^6-HMB)Mn(CO)$_2^+$] is readily accessible by numbers of non or less coordination ligand, such as ether. It can even grab a chloride from dichloromethane to form a neutral (η^6-HMB)Mn(CO)$_2$Cl.

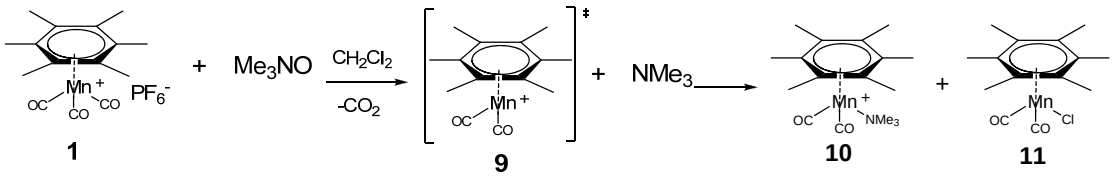

Figure 4-3. Synthesis of (η^6-hexamethylbenzene) manganese dicarbonyl complex using trimethylamine N-oxide

Figure 4-3 shows typical for synthesizing η^6-arene manganese dicarbonyl complex using trimethylamine N-oxide as an oxidant. When dichloromethane is the solvent, a mixture of compound **10** and **11** is the only product. While in the presence of halide (figure 4), compound **12** is the only product instead of **10** and **11** (figure 3). Eyman reported the very first method of synthesizing (η^6-hexamethylbenzene) manganese dicarbonyl hydride (compound **13**) chemically by using tetrabutylammonium borohydride as a hydride source.

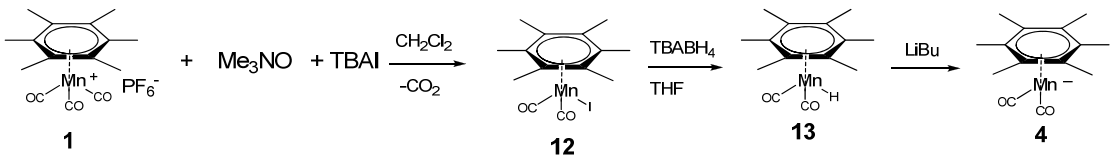

Figure 4-4. Synthesis of (η^6-hexamethylbenzene) manganese dicarbonyl anion.

Further deprotonation of **13** with tetrabutyllithium results in **4** (figure 4-4), which is a very strong nucleophile. It reacts with **1** stoichiometrically to form a

heterodinuclear complex with core structure of Mn-Mn metal-metal bond (compound **5**),[16] with the characteristic bridging CO ligand. Eyman[16] reported hydrogen formation and compound **14** from reaction between **13** and $HBF_4 \cdot Et_2O$. There isn't enough information about the reactivity of **4**, however it is reasonable to believe that **4** would be oxidized and protonated easily by $HBF_4 \cdot Et_2O$ (or even weaker acid) to form **13** or **14** (if excess $HBF_4 \cdot Et_2O$ presents) (figure 4-5).

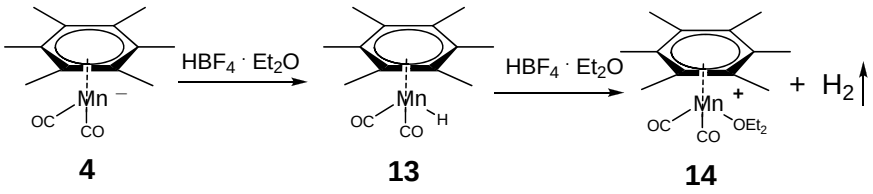

Figure 4-5. Protonation of (η^6-hexamethylbenzene) manganese dicarbonyl anion.

2. Hydrogen formation

Through the above information, we conclude that the reduction product (from compound **1)** compound **4** would react with proton and liberate dihydrogen to affoard a very reactive 16-electron species compound **9**, which will react with solvent or any coordination ligand to sustain its strong desire to become stable 18-electron structure, such as compound **10, 11, 14** and **15 (**if using trifluoroacetic acid as proton source) As discussed in previous chapter (chapter 3), the reduction electrochemistry of compound **10, 14** (in the case of its analog $[(\eta^6\text{-HMB})Mn(CO)_2THF]^+$ cation) is sharing the same reaction pathway with compound **1**[17]. However it might not be the case that when under continuous reduction potential with proton present, unreacted compound **9** might partially be reduced back to compound **4** (the reduction potential

of reducing compound **9** to **4** must be much more positive than the one of compound **1**), and then oxidized and protonated by proton and liberate the dihydrogen gas and compound **9**, ····· This is a full cycle of catalyzing proton reduction via (η^6-hexamethylbenzene) manganese dicarbonyl anion, and the initial starting material **1** is inert to strong acidic environment.

3. Ion analog

The aromatic ion carbonyl complex $(\eta^5\text{-}C_5H_5)Fe(CO)_2H$ shares a lot of similarities with aromatic manganese complexes in my study.[9] According to the calculation and scale established for transition metal hydride by Norton and co-workers[18], the pKa of the $(\eta^6\text{-}C_6H_6)Mn(CO)_2H$ is 26.8, and the pKa of methylated complex $(\eta^6\text{-}C_6Me_6)Mn(CO)_2H$ is in the range between 33 and 35. This makes compound **13** the least acidic and most hydridic compound ever characterized. In comparision, the pKa of $(\eta^5\text{-}C_5H_5)Fe(CO)_2H$ is reported to be 19.4, which is much lower than the Manganese hydride analog. This explains why $(\eta^6\text{-}C_6Me_6)Mn(CO)_2H$ can react with acid easily while $(\eta^5\text{-}C_5H_5)Fe(CO)_2H$ is stable upon acid contacts.

The catalytic cycle is shown below:

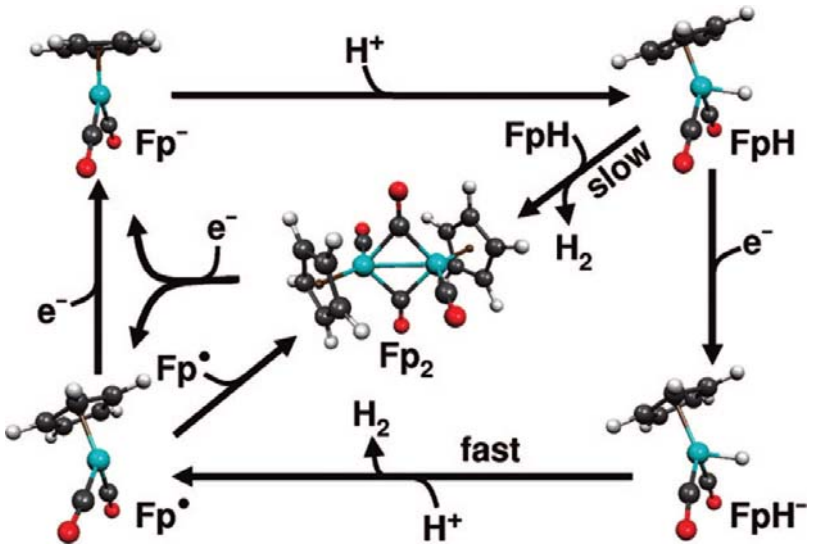

Scheme 4-5. $[(\eta^5\text{-}C_5H_5)Fe(CO)_2]_2$ (Fp_2) reduction followed by catalytic reduction of proton to hydrogen by $(\eta^5\text{-}C_5H_5)Fe(CO)_2^-$ (Fp^-)

In scheme 4-5, $(\eta^5\text{-}C_5H_5)Fe(CO)_2^-$ (Fp^-) anion is formed upon the electrochemical reduction of $[(\eta^5\text{-}C_5H_5)Fe(CO)_2]_2$. Fp^- is then protonated by various kinds of acid to afford a metal hydride complex, FpH, which undergoes further reduction at more negative potentials to afford FpH^-. To finish a full catalytic cycle, FpH^- will be protonated and liberate hydrogen gas and Fp, and then Fp will be reduced by one electron to yield Fp^-. Protonation of Fp^- is found to be the rate determined step. The potential for catalytic reduction of 4-tertbutylphenol is -2.6V vs Fc/Fc^+, with 0.8V overpotential.

4. Electrochemical formation and protonation of Arene-Mn-hydride complex

The direct energetically downhill step of metal hydride protonation to produce molecular hydrogen may be common for sufficiently electron rich metal hydrides and/or sufficiently strong acids among many of the hydrogenase mimics reported thus far. Aromatic ion carbonyls system gives us a good example of how our

aromatic manganese catalyst works. Thus, we proposed a reaction mechanism for the proton reduction catalysis.

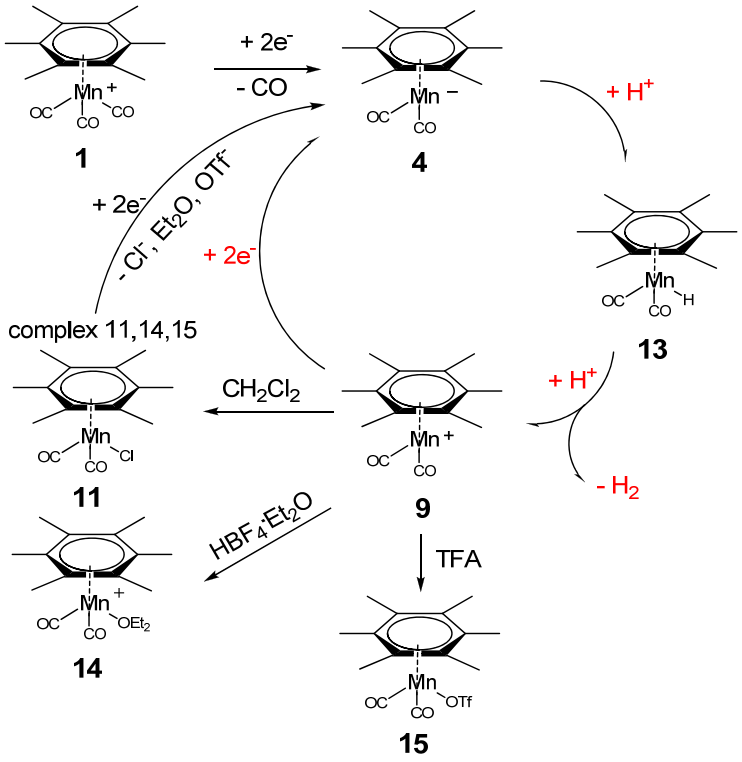

Scheme 4-6. Proposed mechanism of proton reduction catalyzed by (η^6-hexamethylbenzene) manganese dicarbonyl anion.

The cyclic voltammetry (figure 4-7) also support our proposed mechanism. In dichloromethane, when there was acid present (for example, $HBF_4 \cdot Et_2O$), as the acid concentration increasing, the cyclic voltammetry of $[(\eta^6\text{-HMB})Mn(CO)_3]^+$ changed: The reduction peak current kept increasing, the oxidation peak current corresponding to the $[(\eta^6\text{-HMB})Mn(CO)_2]_2$ dimer kept decreasing until fully vanished. We propose that the increase of reduction peak current is the result of two facts: (1) With the presence of acid, the reduction of compound 1 consumes 2-electron instead of

1-electron. (2) Plausible proton catalytic reduction. When the concentration of acid is strong enough, most compound **4** would react with proton instead of compound **1** and liberate dihydrogen. This explains the diminishing of oxidation peak current of compound **5**.

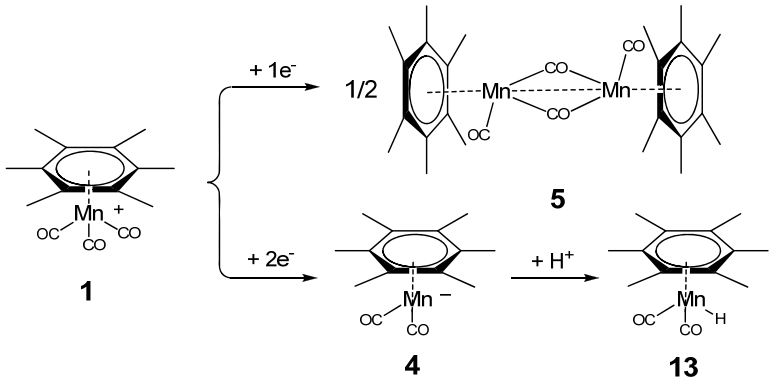

Figure 4-6. Reduction electrochemistry of compound 1 changes from 1-electron without acid to 2-electron with the presence of acid.

With the completely suppression of dimer formation, we expect to see peak current change from 1-electron to 2-electron. The reaction pathway is illustrated in figure 4-6. Note that for a control experiment, when only altering the number of electron transferred from $1e^-$ to $2e^-$, the peak current should increase by 2.85 times.

$$i_p = (2.69\times10^5)n^{3/2}AD^{1/2}v^{1/2}C^*$$

Formula 4-1. The peak current in a cyclic voltammogram containing only one species is described by above fomula at 25 °C where ip is the peak current, n is the number of electrons transferred, A is the electrode area, D is the diffusion coefficient of the species, v is the scan rate and C* is the bulk concentration of the species. n is the number of electrons transferred.

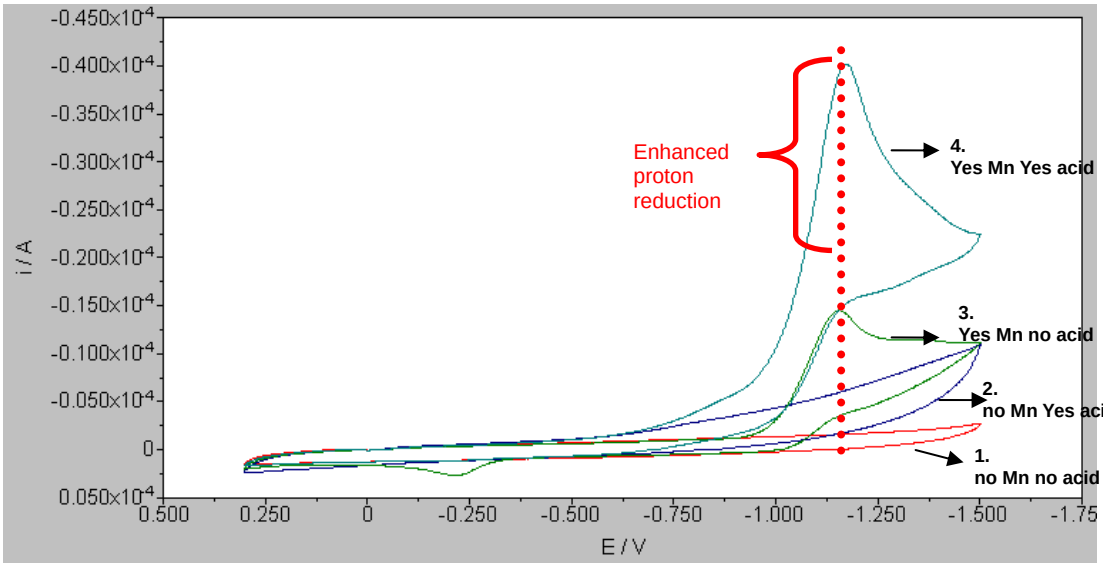

Figure 4-7. CVs of $[(\eta^6\text{-HMB})Mn(CO)_3]PF_6$ with and without the presence of HBF_4 in CH_2Cl_2. Cyclic voltammetry (1). In red, blank solution of dichloromethane with only 0.1M $TBAPF_6$ present. (2). In blue, 50mM HBF_4 with 0.1M $TBAPF_6$ in dichloromethane solution. (3). In green, 1mM $[(\eta^6\text{-HMB})Mn(CO)_3]PF_6$ in the presence of no acid. (4). In light blue, 1mM $[(\eta^6\text{-HMB})Mn(CO)_3]PF_6$ in the presence of 6.6mM HBF_4. Glassy carbon electrode was used and scan rate was 50mV/s, 0.1M $TBAPF_6$ was used as electrolyte. HBF_4 acid is in the form of $HBF_4 \cdot O(CH_2CH_3)_2$. Nitrogen was used to bubble through the solution before experiment and bubble above the solution during the experiment.

From the above CVs in figure 4-7, we did see a big current jump when there is enough acid to suppress the formation of dimer. A reasonable explanation is that, in the CV time scale, the increase of peak current mostly comes from the change of electrons transferred ($1e^-$ to $2e^-$), and $(\eta^6\text{-HMB})Mn(CO)_2H$ would be the primary product. Of course, we can not exclude the formation of dihydrogen from protonation

of (η^6-HMB)$Mn(CO)_2H$, and as a result, partially contributing to the peak current increase. From the extent of current jump, we would point out that, the contribution of peak current increase from proton catalytic reduction is limited. Furthermore, the above CVs also imply that the protonation of (η^6-HMB)$Mn(CO)_2H$ is rate determined step, proton catalytic reduction may not complete a cycle in the CV time scale.

Even though small portion of proton already has been reduced without the presence of our manganese procatalyst (η^6-HMB)$Mn(CO)_3^+$, the generation (η^6-HMB)$Mn(CO)_2H$ would certainly speed up the process of proton reduction.

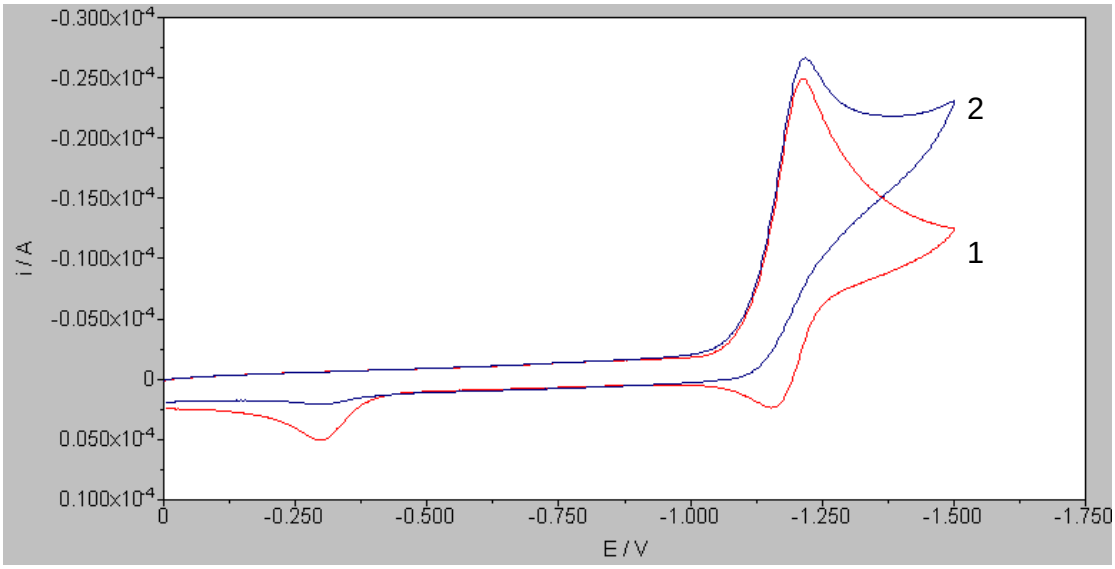

Figure 4-8. CVs of [(η^6-HMB)$Mn(CO)_3$]PF_6 with and without the presence of HBF_4 in acetonitrile. Cyclic voltammetry (1). In red, 1mM [(η^6-HMB)$Mn(CO)_3$]PF_6 in the presence of no acid. (2). In blue, 6.6mM HBF_4 with 0.1M $TBAPF_6$ in dichloromethane solution. Glassy carbon electrode was used and scan rate was 50mV/s, 0.1M $TBAPF_6$ was used as electrolyte. HBF_4 acid is in the form of $HBF_4 \cdot O(CH_2CH_3)_2$. Nitrogen was used to bubble through the solution before

experiment and bubble above the solution during the experiment.

5. Solvent effect

Different solvent was used. Even the formation of dimer was completely suppressed, there was no peak current increase for reduction of $[(\eta^6\text{-HMB})Mn(CO)_3]^+$ in acetonitrile with the same amount of acid present, of which the reaction mechanism is illustrated as following. CV in red (Figure 4-8(1)) implies partially reversibility, which we think is because of surface and solvent effect. Thus, the peak current is a mix of $2e^-$ (ring slippage $(\eta^4\text{-HMB})Mn(CO)_3^-$ as product, reversibility was limited because of fast ring coupled reaction with $(\eta^6\text{-HMB})Mn(CO)_3^+$) and $1e^-$ reduction, it is possible that $2e^-$ reduction might contribute a lot in figure 8 (1). When $1e^-$ reduction is completely suppressed by acid, $2e^-$ reduction primarily contributes to the reduction current but with different reduction product $(\eta^6\text{-HMB})Mn(CO)_2H$. That might be the reason we didn't see big peak current jump. Dichloromethane could be the only solvent suitable for this catalytic reaction. Strong acid such as trifluoroacetic acid could be used as acid source. Weak acid such as benzoic acid didn't support the catalytic reduction.

The efficiency of our catalytic reduction is low because of the slow protonation step. Our catalytic reduction potential is around -1.7V vs Fc/Fc^+, which is quite low compared to -0.9V of the same cobalt catalyst $Co(P^tBu_2NPh_2)(CH_3CN)_3](BF_4)_2$ from Dubios group[2-4].

6. Cp-Mn-NO system

The reduction potential of proton is equal or more negative than the reduction potential of the procatalyst. Since manganese (-1) anion is the initiator of proton

reduction catalytic cycle, we want to confine the structure of this class of catalyst to find a specific procatalyst which could be reduced at a more positive potential, thus getting the proton to be reduced at more positive potential. The nitrosyl substituted analog of cyclopentendienyl manganese tricarbonyl $[(\eta^5\text{-MeCp})Mn(CO)_2NO]BF_4$ caught our attention. $(\eta^5\text{-methylcyclopentadienyl})Mn(CO)_3$ can be electrochemically oxidized by one electron to generate $[(\eta^5\text{-methylcyclopentadienyl})Mn(CO)_3]^+$ cation, and reversibly reduced back. We can use the IR bands of CO ligand as a good reference to demonstrate the electron density of the manganese center. Usually, higher wavenumbers correspond to lower electron density, and less positive reduction potential.

By introducing NO into the $(\eta^5\text{-methylcyclopentadienyl})Mn(CO)_3$ complex, first of all, it will change the oxidation state of the Mn center from 0 to +1; secondly, the electrochemical respondence will be reversed (the electrochemistry of Mn will be swiched from oxidation active to reduction active.).

The electrochemistry of $(\eta^5\text{-MeCp})Mn(CO)_3$ and its analoge with alkyl substitution on the Cp ring was studied. It is chemically reversible oxidation at around +0.6V vs Ag/AgCl. Even though the interpretation of $[(MeCp)Mn(CO)_2NO]^+$ wasn't well established, it was believed that, its electrochemical pathway should mimic the one of $[(\eta^6\text{-HMB})Mn(CO)_3]^+$. Not surprisingly, from the reduction of $[(\eta^5\text{-MeCp})Mn(CO)_2NO]^+$, we did observe similar reductive electrochemistry at much more positive potential when strong acid was present.

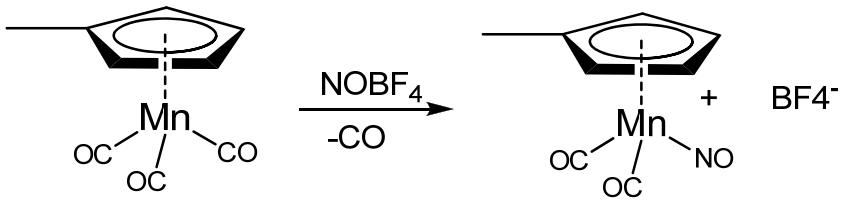

Figure 4-9. Synthesis method of [(η^5-methylcyclopentadienyl)Mn(CO)$_2$NO]BF$_4$

NO can be chemically introduced into the molecule by reacting (η^5-methylcyclopentadienyl)Mn(CO)$_3$ with NOBF$_4$ (Figure 4-9). One carbonyl will be replaced by NO, and Mn (0) will be oxidized to Mn (I), which will change its electrochemistry from oxidation active to reduction active.

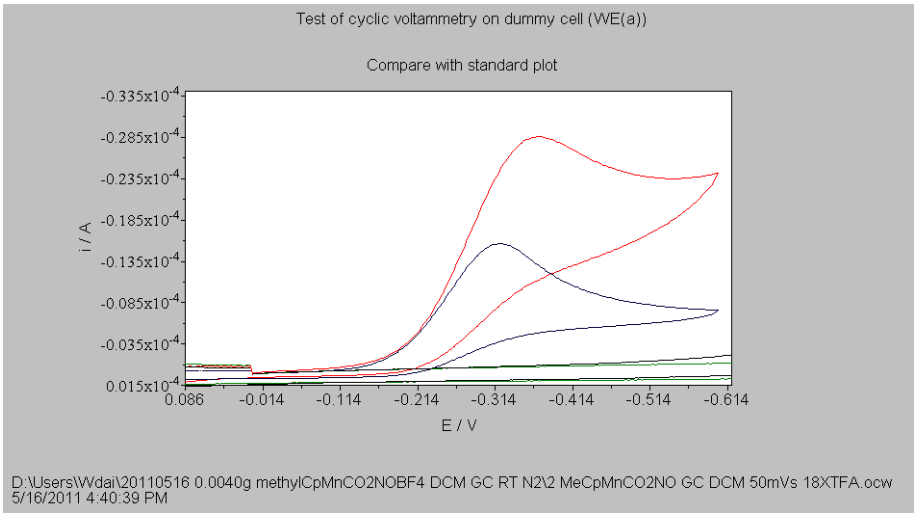

Figure 4-10. Cyclic voltammetry of 1.29mM [(η^5-methylcyclopentadienyl)Mn(CO)$_2$-NO]BF$_4$ with (blue line) and without the presence (red line) of 100mM TFA. Glassy carbon electrode is used and scan rate was 50mV/s, 0.1M TBAPF$_6$ was used as electrolyte. 0.1M trifluoroacetic acid was used as acid source. Nitrogen was used to bubble through the solution before experiment and bubble above the solution during

the experiment.

Based on the similarity between [(η^5-methylcyclopentadienyl)$Mn(CO)_2NO$] BF_4 and [(η^5-hexamethylbenzene)$Mn(CO)_3$]BF_4, the proton reduction mechanism was proposed as following.

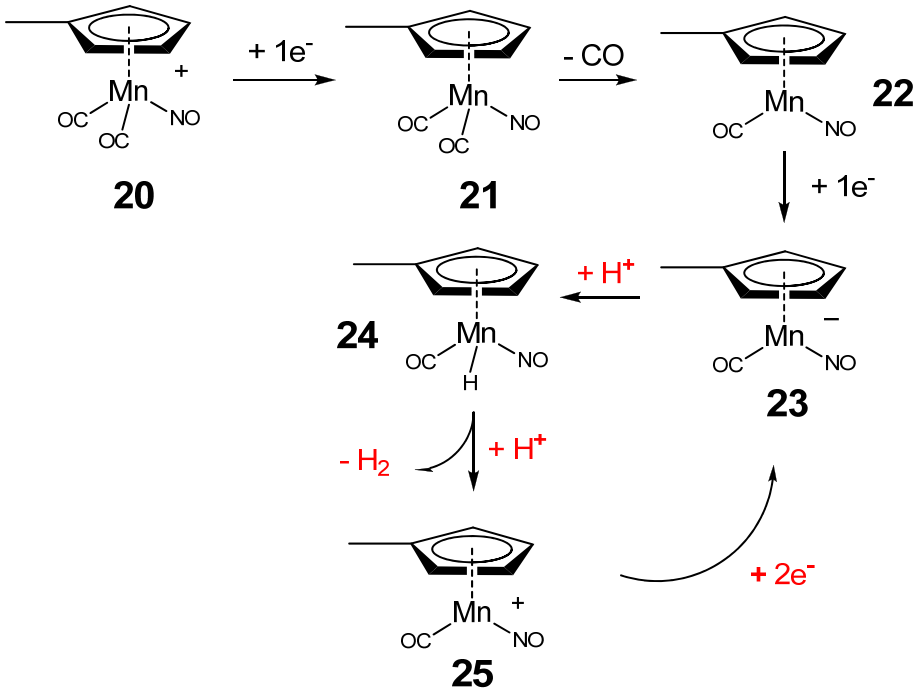

Scheme 4-7. Proposed mechanism of proton reduction catalyzed by [(η^5-methylcyclopentadienyl)$Mn(CO)_2NO$]BF_4

The protonation of compound **13** and **24** is the rate determined step, which is the primary limitation of the low efficiency of aromatic manganese catalyst. Optimization was considered.

7. Optimazation

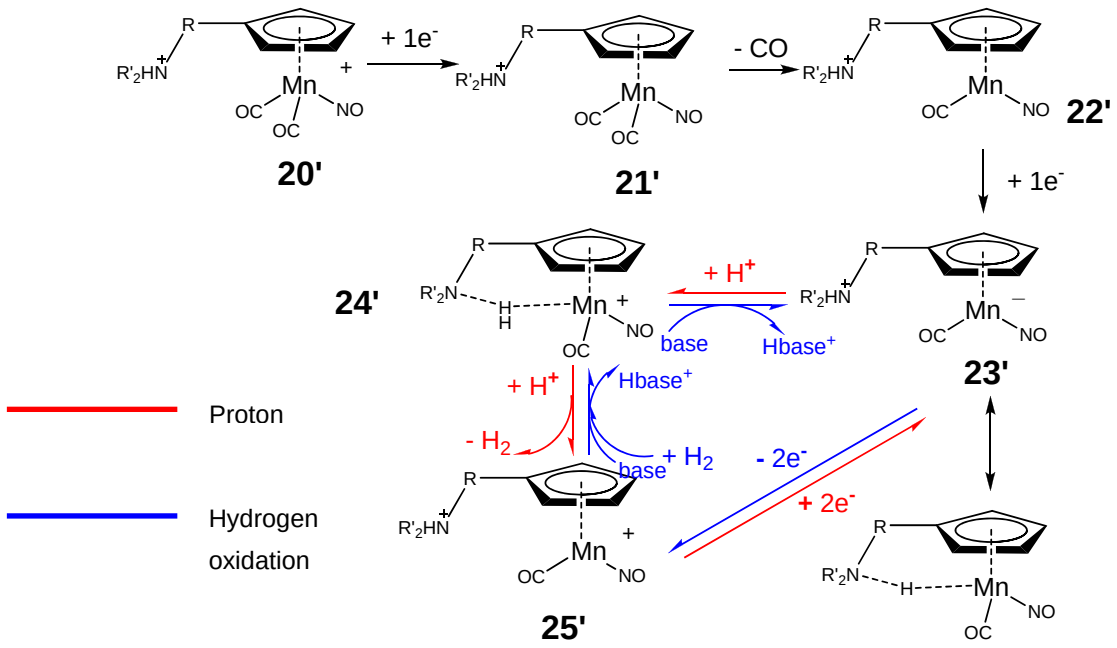

Scheme 4-8. Optimization of $(\eta^5\text{-Cp})Mn(CO)_2NO^+$ procatalyst

The efficiency of our Cp-Mn catalyst is expected to be enhanced by incorporating an amine group onto Cp ring (scheme 4-8). It is preferable that the amine group is sigma bonded through the linker R group to the Cp ligand, thus the amine group could move freely. The existence of the amine group will facilitate the uptake of proton from weaker acid and accelerate the rate determined step.

8. Electronic energy stored as chemical bonding mediated by polyarene-$Mn(CO)_3^+$

In the case of $(\eta^6$-polyarene) manganese tricarbonyl cations, they undergo chemically reversible 2-electron reduction and generate ring slippage $(\eta^4$-polyarene) manganese tricarbonyl anions, which were reported to react with proton and afford $(\eta^5$-cyclohexadienyl) manganese tricarbonyl.[19,20] The reaction is shown in scheme 8. Low temperature NMR was used to capture the transient formation of the ring

slippage metal hydride complex **28'**.

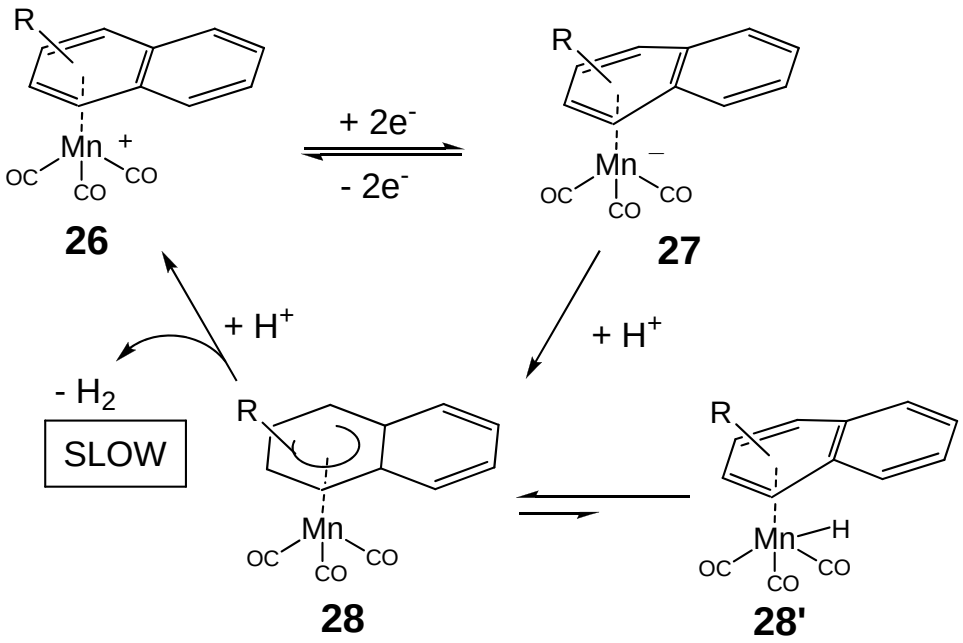

Scheme 4-9. Proposed mechanism of slow hydrogen release, "hydride" generation and storage mediated by (η^6- polyarene) manganese tricarbonyl cation.

Specifically, (η^6- naphthalene) manganese tricarbonyl (R = H), of which the reduction potential is -1V vs Fc/Fc^+, thus, the hydride complex (η^5- hydronaphthalene) manganese tricarbonyl could be produced at -1V with acid presence. The cyclic voltammetry of (η^6- naphthalene) manganese tricarbonyl cation is shown below: it shows nicely reversible 2-electron reduction in dichloromethane at room temperature, however, the reversibility decreases when the concentration of acid increases. The reduction peak potential won't increase much even the reversibility vanished completely. This is because of fast protonation of reduction product **27** and slow protonation of **28**. The reduction product of **26** in the presence of acid is **28** in

the CV time scale (0.1-a few seconds).

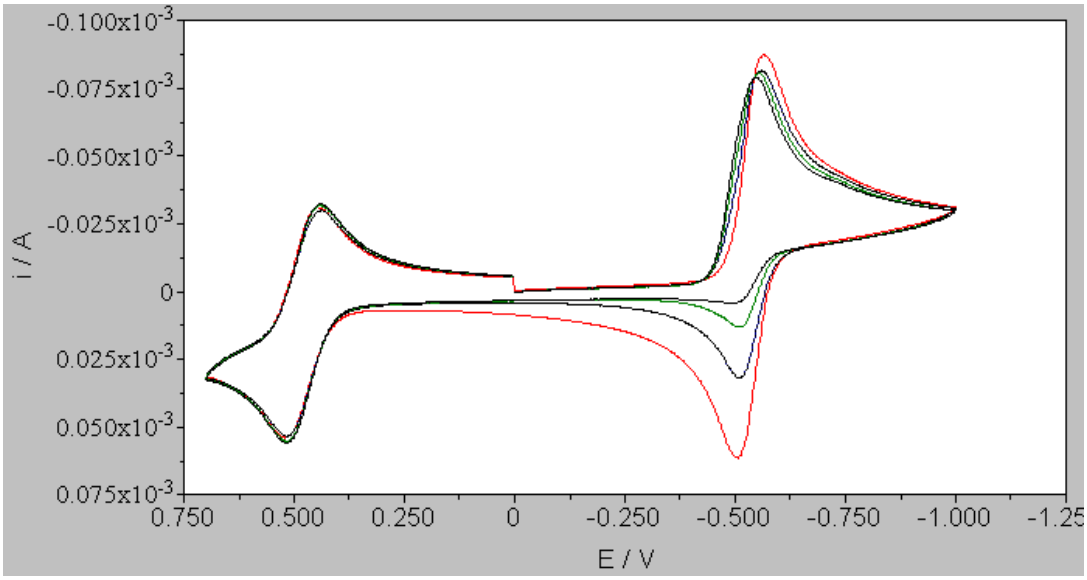

Figure 4-11. CVs of 1mM [(η^6- naphthalene)$Mn(CO)_3$]PF_6 and 1mM ferrocene with the presence of $HBF_4 \cdot Et_2O$ in different concentrations: (a). Red line, no HBF_4 (b). Blue line, 1.1mM HBF_4 (c). Green line, 2.2mM HBF_4 (d). Black line, 3.3mM HBF_4. No further change was observed when up to 6.6 mM HBF_4 was treated.

Chemically synthesized **28** (R = H) was treated with $HBF_4 \cdot Et_2O$ in diethyl ether. After a few minutes, precipitate formed and was characterized as compound **26.**

9. Hydrogen slow release mediated via (η^5-H monoarene)-$Mn(CO)_3$

The same slow hydrogen release reaction was also discovered to be mediated via monoarene manganese tricarbonyl complex. For example, (η^5-H-C_6H_6)$Mn(CO)_3$ was synthesized and treated with strong acid TFA overnight. The hapticity was changed from eta5 back to eta6, the product was confirmed to be (η^6-C_6H_6)$Mn(CO)_3^+$. Similar ring slippage form of (η^4-C_6H_6)$MnH(CO)_3$ was proposed by Brookhart. [21] Based on their proposed mechanism and our experimental data, (η^4-C_6H_6)$MnH(CO)_3$

does exsit as an high energy transient state, thus the protonation is possible but slow and is the rate determined step. In the above case, it took 8 hours for the protonation to be finished.

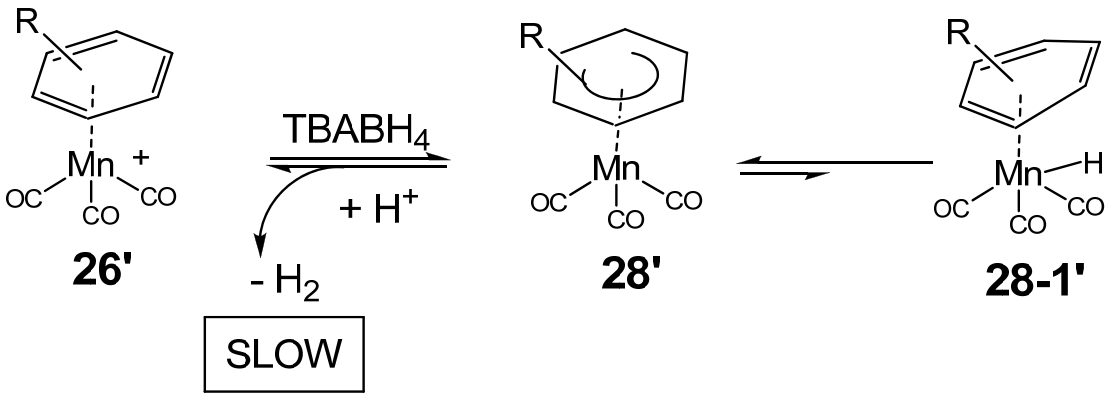

Scheme 4-10. Proposed mechanism of slow hydrogen release mediated via eta6 monoarene manganese tricarbonyl cation. (R = H)

4.4 Conclusions

The reduction potential of proton is equal or more negative than the reduction potential of compound **1** (-1.7 vs Fc/Fc^+). $HBF_4 \cdot Et_2O$ is the proton source, the overpotential of this catalytic proton reduction is around 1.4V, and the efficiency is not high. Nevertheless, aromatic manganese (I) carbonyl complex could be a new class of catalyst for proton reduction. Based on the prototype of compound **1**, optimization of the molecular structure might lead us to more efficient catalyst with smaller overpotential. Different from $(\eta^5\text{-}C_5H_5)Mn(CO)_3$ (which can only be oxidized), $(\eta^5\text{-}C_5H_5)Mn(CO)_2NO^+$ can be reduced at -0.8 V vs Fc/Fc^+. Not surprisingly, in the presence of $HBF_4 \cdot Et_2O$ or trifluoroacetic acid, catalytic property of proton reduction was observed at -0.8V vs Fc/Fc^+ with around 0.5V overpotential.

However, the efficiency was not improved.

The electrochemistry of $(\eta^5\text{-}C_5H_5)Mn(CO)_2NO^+$ has never been studied. We propose that it shares the similar reduction mechanism as of $[(\eta^6\text{-}C_6Me_6)Mn(CO)_3^+]$, thus, similar pathway of catalytic proton reduction. Acetonitrile can not be applied to the above study since its strong nucleophilic property.

The efficiency of our Cp-Mn catalyst is expected to be enhanced by incorporating an amine group onto Cp ring. It is preferable that the amine group is sigma bonded through the linker R group to the Cp ligand. The existence of the amine group will facilitate the uptake of proton from weaker acid and accelerate the rate determined step.

Interestingly, in the case of $(\eta^6$-naphthalene) $Mn(CO)_3^+$, the cyclic voltammetry lost reversibility when there was proton present, which we proposed is because of the formation of η^5-hydronaphthalene complex $(\eta^5\text{-}C_{10}H_9)Mn(CO)_3$ from the reaction between the reduced $(\eta^4$-naphthalene) $Mn(CO)_3^-$ and H^+. Thereafter, hydrogen gas can be liberated gradually when $(\eta^5\text{-}C_{10}H_9)Mn(CO)_3$ is treated with excess acid in dichloromethane.

4.5 References

1. Fontecilla-Camps, J. C.;Volbeda, A.; Cavazza, C.; Nicolet, Y. *Chem. Rev.* **2007**, 107
2. Aaron D. Wilson,† Rachel H. Newell,† Michael J. McNevin,† James T. Muckerman, M. Rakowski DuBois,*,† and Daniel L. DuBois*, *J. Am. Chem. Soc.* **2006**, 128, 358-366
3. M. Rakowski Dubois and Daniel L. Dubois* *Accounts of Chemical Research* **2009** Vol. 42, No. 12. 1974–1982
4. Eric S. Wiedner, Jenny Y. Yang, William G. Dougherty, W. Scott Kassel, R. Morris Bullock, M. Rakowski DuBois, and Daniel L. DuBois*, *Organometallics* **2010**, 29, 5390–5401
5. Greg A. N. Felton, Richard S. Glass, Dennis L. Lichtenberger, and Dennis H. Evans*

   Inorganic Chemistry, Vol. 45, No. 23, **2006** 9181-9184
6. Wilson, A. D.; Shoemaker, R. K.; Meidaner, A.; Muckerman, J. T.; DuBois, D. L.; Rakowski DuBois, *Proc. Natl. Acad. Sci. U.S.A.* **2007**, 104, 6951–6956
7. Louise A. Berben and Jonas C. Peters* *Chem. Commun.*, **2010**, 46, 398–400
8. Xile Hu, Bruce S. Brunschwig, and Jonas C. Peters* *J. am. Chem. Soc.* **2007**, 129, 8988-8998
9. Greg A. N. Felton, Aaron K. Vannucci, Noriko Okumura, L. Tori Lockett, Dennis H. Evans,* Richard S. Glass,* and Dennis L. Lichtenberger* *Organometallics* **2008**, 27, 4671–4679

10. Dmitry A. Valyaev, Mikhail G. Peterleitner, Oleg V. Semeikin , Kamil I. Utegenov, Nikolai A. Ustynyuk*, Alix Sournia-Saquet , Noe, Lugan, Guy Lavigne *Journal of Organometallic Chemistry* 692 (**2007**) 3207–3211

11. James P. Collman,* Paul S. Wagenknecht, and Nathan S. Lewist *J. Am. Chem. Soc*. **1992**, 114, 5665-5673

12. Vincent Artero □, Marc Fontecave *Coordination Chemistry Reviews* 249 (**2005**) 1518–1535

13. Catherine C. Neto, Carl D. Baer, Young K. Chung and Dwight A. Sweigart" *J . Chem. Soc., Chem. Comun.*, **1993** 816-818

14. Bernhardt, R. J.; Eyman, D. P. *Organometallics* **1984**,3,1445.

15. Bernhardt,R. J.;Wilmoth,M.A.; Weers, J. J.;LaBmh, D.M.;Eyman, D. P.; Huffman, J. C. *Organometallics* **1986**,5, 883

16. Peter J. Schlom, Ann M. Morken, Darrell P. Eyman,' Norman C. Baenziger, and Steven J. Schauer *Organometallics* **1993**,12, 3461-3467

17. Chapter 3. Unpublished result of reductive electrochemistry of $(\eta^6$-HMB)$Mn(CO)_2Cl$ and $[(\eta^6$-HMB)$Mn(CO)_2THF]^+$

18. (a) Kristjansdottir, S. S.; Moody, A. E.; Weberg, R. T.; Norton, J. R. *Organometallics* **1988,** 7,1983. (b) Jordan, R. F.; Norton, J. R. *J.Am. Chem. SOC* **1982**,104, 1255. (c) Jordan, R. F.; Norton, J. R. *ACS Symp. Ser.* **1982**, No. 198,403. (d) Moore, E. J.; Sullivan, J. M.; Norton, J. R. *J. Am. Chem. SOC*. **1986**,108,2267. (e) Edidm, R. T.; Sullivan, J. M.; Norton, J. R. *J. Am. Chem. SOC*. **1987**,109,3945.

19. Jacqueline M. Veauthier, Albert Chow, Gideon Fraenkel, Steven J. Geib and N.

John Cooper* *Organometallics* **2000**, 19, 3942-3947

20. Jacqueline M. Veauthier, Albert Chow, Gideon Fraenkel Steven J. Geib and N. John Cooper* *Organometallics 2000*, 19, 661-671

21. W. Lamanna and M. Brookhart* *Journal of the American Chemical Society* **1980** 102 3490-3494

Chapter 5

Direct synthesis of (η^6-aniline) manganese tricarbonyl cation and its analogs

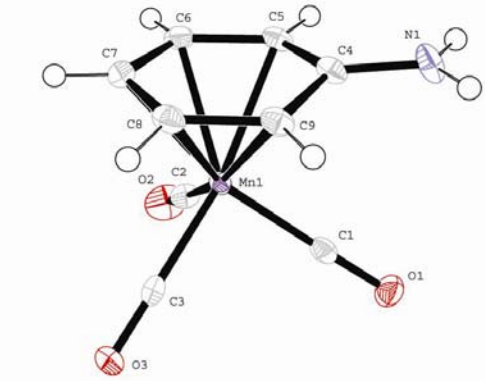

3 (R = H)

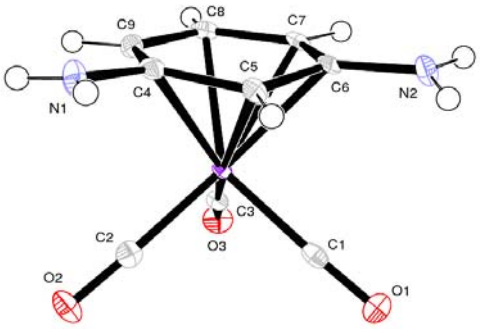

3 (R = m-NH_2)

5.1 Introduction

π-bonded arene manganese carbonyl complexes have applications in interesting areas such as: (1) Organic synthesis of natural and pharmaceutical products[1-2] (2) electrophilic activation and functionalization of arene[3a-g] (3) Supramolecular metal-organometallic coordination framwork based on manganese quinonoid complexes[4-10] (4) surface modification of magnetic nanostructures[11-12] (5) Proton reduction catalysis and hydrogen storage and slow release[13].

The reactivity of arene is greatly enhanced by the coordination of manganese tricarbonyl moiety. Thus, the manganese functionalized arenes are readily accessible by varieties of nucleophiles, which provide us a unique synthetic method of functionalizing arenes with desired functional groups[3a-g].

Right now there are four kinds of method[14] been applied to the synthesis of (η^6-arene) manganese tricarbonyl cation: (1). Fisher-Hafner method[15]; (2). TFA-anhydride method[16-17]; (3). Silver ($AgBF_4$) method[18-20]; (4). Manganese Tricarbonyl Transfer (MTT) method.[21] In order to improve the yield, all the above methods share one similarity: excess mount of desired arene ligand were used, usually over 2 equivalents. However, there are limitations: (1) Electron deficient arene could not coordinate to manganese tricarbonyl moiety. For example, (η^6-o-/m-/p-dichlorobenzene) manganese tricarbonyl cation could not be synthesized via none of the above method since the two chloride atoms would make the benzene ring too electron deficient to sustain the coordination of manganese tricarbonyl moiety.[14] When a benzene ring bearing an adjacent carbonyl, such as benzylic acid,

benzaldehyde, etc, or more than one chloride, bromide or iodide, cyanide, it is difficult to have manganese tricarbonyl π-bonded onto the arene. (2) Electron rich arene could not π-bonded to the manganese moiety directly. Benzene ring with one or two adjacent primary amine group, such as aniline, phenylenediamine or its analog, could not be introduced to manganese tricarbonyl system.[14]

Previously the yield of (η^6-bromobenzene) manganese tricarbonyl was too low to be calculated, and the (η^6-iodidebenzene) manganese tricarbonyl could not even be synthesized. Rose[22] reported the direct synthesis of (η^6-bromo/iodide-benzene) manganese tricarbonyl cation analogs in high yield. They simply introduced an electron donating methoxy group to the benzene ring to make the system more electron rich, and then followed the "silver method", they improved the yield of the anticipating product from none or 8% to around 70%.

η^6-bonded aniline manganese tricarbonyl cation was first introduced by Pauson[23] in 1975. He reported the indirect synthesis method: nucleophilic substitution of the cationic (η^6-chloroarene) manganese tricarbonyl complex by NH_3. However, neither the yield of pure product was reported, nor the crystal structure was obtained. Pike[14] summarized the synthetic scope of eta6-aromatic manganese tricarbonyl in 1994, and found that "no direct route has yet provided the coordinated aniline". Since then, there is no report about the characterization or synthesis of (η^6-aniline) manganese tricarbonyl complex.

Recently, we found a unique direct synthesis method for (η^6-aniline) manganese tricarbonyl complex and its alkyl substituent analogs with high yield. We

are using the MTT method, however, we altered the ligand ratio to be 2.8:1 (MTT: aniline). Trianiline manganese tricarbonyl was formed initially; excess MTT would π-bond to the benzene ring of the aniline and liberate the amine group from the coordination of the first manganese. The yield of aniline analog is 65%. We even got the crystal structure of the (η^6-m-phenylenediamine) manganese tricarbonyl complex which was impossible to be synthesized via indirect method (nucleophilic substitution from halogenoarene manganese tricarbonyl). The scope and reaction mechanism of this direct method was studied and will be discussed in this chapter.

5.2 Experiments

1. Synthesis

[(η^6-aniline) $Mn(CO)_3$]BF_4 Acenaphthene manganese tricaronyl tetrafluoroborate (0.500g, 1.32mmol) and aniline (0.0429ml, 0.47mmol) were combined with 15ml dichloromethane in 20ml pressure tube. The pressure tube was bubbled through nitrogen for 2mins and sealed. It was placed in a 75℃ oil bath for 6hours. The product is a yellow precipitate from the solution. The solution was dried and washed with diethyl ether and dichloromethane once and the compound was recrystallized by diffusing ether into its acetone solution. IR: 2065, 2001 cm^{-1} in acetonitrile. The yield is 65% based on the purified product. Crystal structure was analyzed by single crystal X-ray crystallographic machine.

[(η^6-3,4-dimethylaniline) $Mn(CO)_3$]BF_4 was synthesized following the same procedure as [(η^6-aniline) $Mn(CO)_3$]BF_4 above. IR of it in acetonitrile is 2061, 1996 cm^{-1}.

[(η^6-4-methylaniline) $Mn(CO)_3$]BF_4 was synthesized following the same method listed above; however, it has moderate solubility in dichloromethane, and can only be washed by ether. IR: 2063, 1998 cm^{-1} in acetone.

[(η^6-phenylenediamine) $Mn(CO)_3$]BF_4 was synthesized following the same procedure of [(η^6-aniline) $Mn(CO)_3$]BF_4 above. IR of it in acetonitrile is 2050, 1978 cm^{-1}.

2. Polymerization reaction and diazotization reaction

Polymerization of the aniline functionalized by manganese tricarbonyl moiety failed. [(η^6-aniline) $Mn(CO)_3$]$^+$ could neither be protonated nor diazotized by nitrite.

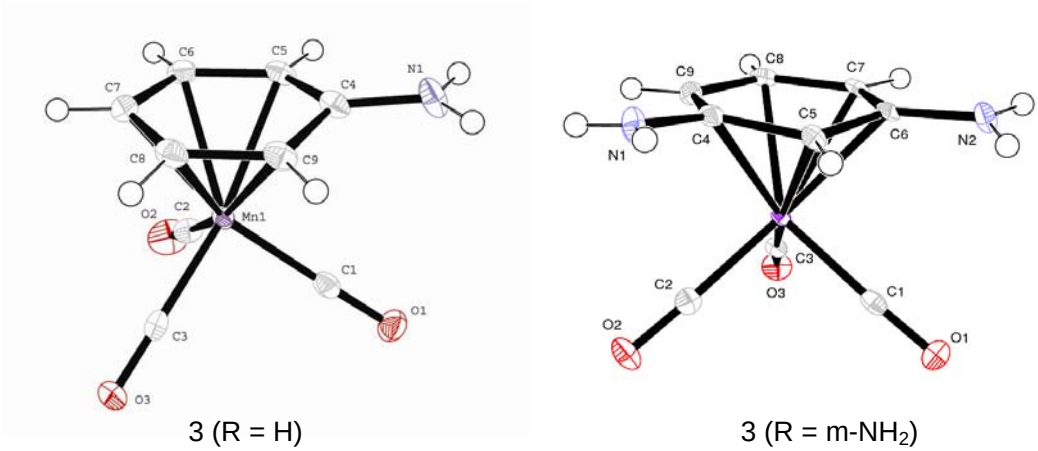

3 (R = H) 3 (R = m-NH_2)

Figure 5-1. Crystal structure of compound **3**

3. Infrared Spectroscopy

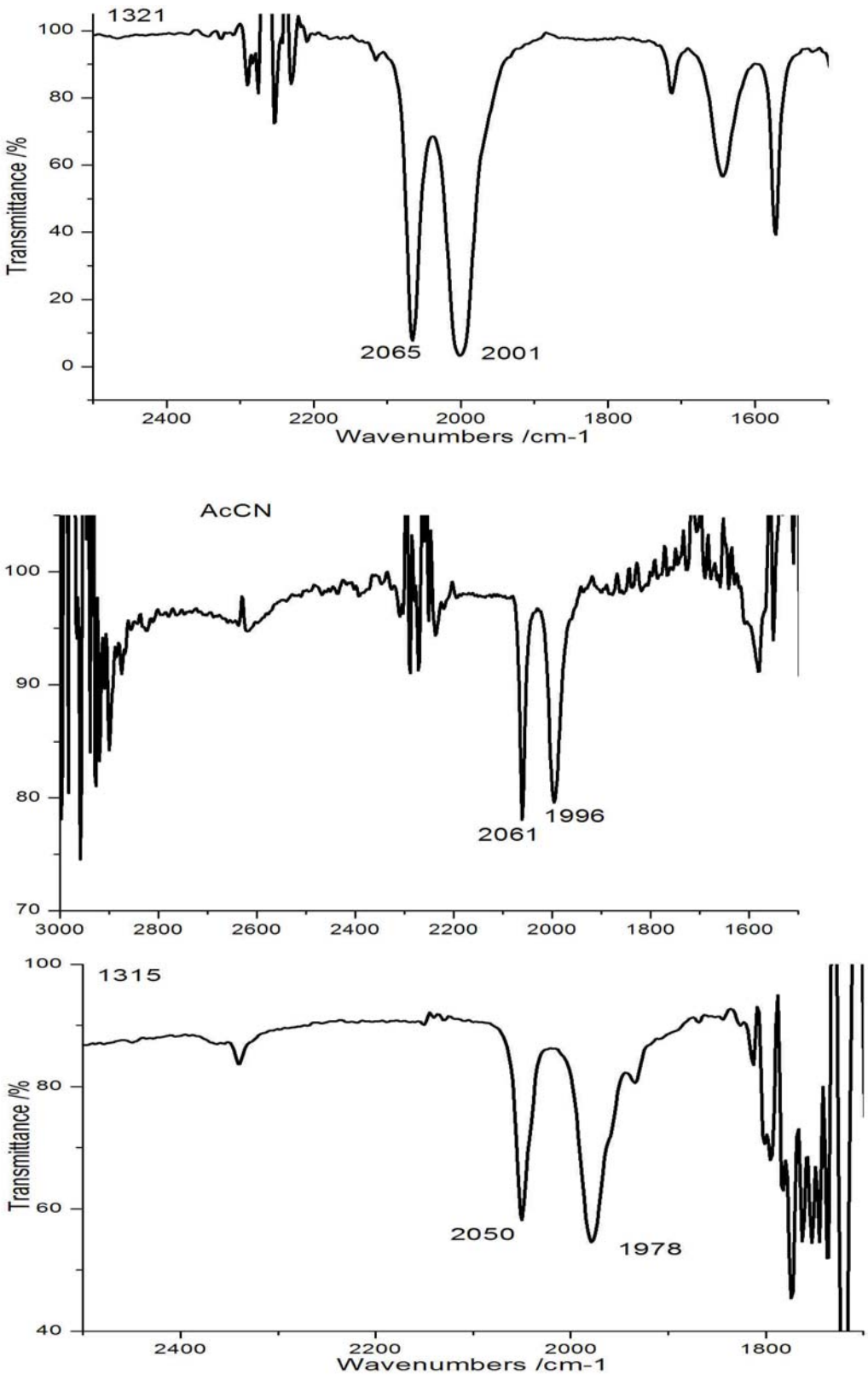

Figure 5-2. IR of the following complexes in acetonitrile

(a). compound 3 (R = H)

(b). compound 3 (R = 3,4-dimethyl)

(c). compound 3 (R = m-NH_2)

From above infrared spectroscopy, as the electron donating group gets stronger, the wavenumbers of the carbonyl group get lower.

4. NMR

NMR in AcCN-D3

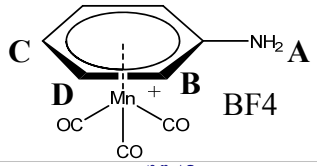

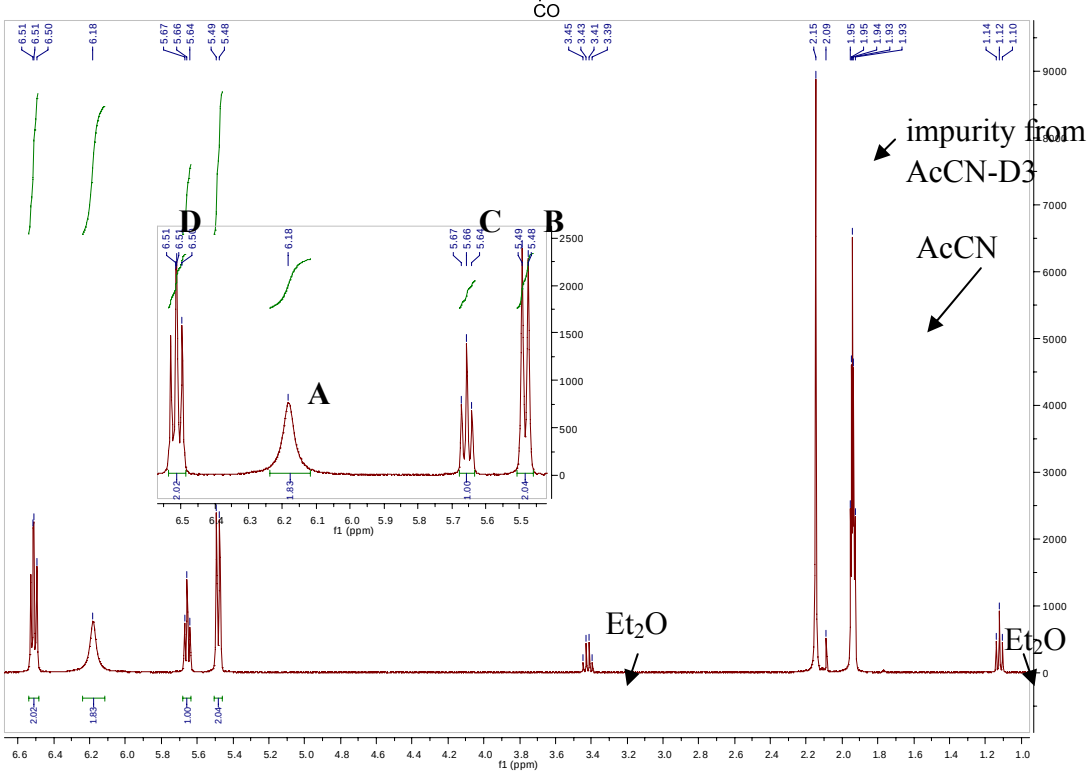

MeCN-D3

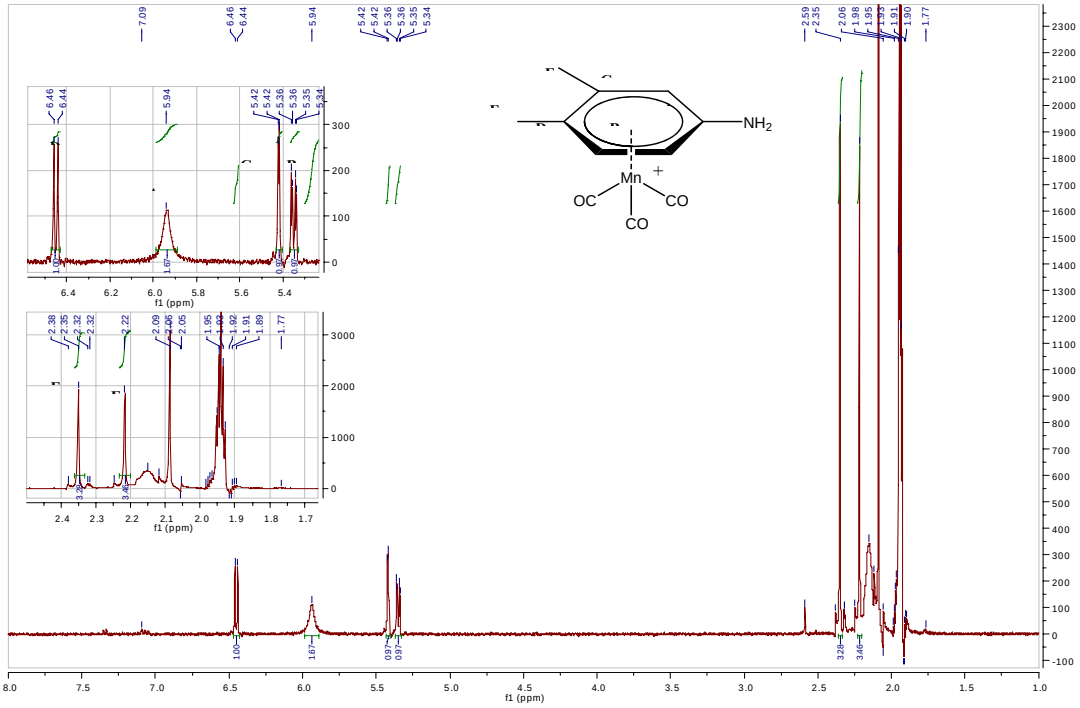

NMR in AcCN-D3

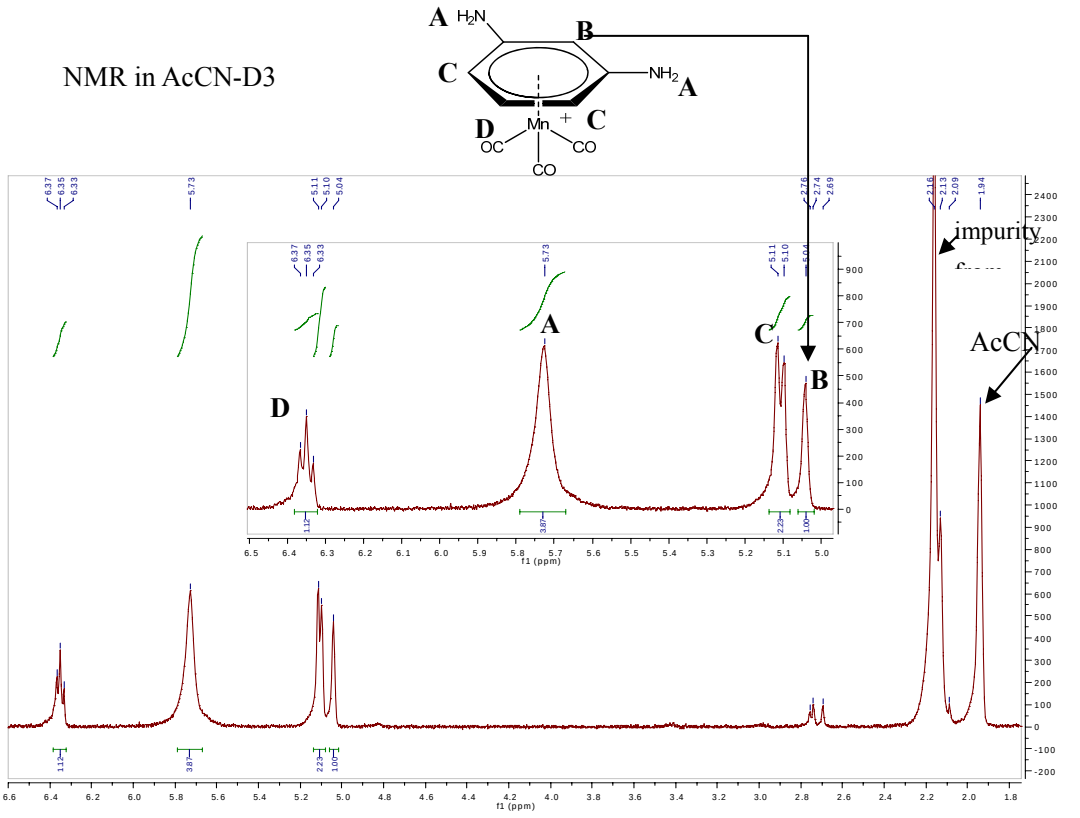

Figure 5-3. NMR of the following complexes in deuterated acetonitrile

(a). compound 3 (R = H)

(b). compound 3 (R = 3,4-dimethyl)

(c). compound 3 (R = m-NH_2)

5. Mass spectrometry: electron spray ionization and fragmentation.

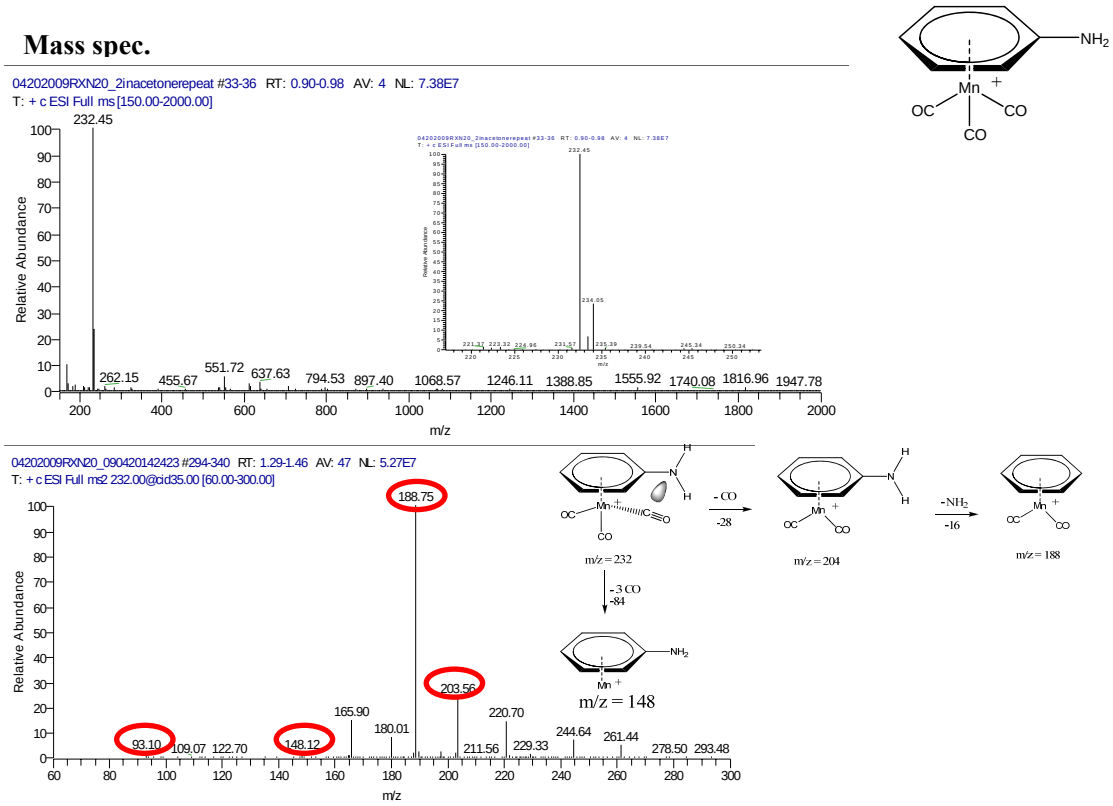

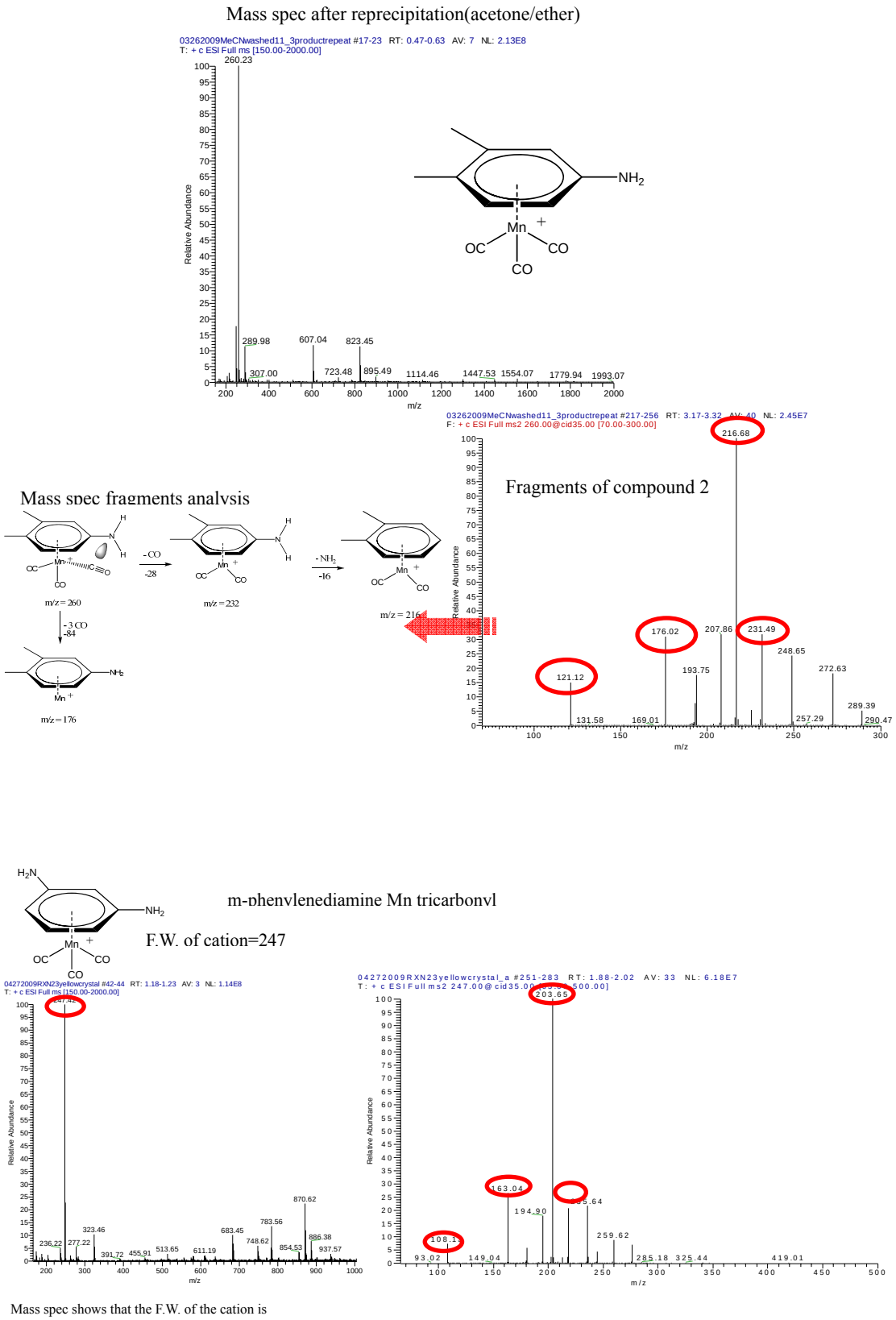

Figure 5-4. Mass spectrometry (electron spray ionization) of the following complexes in 50% acetonitrile/50% H_2O solution

(a). compound 3 (R = H)

(b). compound 3 (R = 3,4-dimethyl)

(c). compound 3 (R = m-NH_2)

The above mass spec. information gives information about ionization and fragmentation of (η^6-aniline) $Mn(CO)_3^+$ and its analogs (compound **3a,b,c**). And it is for the first time that the fragmentation of the arene manganese tricarbonyl cation being analyzed.

5.3. Result and discussion

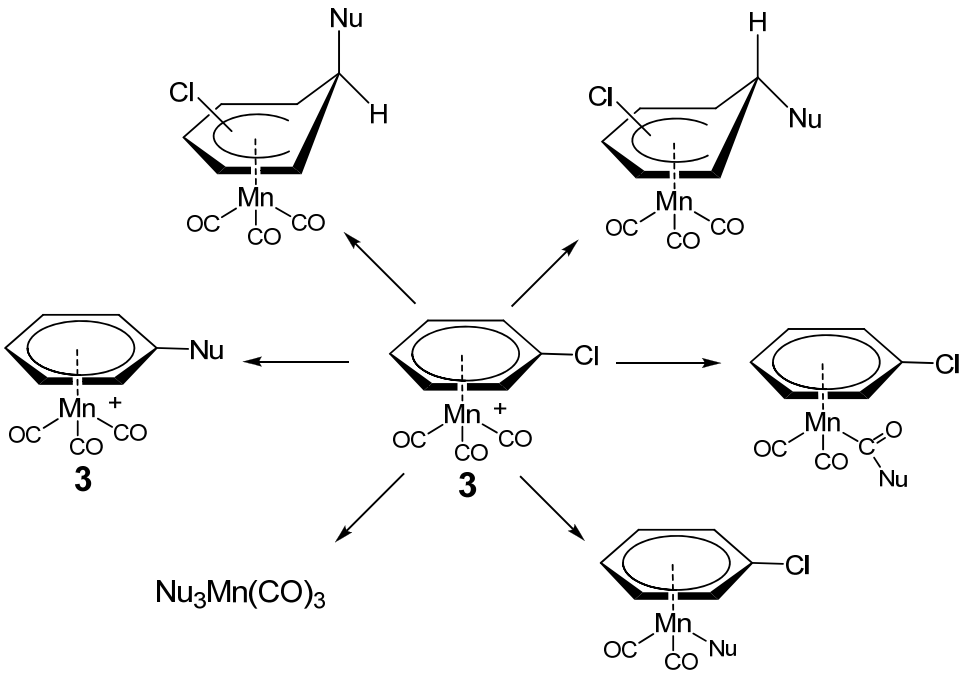

Figure 5-5. **Nucleophilic reactions pathways of (η^6-chlorobenzene) $Mn(CO)_3^+$**. Nucleophiles can react with (η^6-chlorobenzene) $Mn(CO)_3^+$ cation by several alternative pathways which depend on the nature of the nucleophile, solvent, temperature.

Previously, Pauson reported the indirect synthesis of (η^6-aniline) $Mn(CO)_3^+$ by nucleophilic substitution of the chloride from the (η^6-chlorobenzene) $Mn(CO)_3^+$ using ammonia. The yield of the raw product was reported to be 60%.[23]

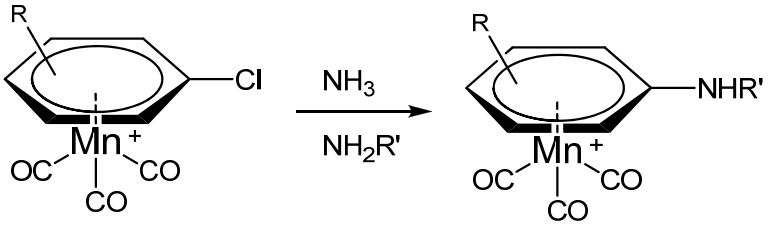

Figure 5-6. How Aniline Manganese Tricarbonyl was made

1. Reaction mechanism

We modified the "MTT" method by altering the MTT : aniline ratio to 2.8 : 1, then after 6 hours of reaction, we got yellow precipitates, which is the [(η^6-aniline) $Mn(CO)_3$]BF_4. Since the aromatic amine is basic, it prefers bonding to the manganese in a η^2 manner and form trianiline manganese tricarbonyl cation instead of (η^6-aniline) manganese tricarbonyl. Initially, we sought ways that would protect the aromatic amine group from coordinating to the manganese moiety. Di-*tert*-butyl dicarbonate is a wildly used amine protection group in organic synthesis, after Boc-protection, the Boc-amine group still prefers bonding to the manganese in a η^2 manner. Instead of being bothered, why don't we accept the fact and consider manganese tricarbonyl as an amine protection group by itself? In fact, three equivalents of anilines are protected by one equivalent of manganese tricarbonyl, and there are three equivalents of arene left for further coordination. The mechanism of the direct synthesis method is

proposed as following:

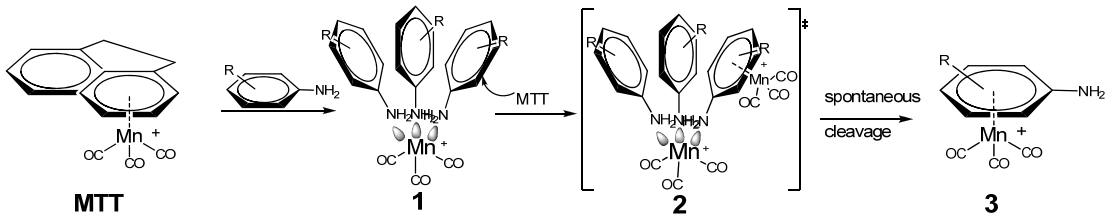

Scheme 5-1. Mechanism of direct synthesis of (η^6-aniline) $Mn(CO)_3^+$ and its analogs (R = alkyl, or m-NH_2 group)

We did one control experiment: trianiline manganese tricarbonyl cation was treated with over one equivalent of MTT, and lead to the formation of [(η^6-aniline) $Mn(CO)_3$]BF_4. Later on, we found out that this reaction could be finished in one step. Simply mixed excess MTT with aniline in the pressure tube, and heated it up to 75℃ for 6 hours, and then we ended up with the η^6 bonded product as precipitate.

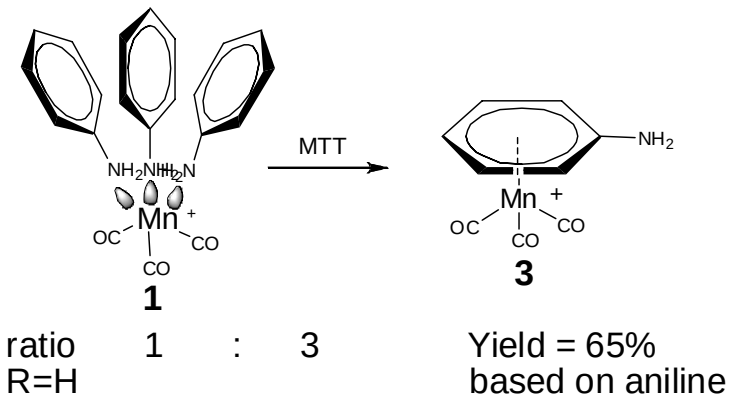

Figure 5-7. Control experiment between compound 1 and MTT

The basicity of the aromatic amine is strongly decreased via coordination of manganese tricarbonyl moiety. The long pair electrons are greatly localized by the

benzene ring. Compound 3 (R = H) could neither be protonated by strong acid, nor bond to electrophile such as MTT, which is in support of the "spontaneous cleavage" mechanism.

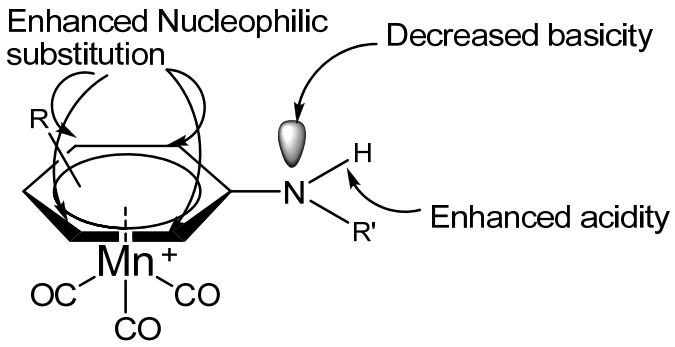

Figure 5-8. Chemical property of aniline after coordination of manganese moiety

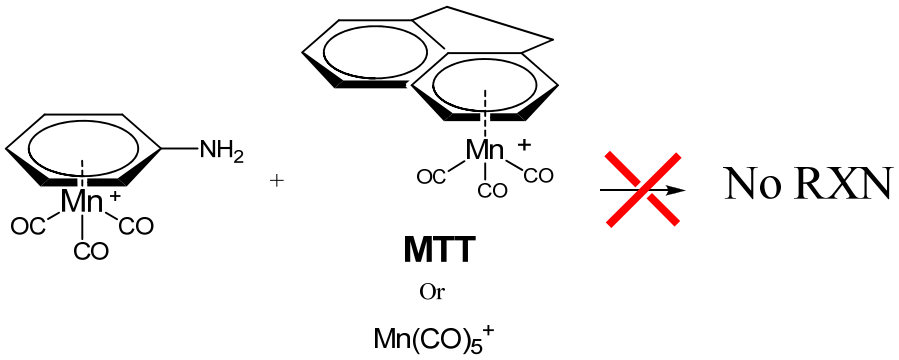

Figure 5-9. Decrease of the basicity of (η^6-aniline) $Mn(CO)_3^+$

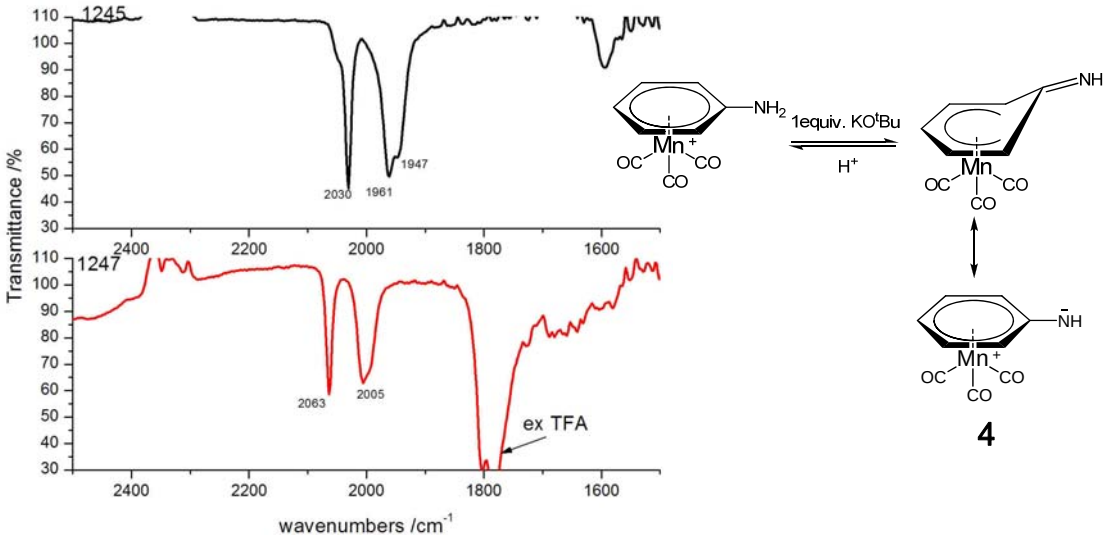

Figure 5-10. Reversible deprotonation

Not being able to be protonated by strong acid, instead, aniline could be deprotonated by strong base after π-bonding to the manganese moiety through the benzene ring. After deprotonation, the product compound 4 is an active nucleophile, and could react with different electrophiles to afford new species, which could be one of its potential applications in organice synthesis.

2. Scope

Other than alkyl-substituted aniline analogs, the scope of our direct synthesis method was investigated. The following aniline analogs bearing heteroatoms were tried.

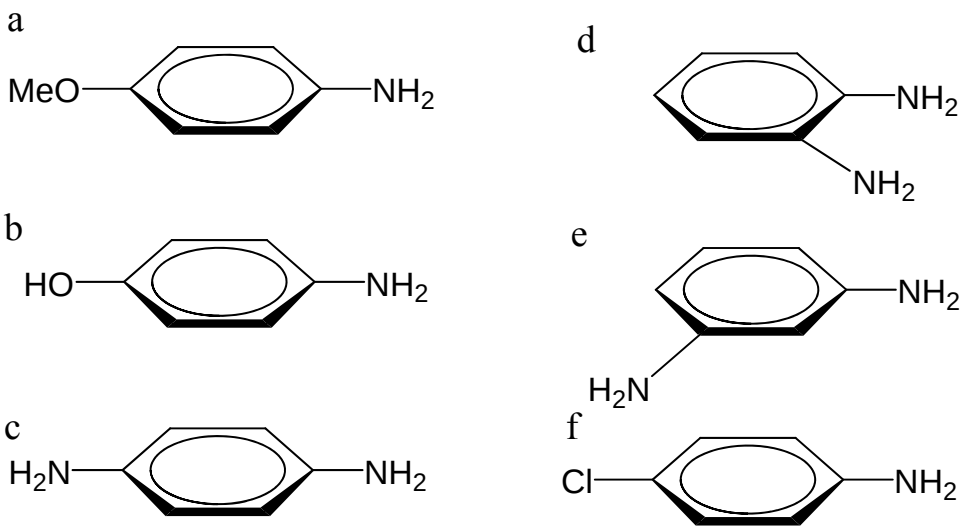

Chart 5-1. Aniline bearing heteroatom: electron donating (a-e) group and electron withdrawing group (f).

Aniline analogs shown above were tested via our direct synthesis method. Unfortunately, only m-phenylenediamine gave positive result. In the case of p/m/o-phenylenediamine, we think that, the basicity of the amine group plays an important role in the crucial step (spontaneous cleavage) of forming eta6-bonding species. When two amine groups are in o/p position, the basicity increases and as a result two amines function as a linkage between two manganese tricarbonyl centers. In the contrary, when the two amines are in meta-position of each other, the basicity doesn't change much. So we may able to have success in a serial of m-functionalized aniline.

As we have limited source of meta-functionalized aniline, we haven't been able to test the following ligand, which seem to be promising: m-methoxylaniline, m-hydroxylaniline, m-chloroaniline (even chloride is not a electron donoting group, but it is still worth trying).

3. Aromatic amine protection — remote protection

Aniline by itself could easily be protonated by strong acid, such as TFA, HBF_4. In another aspect, the most common synthesis of polyaniline is by oxidative polymerization with ammonium peroxodisulfate as an oxidant; also, aniline could be oxidized by nitrite to form diazonium salt. However, after coordination of manganese tricarbonyl moiety, aniline loses its basicity. It could neither be protonated nor oxidized. The best way to understand (η^6-aniline) $Mn(CO)_3^+$ is to consider it as (η^6-toluene) $Mn(CO)_3^+$ since they share very similar chemical property. The amine group is totally neutralized by manganese moiety. Based upon the above discussion, manganese tricarbonyl could be treated as an alternative for protection of aniline and its analogs. The advantage of our method is we can protect the amine group without any modification to the amine. The amine group remains intact. We call it "remote protection".

5.4 Conclusions

To summarize, we reported the first direct synthetic method of (η^6-aniline) $Mn(CO)_3^+$ and its analogs. Primary aromatic amine functionalized by alkyl group could be applied to this one-step method. Secondary and tertiary aromatic amines haven't been tried. However, we are confident that our direct synthesis method could

be applied.

Compared with indirect method, our one-step method is much convenient. More importantly, aniline with different functional group could be activated directly. Sometimes it is difficult to find a chlorobenzene analog to make a detour. For example, it is not possible to synthesize (η^6-dichlorobenzene) manganese tricarbonyl catoin, thus, we could not synthesize the phenylenediamine manganese tricarbonyl by nucleophilic substitution. It is encouraging that (η^6-m-phenylenediamine) manganese tricarbonyl catoin could be synthesized. We will work on the possibility of loading manganese moiety onto other meta-functionalized aniline analogs bearing heteroatoms.

By the coordination of the manganese tricarbonyl moiety to the benzene ring functionalized by amine group, the basicity of the amine group is greatly diminished. It might be an alternative for aromatic amine protection method. To remove the manganese moiety, we can simply leave the compound in acetonitrile for days or heat for a few hours.

Furthermore, (η^6-aniline) $Mn(CO)_3^+$ is an important precursor for the study in another interesting area: heterogeneous electrochemistry, which will be discussed in the next chapter.

5.5 X-ray crystal structure data

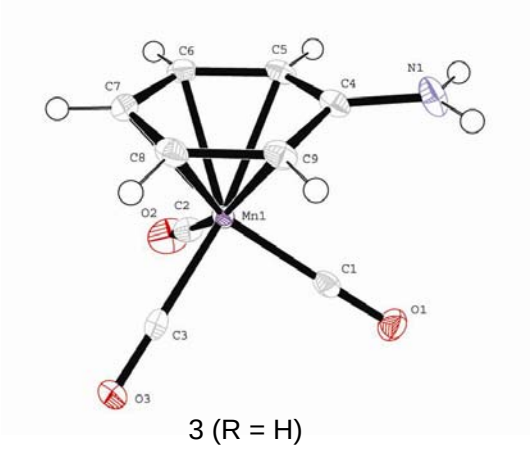

3 (R = H)

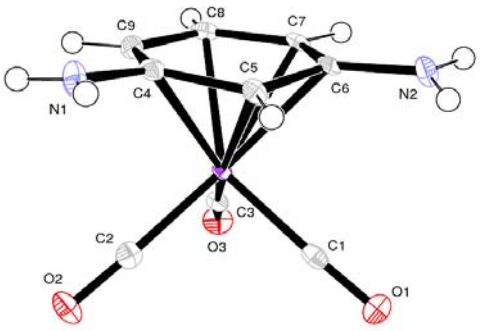

3 (R = m-NH_2)

Crystal structure of compound **3**

Table 5-C1-1. Crystal data and structure refinement for 3 (R = m-NH_2)

Identification code	**3** (R = m-NH_2)	
Empirical formula	C9 H8 B F4 Mn N2 O3	
Formula weight	333.92	
Temperature	100(2) K	
Wavelength	1.54178	
Crystal system	Triclinic	
Space group	P-1	
Unit cell dimensions	a = 6.70060(10) Å	α= 90.9980(10)°
	b = 9.00050(10) Å	β=106.5300(10)º
	c = 10.32920(10) Å	γ = 90.0710(10)°
Volume	597.092(13) $Å^3$	
Z	2	
Density (calculated)	1.857 Mg/m^3	
Absorption coefficient	9.615 mm^{-1}	
F(000)	332	
Crystal size	0.41 x 0.26 x 0.21 mm^3	
Theta range for data collection	4.47 to 67.00?	
Index ranges	-7<=h<=7, -10<=k<=10, -12<=l<=12	
Reflections collected	10061	
Independent reflections	2066 [R(int) = 0.0357]	
Completeness to theta = 67.00°	96.9 %	
Absorption correction	Numercial	
Max. and min. transmission	0.2350 and 0.1110	
Refinement method	Full-matrix least-squares on F^2	
Data / restraints / parameters	2066 / 0 / 213	
Goodness-of-fit on F^2	1.100	
Final R indices [I>2sigma(I)]	R1 = 0.0293, wR2 = 0.0744	
R indices (all data)	R1 = 0.0295, wR2 = 0.0746	
Largest diff. peak and hole	0.342 and -0.651 e. $Å^{-3}$	

Table 5-C1-2. Atomic coordinates (x 10^4) and equivalent isotropic displacement parameters (Å ^{2}x 10^3) U(eq) is defined as one third of the trace of the orthogonalized U^{ij} tensor.

	x	y	z	U(eq)
Mn(1)	1410(1)	2331(1)	8498(1)	8(1)
N(1)	2963(3)	3154(2)	5727(2)	16(1)
N(2)	-1096(3)	-717(2)	6868(2)	15(1)
O(1)	2686(2)	-452(2)	9979(2)	19(1)
O(2)	5647(2)	3642(2)	9296(2)	19(1)
O(3)	518(2)	3603(2)	10931(1)	18(1)
C(1)	2225(3)	641(2)	9428(2)	13(1)
C(2)	4027(3)	3119(2)	9008(2)	13(1)
C(3)	865(3)	3148(2)	9982(2)	13(1)
C(4)	1481(3)	2740(2)	6287(2)	12(1)
C(5)	1161(3)	1217(2)	6504(2)	11(1)
C(6)	-632(3)	738(2)	6869(2)	11(1)
C(7)	-1801(3)	1825(2)	7337(2)	12(1)
C(8)	-1364(3)	3346(2)	7243(2)	13(1)
C(9)	306(3)	3818(2)	6785(2)	13(1)
B(1)	5866(3)	2559(2)	3343(2)	14(1)
F(1)	5048(2)	3920(1)	3597(1)	27(1)
F(2)	4685(2)	1951(2)	2133(1)	28(1)
F(3)	7919(2)	2770(1)	3328(1)	26(1)
F(4)	5822(2)	1576(1)	4368(1)	22(1)

Table 5-C1-3. Bond lengths [Å] and angles [°]

Mn(1)-C(1)	1.813(2)	O(2)-C(2)	1.139(2)
Mn(1)-C(3)	1.8179(19)	O(3)-C(3)	1.139(2)
Mn(1)-C(2)	1.8201(19)	C(4)-C(5)	1.419(3)
Mn(1)-C(8)	2.1552(18)	C(4)-C(9)	1.428(3)
Mn(1)-C(7)	2.1878(18)	C(5)-C(6)	1.426(3)
Mn(1)-C(9)	2.1932(18)	C(5)-H(5)	0.92(3)
Mn(1)-C(5)	2.2380(17)	C(6)-C(7)	1.416(3)
Mn(1)-C(6)	2.3151(17)	C(7)-C(8)	1.411(3)
Mn(1)-C(4)	2.3337(18)	C(7)-H(7)	0.93(2)
N(1)-C(4)	1.338(3)	C(8)-C(9)	1.401(3)
N(1)-H(1)	0.86(3)	C(8)-H(8)	0.97(3)
N(1)-H(2)	0.80(3)	C(9)-H(9)	0.92(3)
N(2)-C(6)	1.346(2)	B(1)-F(2)	1.378(2)
N(2)-H(3)	0.80(3)	B(1)-F(3)	1.393(2)
N(2)-H(4)	0.85(3)	B(1)-F(1)	1.394(2)
O(1)-C(1)	1.143(3)	B(1)-F(4)	1.398(3)

C(1)-Mn(1)-C(3)	89.23(8)	C(7)-Mn(1)-C(5)	66.80(7)
C(1)-Mn(1)-C(2)	92.99(8)	C(9)-Mn(1)-C(5)	66.90(7)
C(3)-Mn(1)-C(2)	90.82(8)	C(1)-Mn(1)-C(6)	84.14(7)
C(1)-Mn(1)-C(8)	140.01(8)	C(3)-Mn(1)-C(6)	129.07(7)
C(3)-Mn(1)-C(8)	89.51(8)	C(2)-Mn(1)-C(6)	139.83(7)
C(2)-Mn(1)-C(8)	126.99(8)	C(8)-Mn(1)-C(6)	66.20(6)
C(1)-Mn(1)-C(7)	102.93(8)	C(7)-Mn(1)-C(6)	36.52(7)
C(3)-Mn(1)-C(7)	97.87(7)	C(9)-Mn(1)-C(6)	78.35(7)
C(2)-Mn(1)-C(7)	161.89(8)	C(5)-Mn(1)-C(6)	36.44(6)
C(8)-Mn(1)-C(7)	37.90(7)	C(1)-Mn(1)-C(4)	125.46(7)
C(1)-Mn(1)-C(9)	159.87(8)	C(3)-Mn(1)-C(4)	145.26(7)
C(3)-Mn(1)-C(9)	109.51(8)	C(2)-Mn(1)-C(4)	85.97(7)
C(2)-Mn(1)-C(9)	94.00(8)	C(8)-Mn(1)-C(4)	65.76(7)
C(8)-Mn(1)-C(9)	37.58(7)	C(7)-Mn(1)-C(4)	77.82(7)
C(7)-Mn(1)-C(9)	68.15(7)	C(9)-Mn(1)-C(4)	36.62(7)
C(1)-Mn(1)-C(5)	93.08(7)	C(5)-Mn(1)-C(4)	36.09(6)
C(3)-Mn(1)-C(5)	164.63(8)	C(6)-Mn(1)-C(4)	64.36(6)
C(2)-Mn(1)-C(5)	104.22(7)	C(4)-N(1)-H(1)	121.2(19)
C(8)-Mn(1)-C(5)	78.97(7)	C(4)-N(1)-H(2)	118.3(18)

H(1)-N(1)-H(2)	120(3)	C(8)-C(7)-C(6)	119.75(17)
C(6)-N(2)-H(3)	120.0(18)	C(8)-C(7)-Mn(1)	69.80(10)
C(6)-N(2)-H(4)	117.6(19)	C(6)-C(7)-Mn(1)	76.64(10)
H(3)-N(2)-H(4)	121(3)	C(8)-C(7)-H(7)	120.7(14)
O(1)-C(1)-Mn(1)	177.51(16)	C(6)-C(7)-H(7)	119.4(14)
O(2)-C(2)-Mn(1)	177.95(17)	Mn(1)-C(7)-H(7)	128.5(15)
O(3)-C(3)-Mn(1)	177.18(17)	C(9)-C(8)-C(7)	121.60(16)
N(1)-C(4)-C(5)	120.56(17)	C(9)-C(8)-Mn(1)	72.68(10)
N(1)-C(4)-C(9)	121.08(17)	C(7)-C(8)-Mn(1)	72.30(10)
C(5)-C(4)-C(9)	118.14(16)	C(9)-C(8)-H(8)	119.8(15)
N(1)-C(4)-Mn(1)	134.15(13)	C(7)-C(8)-H(8)	118.4(15)
C(5)-C(4)-Mn(1)	68.28(10)	Mn(1)-C(8)-H(8)	123.3(15)
C(9)-C(4)-Mn(1)	66.34(10)	C(8)-C(9)-C(4)	119.30(17)
C(4)-C(5)-C(6)	120.98(17)	C(8)-C(9)-Mn(1)	69.74(10)
C(4)-C(5)-Mn(1)	75.63(10)	C(4)-C(9)-Mn(1)	77.05(11)
C(6)-C(5)-Mn(1)	74.72(10)	C(8)-C(9)-H(9)	118.0(16)
C(4)-C(5)-H(5)	117.8(16)	C(4)-C(9)-H(9)	122.6(16)
C(6)-C(5)-H(5)	120.7(15)	Mn(1)-C(9)-H(9)	125.6(17)
Mn(1)-C(5)-H(5)	128.9(16)	F(2)-B(1)-F(3)	110.81(17)
N(2)-C(6)-C(7)	121.13(17)	F(2)-B(1)-F(1)	110.42(18)
N(2)-C(6)-C(5)	120.60(17)	F(3)-B(1)-F(1)	109.03(16)
C(7)-C(6)-C(5)	118.07(16)	F(2)-B(1)-F(4)	108.09(16)
N(2)-C(6)-Mn(1)	132.73(13)	F(3)-B(1)-F(4)	109.24(17)
C(7)-C(6)-Mn(1)	66.84(9)	F(1)-B(1)-F(4)	109.23(16)
C(5)-C(6)-Mn(1)	68.83(10)		

Symmetry transformations used to generate equivalent atoms:

Table 5-C1-4. Anisotropic displacement parameters ($Å^2 x\ 10^3$)for p1bar. The anisotropic displacement factor exponent takes the form: $-2\ ^2[\ h^2 a^{*2} U^{11} + ... + 2\ h\ k\ a^*\ b^*\ U^{12}\ ]$

	U^{11}	U^{22}	U^{33}	U^{23}	U^{13}	U^{12}
Mn(1)	8(1)	8(1)	8(1)	-2(1)	2(1)	-1(1)
N(1)	19(1)	15(1)	18(1)	-2(1)	10(1)	-5(1)
N(2)	14(1)	11(1)	19(1)	-3(1)	5(1)	-4(1)
O(1)	21(1)	15(1)	21(1)	5(1)	4(1)	1(1)
O(2)	12(1)	20(1)	25(1)	-5(1)	5(1)	-5(1)
O(3)	21(1)	19(1)	15(1)	-5(1)	6(1)	3(1)
C(1)	11(1)	18(1)	11(1)	-5(1)	3(1)	-3(1)
C(2)	16(1)	11(1)	12(1)	-3(1)	5(1)	2(1)
C(3)	10(1)	13(1)	14(1)	0(1)	1(1)	-1(1)
C(4)	13(1)	16(1)	7(1)	-2(1)	1(1)	-3(1)
C(5)	13(1)	11(1)	9(1)	-4(1)	3(1)	-1(1)
C(6)	10(1)	13(1)	7(1)	-3(1)	-1(1)	-2(1)
C(7)	7(1)	17(1)	9(1)	-2(1)	0(1)	-2(1)
C(8)	10(1)	16(1)	10(1)	-2(1)	-1(1)	2(1)
C(9)	17(1)	10(1)	12(1)	-1(1)	0(1)	-2(1)
B(1)	12(1)	12(1)	16(1)	-1(1)	3(1)	-1(1)
F(1)	28(1)	14(1)	43(1)	-2(1)	18(1)	2(1)
F(2)	27(1)	39(1)	16(1)	-5(1)	1(1)	-6(1)
F(3)	16(1)	21(1)	44(1)	-1(1)	14(1)	-3(1)
F(4)	24(1)	22(1)	19(1)	5(1)	4(1)	0(1)

Table 5-C1-5. Hydrogen coordinates (x 10^4) and isotropic displacement parameters (A^2x 10^3)

	x	y	z	U(eq)
H(1)	3650(40)	2510(30)	5410(30)	27(7)
H(2)	3290(40)	4010(30)	5770(30)	15(6)
H(3)	-270(40)	-1330(30)	6790(30)	17(6)
H(4)	-2140(50)	-960(30)	7130(30)	25(7)
H(5)	2040(40)	540(30)	6280(30)	15(6)
H(7)	-2910(40)	1530(30)	7650(20)	12(5)
H(8)	-2180(40)	4070(30)	7580(30)	16(6)
H(9)	580(40)	4820(30)	6800(30)	21(6)

Table 5-C1-6. Hydrogen bonds

D-H...A	d(D-H)	d(H...A)	d(D...A)	<(DHA)
N(1)-H(1)...F(4)	0.86(3)	2.20(3)	3.021(2)	160(3)
N(1)-H(2)...F(1)#1	0.80(3)	2.16(3)	2.932(2)	162(2)
N(2)-H(3)...F(3)#2	0.80(3)	2.07(3)	2.868(2)	175(3)
N(2)-H(4)...F(2)#3	0.85(3)	2.25(3)	3.087(2)	171(3)
N(2)-H(4)...F(4)#3	0.85(3)	2.57(3)	3.149(2)	127(2)

Symmetry transformations used to generate equivalent atoms:

#1 -x+1,-y+1,-z+1 #2 -x+1,-y,-z+1 #3 -x,-y,-z+1

Table 5-C2-1. Crystal data and structure refinement for 3 (R = H).

Identification code	3 (R = H)	
Empirical formula	C9 H7 B F4 Mn N O3	
Formula weight	318.91	
Temperature	100(2) K	
Wavelength	1.54178	
Crystal system	Monoclinic	
Space group	P2(1)/c	
Unit cell dimensions	a = 10.1479(2)	α= 90 º
	b = 9.8810(2)	β= 113.0580(10) º
	c = 12.7269(2)	γ= 90 º
Volume	1174.19(4) A^3	
Z	4	
Density (calculated)	1.804 Mg/m^3	
Absorption coefficient	9.720 mm^{-1}	
F(000)	632	
Crystal size	0.28 x 0.26 x 0.19 mm^3	
Theta range for data collection	4.74 to 66.96?	
Index ranges	-12<=h<=12, -11<=k<=10, -14<=l<=15	
Reflections collected	12393	
Independent reflections	2047 [R(int) = 0.0295]	
Completeness to theta = 66.96º	98.0 %	
Absorption correction	Numerical	
Max. and min. transmission	0.2651 and 0.1752	
Refinement method	Full-matrix least-squares on F^2	
Data / restraints / parameters	2047 / 0 / 200	
Goodness-of-fit on F^2	1.095	
Final R indices [I>2sigma(I)]	R1 = 0.0236, wR2 = 0.0617	
R indices (all data)	R1 = 0.0242, wR2 = 0.0620	
Largest diff. peak and hole	0.218 and -0.603 $e.A^{-3}$	

Table 5-C2-2. Atomic coordinates (x 10^4) and equivalent isotropic displacement parameters (A^2x 10^3) for3 (R = H). U(eq) is defined as one third of the trace of the orthogonalized U^{ij} tensor.

	x	y	z	U(eq)
Mn(1)	2450(1)	4302(1)	2386(1)	12(1)
O(1)	174(1)	6124(1)	897(1)	23(1)
O(2)	4118(2)	4587(2)	939(1)	33(1)
O(3)	4049(1)	6603(1)	3803(1)	21(1)
N(1)	-915(2)	2918(2)	1576(1)	22(1)
C(1)	1073(2)	5429(2)	1468(1)	16(1)
C(2)	3482(2)	4489(2)	1496(2)	20(1)
C(3)	3431(2)	5719(2)	3251(2)	16(1)
C(4)	491(2)	2881(2)	2186(1)	16(1)
C(5)	1452(2)	2303(2)	1746(2)	17(1)
C(6)	2916(2)	2152(2)	2446(2)	18(1)
C(7)	3489(2)	2667(2)	3563(2)	19(1)
C(8)	2573(2)	3375(2)	3961(1)	18(1)
C(9)	1117(2)	3540(2)	3272(1)	17(1)
B(1)	2643(2)	8831(2)	1164(2)	16(1)
F(1)	2423(1)	9009(1)	2170(1)	31(1)
F(2)	3712(1)	9706(1)	1167(1)	20(1)
F(3)	1376(1)	9141(1)	238(1)	31(1)
F(4)	3021(1)	7506(1)	1065(1)	30(1)

Table 5-C2-3. Bond lengths [A] and angles [º] for 3 (R = H).

Mn(1)-C(1)	1.8113(17)	C(4)-C(5)	1.420(2)
Mn(1)-C(3)	1.8174(17)	C(4)-C(9)	1.432(2)
Mn(1)-C(2)	1.8292(18)	C(5)-C(6)	1.410(2)
Mn(1)-C(8)	2.1622(17)	C(5)-H(5)	0.963(19)
Mn(1)-C(6)	2.1723(17)	C(6)-C(7)	1.404(3)
Mn(1)-C(7)	2.1750(17)	C(6)-H(6)	0.93(2)
Mn(1)-C(9)	2.2052(16)	C(7)-C(8)	1.407(3)
Mn(1)-C(5)	2.2238(16)	C(7)-H(7)	0.93(2)
Mn(1)-C(4)	2.3640(16)	C(8)-C(9)	1.401(2)
O(1)-C(1)	1.145(2)	C(8)-H(8)	0.95(2)
O(2)-C(2)	1.134(2)	C(9)-H(9)	0.91(2)
O(3)-C(3)	1.142(2)	B(1)-F(4)	1.384(2)
N(1)-C(4)	1.332(2)	B(1)-F(2)	1.386(2)
N(1)-H(1)	0.84(2)	B(1)-F(3)	1.396(2)
N(1)-H(2)	0.89(2)	B(1)-F(1)	1.394(2)
C(1)-Mn(1)-C(3)	91.09(7)	C(7)-Mn(1)-C(9)	67.86(7)
C(1)-Mn(1)-C(2)	91.27(8)	C(1)-Mn(1)-C(5)	100.61(7)
C(3)-Mn(1)-C(2)	89.23(8)	C(3)-Mn(1)-C(5)	165.64(7)
C(1)-Mn(1)-C(8)	127.51(7)	C(2)-Mn(1)-C(5)	98.73(7)
C(3)-Mn(1)-C(8)	86.92(7)	C(8)-Mn(1)-C(5)	79.37(6)
C(2)-Mn(1)-C(8)	141.07(7)	C(6)-Mn(1)-C(5)	37.39(6)
C(1)-Mn(1)-C(6)	136.60(7)	C(7)-Mn(1)-C(5)	67.70(6)
C(3)-Mn(1)-C(6)	132.21(7)	C(9)-Mn(1)-C(5)	66.49(6)
C(2)-Mn(1)-C(6)	87.17(7)	C(1)-Mn(1)-C(4)	83.81(7)
C(8)-Mn(1)-C(6)	67.67(7)	C(3)-Mn(1)-C(4)	139.54(7)
C(1)-Mn(1)-C(7)	160.90(7)	C(2)-Mn(1)-C(4)	130.85(7)
C(3)-Mn(1)-C(7)	98.75(7)	C(8)-Mn(1)-C(4)	65.74(6)
C(2)-Mn(1)-C(7)	105.12(7)	C(6)-Mn(1)-C(4)	65.48(6)
C(8)-Mn(1)-C(7)	37.85(7)	C(7)-Mn(1)-C(4)	78.07(6)
C(6)-Mn(1)-C(7)	37.68(7)	C(9)-Mn(1)-C(4)	36.32(6)
C(1)-Mn(1)-C(9)	93.87(7)	C(5)-Mn(1)-C(4)	35.89(6)
C(3)-Mn(1)-C(9)	104.71(7)	C(4)-N(1)-H(1)	119.7(14)
C(2)-Mn(1)-C(9)	165.02(7)	C(4)-N(1)-H(2)	119.6(14)
C(8)-Mn(1)-C(9)	37.40(6)	H(1)-N(1)-H(2)	121(2)
C(6)-Mn(1)-C(9)	79.43(7)	O(1)-C(1)-Mn(1)	178.01(15)

O(2)-C(2)-Mn(1)	179.07(16)	F(4)-B(1)-F(2)	110.19(14)
O(3)-C(3)-Mn(1)	179.43(15)	F(4)-B(1)-F(3)	109.13(14)
N(1)-C(4)-C(5)	121.70(16)	F(2)-B(1)-F(3)	109.05(14)
N(1)-C(4)-C(9)	121.27(16)	F(4)-B(1)-F(1)	110.67(15)
C(5)-C(4)-C(9)	116.77(15)	F(2)-B(1)-F(1)	108.99(14)
N(1)-C(4)-Mn(1)	135.26(12)	F(3)-B(1)-F(1)	108.78(14)
C(5)-C(4)-Mn(1)	66.67(9)		
C(9)-C(4)-Mn(1)	65.79(9)		
C(6)-C(5)-C(4)	120.68(15)		
C(6)-C(5)-Mn(1)	69.32(9)		
C(4)-C(5)-Mn(1)	77.45(10)		
C(6)-C(5)-H(5)	120.3(10)		
C(4)-C(5)-H(5)	118.8(10)		
Mn(1)-C(5)-H(5)	129.9(11)		
C(7)-C(6)-C(5)	121.14(16)		
C(7)-C(6)-Mn(1)	71.27(10)		
C(5)-C(6)-Mn(1)	73.29(9)		
C(7)-C(6)-H(6)	118.7(13)		
C(5)-C(6)-H(6)	120.0(13)		
Mn(1)-C(6)-H(6)	124.6(12)		
C(6)-C(7)-C(8)	118.35(16)		
C(6)-C(7)-Mn(1)	71.06(10)		
C(8)-C(7)-Mn(1)	70.58(9)		
C(6)-C(7)-H(7)	119.1(12)		
C(8)-C(7)-H(7)	122.4(12)		
Mn(1)-C(7)-H(7)	125.1(12)		
C(9)-C(8)-C(7)	121.10(16)		
C(9)-C(8)-Mn(1)	72.96(10)		
C(7)-C(8)-Mn(1)	71.56(10)		
C(9)-C(8)-H(8)	118.9(12)		
C(7)-C(8)-H(8)	119.5(12)		
Mn(1)-C(8)-H(8)	120.9(12)		
C(8)-C(9)-C(4)	120.73(16)		
C(8)-C(9)-Mn(1)	69.63(9)		
C(4)-C(9)-Mn(1)	77.89(10)		
C(8)-C(9)-H(9)	119.6(13)		
C(4)-C(9)-H(9)	119.6(13)		
Mn(1)-C(9)-H(9)	127.0(13)		

Symmetry transformations used to generate equivalent atoms:

Table 5-C2-4. Anisotropic displacement parameters ($A^2 \times 10^3$)for p21onc. The anisotropic displacement factor exponent takes the form: $-2\ ^2[\ h^2 a^{*2} U^{11} + ... + 2\ h\ k\ a^*\ b^*\ U^{12}\ ]$

	U^{11}	U^{22}	U^{33}	U^{23}	U^{13}	U^{12}
Mn(1)	11(1)	12(1)	12(1)	-2(1)	4(1)	-1(1)
O(1)	21(1)	22(1)	20(1)	-2(1)	1(1)	5(1)
O(2)	40(1)	33(1)	40(1)	2(1)	31(1)	3(1)
O(3)	18(1)	17(1)	23(1)	-6(1)	2(1)	-2(1)
N(1)	14(1)	32(1)	19(1)	-9(1)	6(1)	-7(1)
C(1)	17(1)	17(1)	15(1)	-6(1)	6(1)	-4(1)
C(2)	23(1)	15(1)	23(1)	-2(1)	9(1)	2(1)
C(3)	12(1)	19(1)	16(1)	3(1)	4(1)	5(1)
C(4)	18(1)	16(1)	16(1)	-1(1)	8(1)	-5(1)
C(5)	20(1)	13(1)	18(1)	-5(1)	7(1)	-5(1)
C(6)	19(1)	11(1)	25(1)	-1(1)	9(1)	0(1)
C(7)	16(1)	14(1)	21(1)	4(1)	3(1)	0(1)
C(8)	23(1)	16(1)	13(1)	0(1)	5(1)	-5(1)
C(9)	19(1)	16(1)	18(1)	-2(1)	11(1)	-4(1)
B(1)	16(1)	14(1)	18(1)	-1(1)	7(1)	-2(1)
F(1)	41(1)	35(1)	27(1)	0(1)	23(1)	-4(1)
F(2)	17(1)	19(1)	25(1)	1(1)	9(1)	-4(1)
F(3)	19(1)	32(1)	29(1)	-2(1)	-4(1)	-2(1)
F(4)	33(1)	15(1)	48(1)	0(1)	22(1)	1(1)

5.6 References

1. Anthony J. Pearson* and Paul R. Bruhn *J. Org. Chem.* **1991**. 56, 70927097
2. Pearson, A. J and Shin, H. *Tetrahedron* **1992** 48, 7527-7538
3. (a) Rose-Munch, F.; Rose, E. Eur. J. *Inorg. Chem.* **2002**, 1269. (b) Auffrant, A.; Prim, D.; Rose-Munch, F.; Rose, E.; Schouteeten, S.; Vaissermann, J. *Organometallics* **2003**, 22, 1898. (c) Prim, D.; Andrioletti, B.; Rose-Munch, F.; Rose, E.; Couty, F. *Tetrahedron 2004*, 60, 3325. (d) Ku¨ndig, E. P.; Pape, A. Top. *Organomet. Chem.* **2004**, 7, 71. (e) Sweigart, D. A.; Reingold, J. A.; Son, S. U. *Comprehensive Organometallic Chemistry III*; Crabtree, R. H., Mingos, D. M. P., Eds.; Elsevier: Oxford, U.K., **2006**; Vol. 5, Chapter 10, pp 761-814. (f) Jacques, B.; Chavarot, M.; Rose-Munch, F.; Rose, E. *Angew. Chem., Int. Ed.* **2006**, 45, 3481. (g) Jacques, B.; Chanaewa, A.; Chavarot-Kerlidou, M.; Rose-Munch, F.; Rose, E.; Ge´rard, H. *Organometallics* **2008**, 27, 626.
4. J. A. Reingold, S. U. Son, G. B. Carpenter and D. A. Sweigart, *J. Inorg. Organomet. Polym.*, **2006** 16, 1, 1-13.
5. J. A. Reingold, M. Jin and D. A. Sweigart, *Inorg. Chim. Acta*, **2006** 359, 1983.
6. M. Oh, J. A. Reingold and D. A. Sweigart, *Macromolecules Containing Metal and Metal-Like Elements* , **2005** John Wiley, Vol. 5, Chapter 10, 259.
7. M. Oh, G. B. Carpenter and D. A. Sweigart, *Acc. Chem. Res*., **2004** 37, 1.
8. M. Oh, G. B. Carpenter and D. A. Sweigart *Angew. Chem. Int. Ed.*, **2003** 42, 2025.
9. M. Oh, G. B. Carpenter and D. A. Sweigart, *Organometallics*, **2003** 22, 1437.

10. M. Oh, G. B. Carpenter and D. A. Sweigart, *Angew.* **2002** *Chem. Int. Ed.*, 41, 3650.

11. Sang Bok Kim, Chen Cai, Shouheng Sun, and Dwight A. Sweigart, *Angew. Chem. Int. Ed.*, **2009** 48, 2907 –2910.

12. Sang Bok Kim, Chen Cai, Jaemin Kim, Shouheng Sun, and Dwight A. Sweigart, *Organometallics*, **2009** 28, 5341–5348.

13. Chapter 4. Proton reduction catalyzed by aromatic manganese carbonyl complexes Manuscript in process.

14. J. Derek Jackson, Sharon J. Villa, Deborah S. Bacon, and Robert D. Pike* *Organometallics* **1994,** *13,* 3972-3980

15. (a) Fischer, E. O. and Hafner, W. Z.*Naturforsch.*, B **1966**, 10, 665. (b) Fischer, E. O. and Seus, D. *Chem. Ber.* **1956**,89,1809. (c) Cofield, T. H.; Sandel, V.; Closson, R. D. *J. Am. Chem. Soc.* **1967**, 79, 5826.

16. Rybinskaya, M. I.; Kaganovich, V. S.; Kydinov, A. R. *Izu. &ad. Nauk SSR*, *Ser. A Khim*. **1984**,885.

17. Pearson, A. J.; Shin, H. *Tetrahedron* **1992**, 48, 7527.

18. Pearson, A. J.; Richards, I. C. *J. Organomet. Chem.* **1983**,258, C41

19. (a) Mews, R. *Angew. Chem., Int. Ed. Engl.* **1975**, 14, 640. (b) Wimmer, F. L.; Snow, M. R. *Aust. J. Chem.* **1978**, 31,267. (c) Uson, R.; Riera, V.; Gimeno, J.; Laguna, M.; Gamasa, M. P. *J. Chem. SOC., Dalton Trans.* **1974**, 966. (d) Cotton, F. A.; Darensbourg, D. J.; Kolthammer, W. S. *Inorg. Chem.* **1981**, 20, 1287. (e) Schmidt, S. P.; Nitschze, J.; Trogler, W. C. *Inorg. Synth.* **1989**,26, 113.

20. Basin, K. K.; Balkeen, W. G.; Pauson, P. L. *J. Organomet. Chem.* **1981**, 204, C 25.

21. S. Sun, L. K. Yeung, S. R. Switzer, T.-Y. Lee, S. S. Lee, Y. K. Chung, R. D. Pike, and D. A. Sweigart, *Organometallics*, **1995** 14, 2613.

22. Antoine Eloi, Franc-oise Rose-Munch,* Eric Rose,* and Petra Lennartz *Organometallics* **2009**, 28, 5757–5764

23. Peter L. Pauson and John A. Segal, *J.C.S. Dalton* **1975** 1677-1682

Chapter 6

Surface electrochemistry of aromatic manganese tricarbonyl complexes using diazonium attachment and physical surface modification

—— organometallic electrode

6.1 Introduction

As already being discussed in chapter 3, the electrochemistry of monoarene manganese tricarbonyl in homogeneous solution is investigated: Compared with the far greater reactivity of the polyarene $Mn(CO)_3^+$complexes,[1,2] monoarene [HMB $Mn(CO)_3$]PF_6 and it's analogs exhibit quite stable properties. It is reduced irreversibly by one electron at much more negative potential to give $19e^-$ unstable radical at room temperature, the free radicals will dissociate one carbonyl from the $Mn(CO)_3^+$ moiety followed by dimerization to afford a green color bimetallic compound with a metal-metal bond.[3]

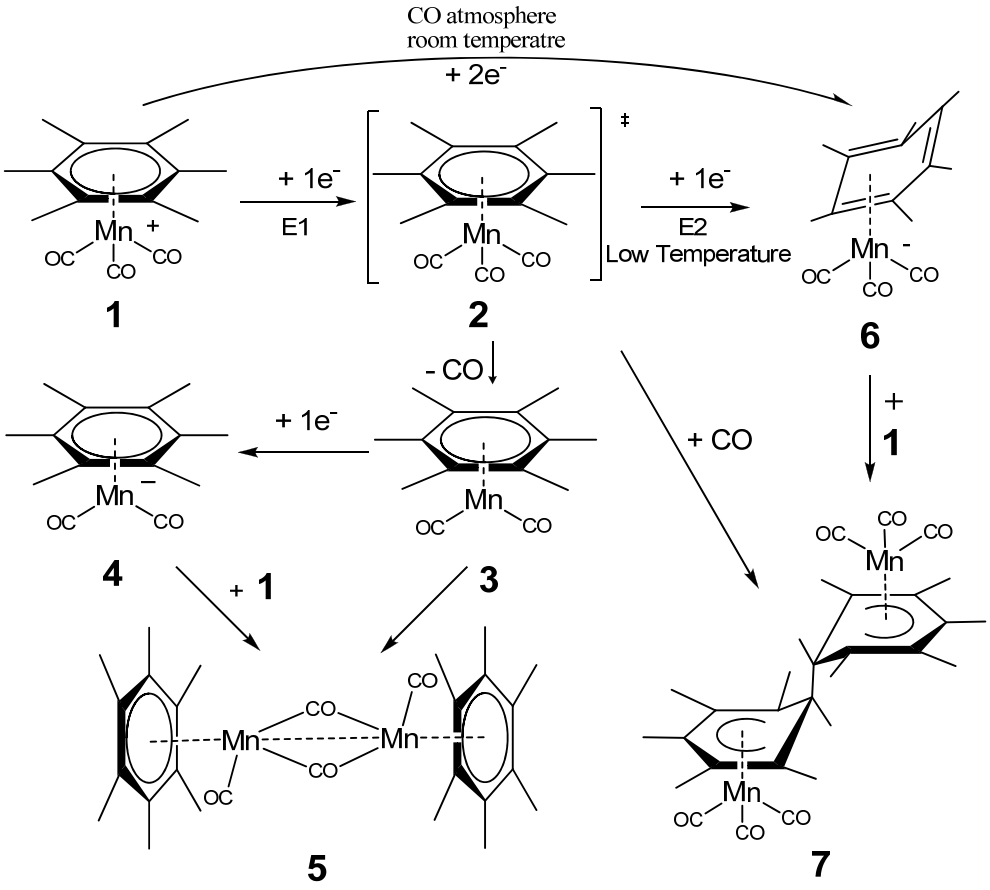

Figure 6-1. Mechanism of electrochemistry of $(\eta^6\text{-HMB})Mn(CO)_3^+$

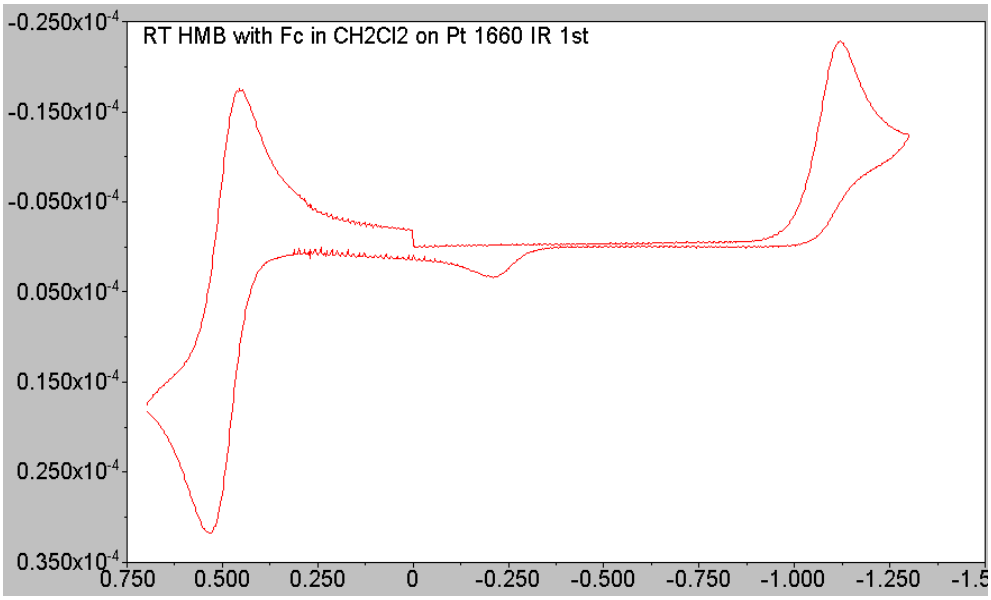

Figure 6-2. CV of 1mM compound **1** at room temperature on Pt electrode. 1mM ferrocene was used as an internal potential standard. Scan rate is 0.50V/s.[4]

The monoarene manganese tricarbonyl loses its chemical reverisibility under applied potential and decomposed to a green color manganese dimer. There is no chemical reversibility observed for monoarene manganese tricarbonyl. Electrochemist prefers reversibility not only because that it indicates the stability under reduction or oxidation, but also the potential application as an electrocatalyst. If the decomposition, in another word, dimerization of the complex 1 could be stopped, the electrochemistry could very possibly be chemically reversible. Enabling the reversibility of complex 1 would widen the scope of our view of electrochemistry of monoarene manganese complex. A redox active complex would be more attractive, might have potential applications in catalysis and sensor.

1. The following methods might stop the dimerization:

1). Excess CO was bubbled into the solution where cyclic voltammetry is conducted. Excess carbon monoxide might prevent complex 1 from losing CO after reduction, hence, stop the dimerizaton (discussed in chapter 3).

2). Physical attachment: powder of complex 1 was loaded onto the surface of the electrode. CV was conducted in aqueous solution since complex 1 has no solubility in aqueous solution. Ideally, the complex 1 on the surface of the electrode would not dissolve into the aqueous solution, so under the applied reductive potential, even losing CO ligand, two of them can not move freely to dimerize.

3). Chemical attachment: diazonium attachment is one of the wildly used chemical attachments. The precursor has already been synthesized (chapter 5). So in this

chapter, I will take it from there.

For the purpose of applying our research to more interesting and applicable areas, like surface electrocatalyst, bio-sensor, we want to combine the previous work with the chemical modified electrode, that is, we will try to load our Mn, Re or any other promising transition metal moiety to the surface of the commonly used electrodes, like Pt, Glassy Carbon, Au. Furthermore, covalent attachment is the most promising attachment method for our research, since it's a stronger attachment to the substrate surface, and it might be stronger enough to undergo high activation energy barrier (high temperature, high pressure). What we know mostly is the interaction between the aryl group and the metal moiety on a conductive substrate and what we are most interested is how differently it will behave if it is directly attached to the substrate other than moving freely in the solution.

The surface modification of the conductive substrate —— "electrode surface synthesis", was introduced by Royce. W. Murray[5] and his colleagues at early 1970s. For the first time, the conductive substrate tin dioxide electrode was chemically functionalized with amine group through covalent bond, which was a milestone, because amine surface was much reactive and could be further modified by other desired functional groups via linker chemistry.

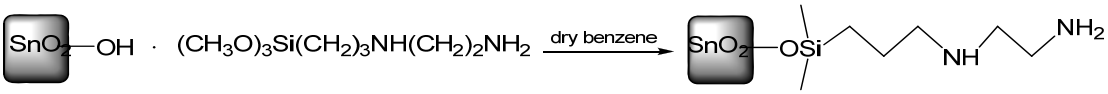

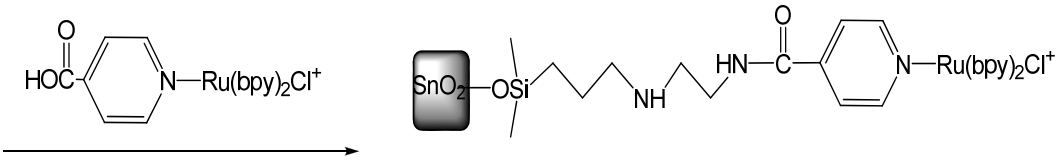

Figure 6-3. Surface modification of Tin dioxide with ruthenium complex

There are several methods of strong attachment for modifying electrode surface, in another word, chemical bonding: diazonium salt based attachment, click chemistry, spontaneous oxidation of primary amine to form a C-N bond on glass carbon electrode. Of which, diazonium based attachment is most convenient and straightforward method in our case.

Geiger[6] reported the first chemically modified electrode by aromatic cobalt and manganese complexes. He successfully loaded cobaltocenium and cyclopentadienyl manganese tricarbonyl[7] complex onto the surface of glassy carbon electrode using diazonium based attachment.

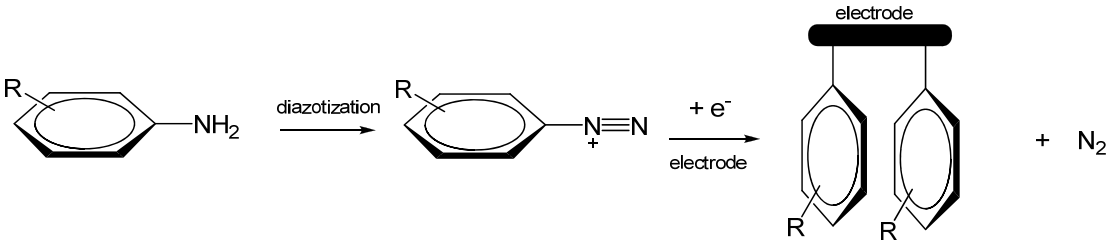

Scheme 6-1. Mechanism of surface modification using diazonium attachment.

Not alike aniline by itself, manganese tricarbonyl functionalized aniline complex (η^6-aniline) $Mn(CO)_3^+$ could not be diazotized by nitrite. So we change its hapticity from eta6 to eta5 to make the π system more electron rich. (η^5-aminocyclohexadienyl) manganese tricarbonyl was synthesized and diazotized to

afford (η^5-cyclohexadienyldiazonium) manganese tricarbonyl complex. This cyclohexadienyl manganese tricarbonyl diazonium complex can be reduced to liberate nitrogen and form a bond between the cyclohexadienyl group and electrode surface. The substituted hydrogen could be removed by treating with CPh_3^+ or strong acid thereafter. Herein, we want to report a unique method for surface modification of electrode by (η^6-aromatic) manganese tricarbonyl cation. We want to compare its reductive electrochemistry before and after electrode surface modification, and we expect to see that the chemical reversibility shows up. No preliminary data has been acquired yet. We are still working on the purification and characterization of the intermediates. $(\eta^6\text{-}C_6H_5NHC_6H_4NH_2)Mn(CO)_3^+$ was synthesized from nucleophilic substitution of $(\eta^6\text{-}C_6H_5Cl)Mn(CO)_3^+$ by p-phenylenediamine, then it was diazotized to afford $(\eta^6\text{-}C_6H_5NHC_6H_4N_2)Mn(CO)_3^{2+}$. We can see that partial reversibility shows up in the CV time scale (scheme 6-2).

In the meanwhile, taking advantage of the solubility of arene manganese tricarbonyl complex, we have done their heterogeneous electrochemistry by physical attachment.

(η^5-aminocyclohexadienyl) manganese tricarbonyl mediated slow hydrogen release is the side reaction when it is treated with acid. Other (η^5-hydrocyclohexadienyl) manganese tricarbonyl analogs show similar properties of hydrogen release. The amine group of $(\eta^5\text{-}C_6H_6NH_2)Mn(CO)_3$ facilitates the hydrogen release reaction.

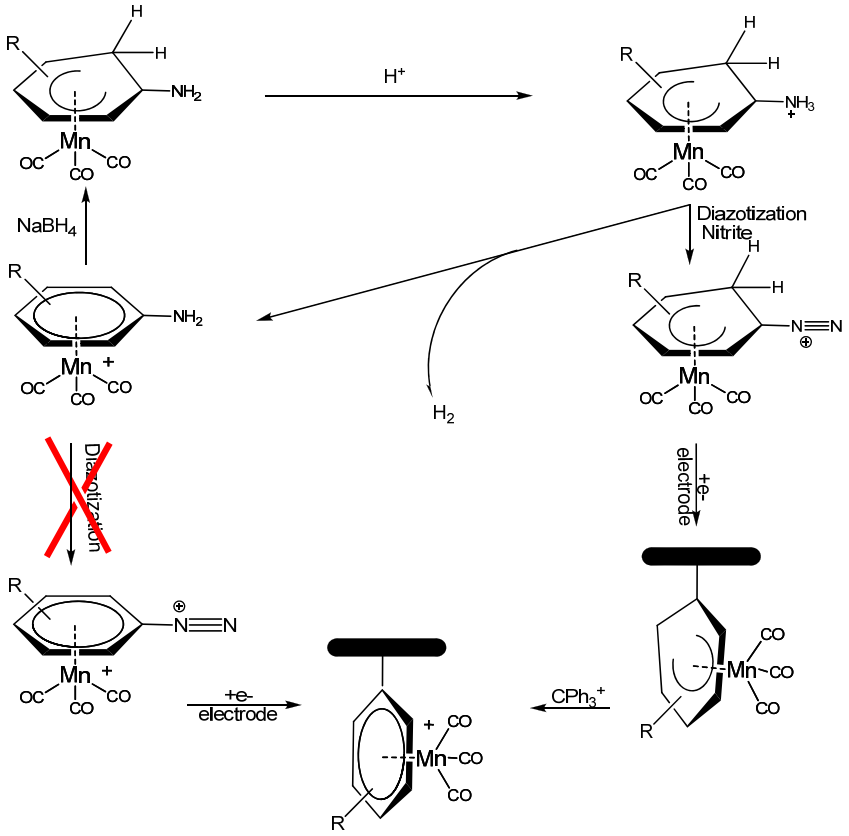

Scheme 6-2. Surface modification of electrode by aromatic manganese tricarbonyl cation through diazonium attachment & slow hydrogen release as side reaction.

In the meanwhile, taking advantage of the solubility of arene manganese tricarbonyl complex, we have done their heterogeneous electrochemistry by physical attachment.

6.2 Experimental

1. Synthesis

$(\eta^5$-$HC_6H_5NH_2)Mn(CO)_3$ The synthesis method of this (η^5-aminocyclohexadienyl) manganese tricarbonyl cation is straightforward. $[(\eta^6$-aniline$)Mn(CO)_3]BF_4$ (0.638g, 2.00mmol) and tetrabutylammonium borohydride

(0.566g, 2.20mmol) were combined with 20ml dichloromethane in a 50ml round bottom flask in ice bath. The reaction mixture was stirred for 30mins in ice bath and then 30mins at room temperature. The product was purified by running through the silica gel column using dichloromethane as eluent. IR in dichloromethane: 2005 and 1923 cm^{-1} ; in ether: 2007, 1930 and 1917 cm^{-1}.

$[(\eta^5\text{-}HC_6H_5N_2)Mn(CO)_3]BF_4$ The diazotization of $(\eta^5\text{-}HC_6H_5NH_2)Mn(CO)_3$ was conducted in acetone solution. $(\eta^5\text{-}HC_6H_5NH_2)Mn(CO)_3$ (0.233g, 1.00mmol), excess amount of $HBF_4 \cdot Et_2O$ and t-butyl nitrite (0.158ml, 1.20mmol) were combined with 20ml acetone in a 50ml round bottom flask in ice bath. The reaction mixture was stirred for 60mins in ice bath. The color of the solution changed from yellow to orange red. After reaction, solvent was dried to minimum amount and excess amount of ether was added to precipitate the product. Orange red solid were washed several times by ether. Dichloromethane was used to dissolve any soluble species until nothing could be dissolved. Then the dichloromethane solution was combined and dried to minimum amount and was treated with excess ether to precipitate the yellow salt in it. The yellow salt is the desired (η^5-cyclohexadienyldiazonium) manganese tricarbonyl complex. IR of it in dichloromethane is 2065 2004 cm^{-1} for CO; 2291 cm^{-1} for diazonium. The leftover yellow compound is **$[(\eta^6\text{-aniline})\ Mn(CO)_3]BF_4$.** It came from a side reaction of the above diazotization. We can reuse the aniline manganese complex.

$[(\eta^6\text{-chlorobenzene})Mn(CO)_3]PF_6$ $Mn(CO)_5Br$ (2.749g, 10.00mmol) and $AlCl_3$ (2.414g, 20.00mmol) were combined with 30ml chlorobenzene in 100ml round

bottom flask. The mixture was heated to reflux for 8 hours. After reaction, the mixture was cooled down and washed by 15ml of DI water several times. The water solution was combined and washed by toluene two times and hexane two times. Then, excess amount of 45% HPF_6 was added to the water solution to precipitate the product. The mixture was filtered and precipitate was washed by ether three times. The yield of the product is 60%. Recrystallization was taken by slow evaporation of ether into its acetone solution. IR of it in acetone is 2084, 2032 cm^{-1}.

$[(\eta^6\text{-}p\text{-}C_6H_5NHC_6H_4NH_2)Mn(CO)_3]PF_6$ $[(\eta^6\text{-chlorobenzen})Mn(CO)_3]PF_6$ (0.397g, 1.00mmol) and p-phenylenediamine (0.225g, 2.08mmol)were dissolved in 4ml and 2ml of acetone separately. The manganese solution was added into the phenylenediamine solution drop by drop while the solution was kept stirring. Precipitate formed instantaneously. After two solution was combined, the precipitate was removed. The left over acetone solution was dried to minimum amount and treated with excess amount of ether. The product precipitated out and recrystallized via slow evaporation of ether into its acetone solution. The yield is 90%. IR of it in acetone is 2063, 1998 cm^{-1}.

$[(\eta^6\text{-}C_6H_5NHC_6H_4N_2)Mn(CO)_3](BF_4)_2$ Similar method was applied to the diazotization of $[\eta^6\text{-}p\text{-}C_6H_5NHC_6H_4NH_2)Mn(CO)_3]PF_6$. $[\eta^6\text{-}p\text{-}C_6H_5NHC_6H_4NH_2)$ $Mn(CO)_3]PF_6$ (0.936g, 2.00mmol), excess amount of $HBF_4 \cdot Et_2O$ and t-butyl nitrite (0.316ml, 2.40mmol) were combined with 20ml acetone in a 50ml round bottom flask in ice bath. The reaction mixture was stirred for 60mins in ice bath. The color of the solution changed from yellow to orange red. After reaction, solvent was dried to

minimum amount and excess amount of ether was added to precipitate the product. Orange red solid were washed several times by ether and dichloromethane. The orange yellow salt is the desired manganese tricarbonyl diazonium dication complex. IR of it in acetone is 2073, 2014 cm^{-1} for carbonyls and a small peak at 2258 cm^{-1} for the diazonium.

2. Surface modification of glassy carbon electrode via reduction of diazonium salt

1mM of the diazonium salt, 0.1M $TBAPF_6$ electrolyte and 10ml acetonitrile were combined in a cyclic voltammetry cell. Nitrogen was used to bubble through and above the whole system before and after electrochemistry experiment. Fresh polished glassy carbon electrode was used. The reduction potential was kept at -0.6V for 600s with the solution being stirred all the time. After the electrolysis, the electrode was rinsed thoroughly by acetonitrile to remove any chemical that might attach to the surface physically. Sonication was also used to clean the surface of the electrode. After sonication, electrode was kept dry in the nitrogen.

3. To test the electrochemical signal from the modified electrode.

A blank dichloromethane solution was prepared with 0.1M $TBAPF_6$ electrolyte. Again, nitrogen was bubbled through and above the solution in the cell before and after cyclic voltammetry experiment. Since (η^6-arene) manganese tricarbonyl cation is reductive active electrochemically. Potential was set to start from 0V to -1.5V vs Ag/AgCl.

4. Physical attachment

1mM of $[(\eta^6\text{-HMB})Mn(CO)_3]PF_6$ solution in acetone was prepared. The glassy carbon electrode was dipped into the solution for 3s, and then was lifted. Nitrogen was used to dry the surface of the electrode. Blank aqueous solution with 0.1M KCl was used to test the electrochemical signal from the modified electrode. 1mM of $[(\eta^6\text{-benzene})Mn(CO)_3]PF_6$ solution in acetone was tried also. Instead using aqueous solution, blank dichloromethane solution with 0.1M $TBAPF_6$ was used, since the bad solubility of $[(\eta^6\text{-benzene})Mn(CO)_3]PF_6$ in dichloromethane.

In the above case, even $[(HMB)Mn(CO)_3]PF_6$ dissolves well in dichloromethane, its solution could not be used for unknown reason. Not signal could be detected if pretreating the electrode surface with $[HMB\ Mn(CO)_3]PF_6$ dichloromethane solution. We thought that, dichloromethane solution might result in bad contact between the compound and the electrode surface.

6.3 Result and discussion

Surface modification is a method which brings two types of surface together. Organometallic electrode: also called chemically modified electrodes, that is the study of electroactive monolayers and thicker films on the conductive substrates. This aspect of electrochemistry is more and more active in recent years. A lot of people have put their effort into this area and a number of publications related to the preparation, characterization, application and electrochemical behavior of chemically modified electrodes are available [8-13]. Modification of electrode surfaces for catalytic or analytical purposes and biotechnological applications currently attracts

considerable attention because of potential applications in areas such as electrocatalysis, sensor development and semiconductor productions.

There are many ways of modifying the surface of the conductive substrates, such as: irreversible adsorption,[12] covalent attachment of a monolayer, and coating the electrode with films of polymers or other materials[12]. Of which, chemical modification is preferred not only because it provides the strongest attachment but also it fundamentally changed the chemical and physical properties of the conductive substrate, which give versatile surface modified with desired functional group.

The purpose of heterogeneous electrochemistry study is to achieve the electrochemical reductive reversibility by covalent attachment of arene manganese tricarbonyl using diazonium-base chemistry or simply physical adsorption attachment. Physical separation of manganese compound may stop the dimerization after one-electron reduction and result in reductive reversibility. Organometallic electrode is a new concept in the area of heterogeneous electrochemistry. One of my projects is focused on covalent attachment of arene manganese tricarbonyl using diazonium-base chemistry and collecting and analyzing e-chem signal from the surface functionalized electrode.

As already being discussed in chapter 5, aniline is deactivated after the coordination of manganese moiety. Thus, we need to add a hydride to change the hapticity of (η^6-aniline) $Mn(CO)_3^+$ from eta6 to eta5 in order to reactivate this manganese functionalized aniline. The strategy is illustrated in scheme 6-2.

1. Side reaction

The diazotization of $(\eta^5\text{-}HC_6H_5NH_2)Mn(CO)_3$ leads to side reaction with $(\eta^6\text{-aniline})Mn(CO)_3$ as byproduct. The slow hydrogen release reaction was discussed in chapter 4 and the mechanism was discussed. The key intermediate is a formation of ring slippage $(\eta^4\text{-R-}C_6H_5)MnH(CO)_3$. In the above case, aromatic amine is a base with moderate strength, the incorporation of amine will facilitate the uptake of proton and interaction between N-H-Mn, thus accelerate the hydrogen liberation and indeed, Inspired by this side reaction, we are trying to optimize our $CpMn(CO)_2NO^+$ pre-catalyst by incorporating an amine group to the aromatic hydrocarbon ring.

Diazotization of $(\eta^5\text{-}HC_6H_5NH_2)Mn(CO)_3$ leads to the formation of its diazonium analog $[(\eta^5\text{-}HC_6H_5N_2)Mn(CO)_3]BF_4$. Experiment was held at this step; we are in the process of confirming the existence of this reactive species which contains hydride and diazonium cation. Molecular internal redox reaction between oxidant diazonium salt and reductant hydride would result in explosion.

2. Direct diazotization

Compared with the above indirect diazotization method, direct diazotization method was applied. See the following scheme.

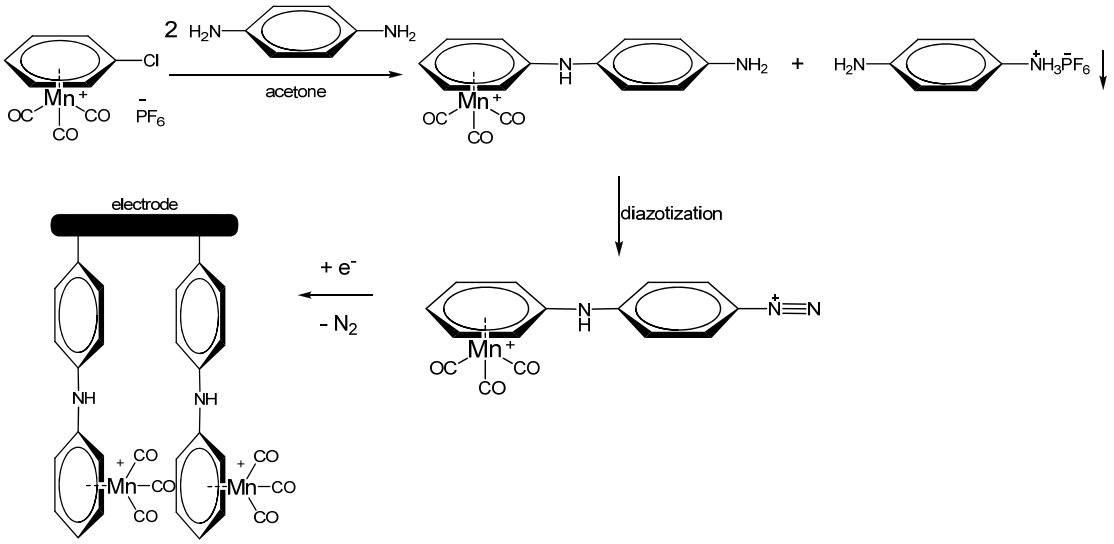

Scheme 6-3. Reaction pathway for indirect diazotization without changing hapticity.

By incorporating p-phenylenediamine as a linker, we not only introduce free aniline into our system; but also keep the hapticity unchanged (scheme 6-3). Compared with the indirect method, this strategy is straight forward and more convenience. However, a nitrogen heteroatom was introduced into the system after surface modification. We lack information about good interpretation of homogeneous electrochemistry of N-phenyl-aniline manganese tricarbonyl complex, so their heterogeneous electrochemistry remains unclarified. But it is for the first time that, eta6 aromatic manganese tricarbonyl cation was successfully introduced onto the surface of glassy carbon electrode. The cyclic voltammetry of the surface modified electrode in blank solvent is shown in figure 6-4.

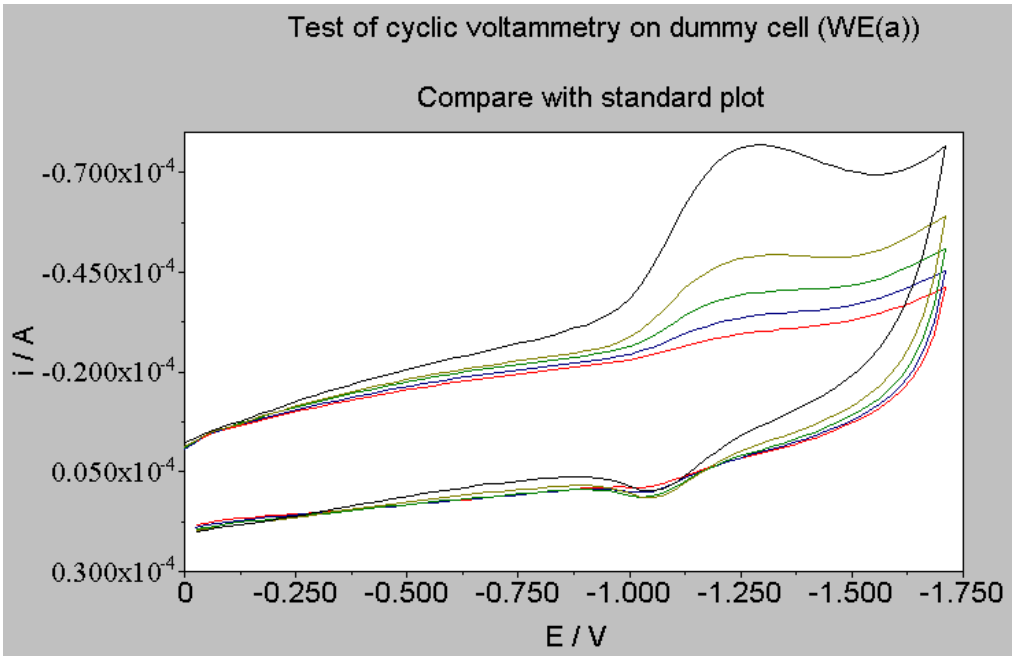

Figure 6-4. Continuous five scans of cyclic voltammetry of $(\eta^6\text{-p-}C_6H_5NHC_6H_4\text{-})Mn(CO)_3^+$ modified glassy carbon electrode in blank dichloromethane solution with 0.1M $TBAPF_6$ at room temperature. The scan rate is 5V/s.

The electrode was rinsed carefully to remove any physical adsorption. From the above continuous five scans, partially chemical reversibility was observed; however, each scan lost around 80% reversibility, therefore at fifth scan (red line), no peak could be observed any more. We could not give a reasonable explanation about the generation of reversibility and we are not sure about the whether it is two electrons or one electron reduction.

3. Physical attachment

One drop of 1mM $[(HMB)Mn(CO)_3]PF_6$ acetone solution was dried directly on the surface of the glassy carbon electrode. The adsorbed complex

[(HMB)Mn(CO)$_3$]PF$_6$, which is insoluble in water, produced a chemically irreversible reduction at E_p = -1.27 *V*. The peak current became greatly diminished after the first scan cycle. Since the formation of dimer **5** or ring coupled dimanganese complex **7** should be sterically difficult, our interpretation is that formation of anionic **4** occurs, but is very rapidly followed by protonation by the medium (water) to give the known and electrochemically-inactive (η^6-C$_6$Me$_6$)Mn(CO)$_2$H. This explanation is consistent with the diminished reduction current observed on the 2nd scan.

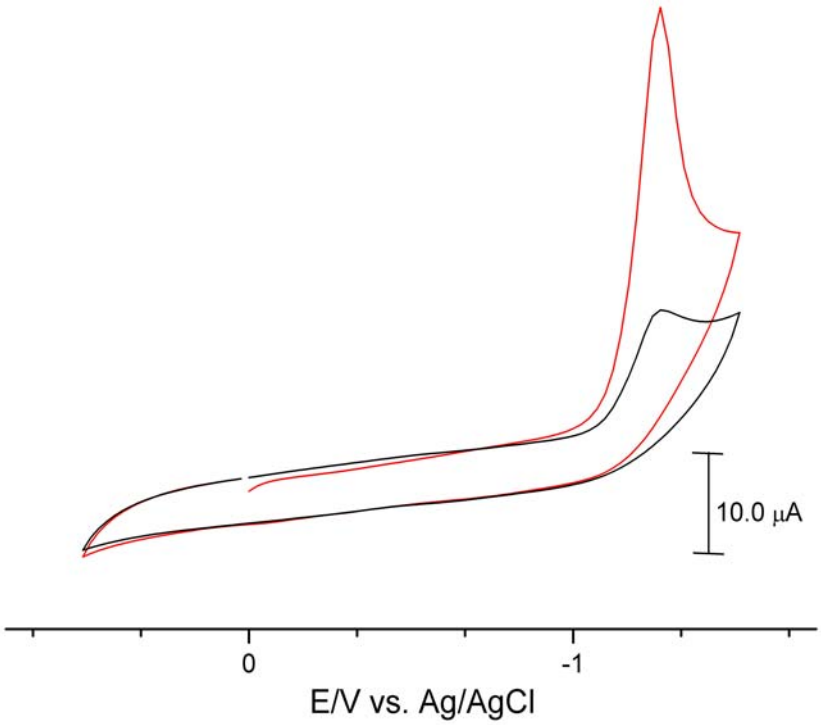

Figure 6-5. CVs of solid [(η^6-C$_6$Me$_6$)Mn(CO)$_3$]PF$_6$ (**1**) deposited from a 1 mM acetone solution onto a 3.0 mm diameter glassy carbon working electrode by evaporation at 20 ^{o}C. The CV medium was 1.0 M KCl in water under N$_2$. The

scan rate was 0.50 V s^{-1}. The first scan is shown in red and the second is shown in black.

Similar physical attachment experiment was applied to $[(\eta^6\text{-}C_6H_6)Mn(CO)_3]PF_6$. Dichloromethane solution was used since $[(\eta^6\text{-benzene})Mn(CO)_3]PF_6$ has limited solubility in CH_2Cl_2.

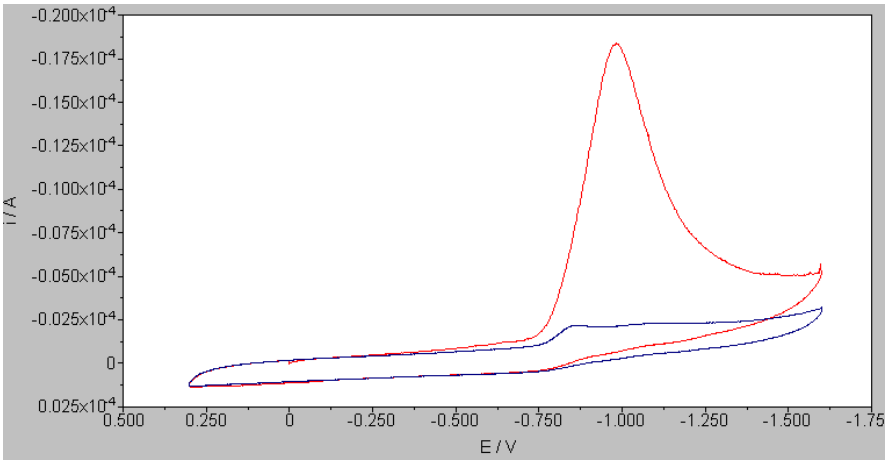

Figure 6-6. CVs of solid $[(\eta^6\text{-}C_6H_6)Mn(CO)_3]PF_6$ deposited from a unknown concentration acetone solution onto a 3.0 mm diameter glassy carbon working electrode by evaporation under nitrogen at 20 ^oC. The CV medium was 1.0 M KCl in water under N_2. The scan rate was 0.05 V s^{-1}. The first scan is shown in red and the second is shown in blue.

In the above CVs, the solvent was changed to non-nucleophilic CH_2Cl_2. The electrochemistry of benzene manganese tricarbonyl cation mimics the one of compound 1.[3] Similar anion $(\eta^6\text{-}C_6H_6)Mn(CO)_2^-$ formed after major reduction at -0.95 V, however it stayed as anion or partially dissolved in the solution. No peak for the dimer was found, and the peak current for the continuous second scan vanished (in

blue).

Taking advantage of solubility of our interested complexes, physical attachment method could be easily applied into heterogeneous electrochemistry study. Compared with chemical modification, its flexibility and renewability are advantageous, however, it lacks durability and the concentration of the modification could not be well controlled.

6.4 Conclusions.

In this chapter, different surface modification methods were applied to heterogeneous electrochemistry study of eta6 aromatic manganese tricarbonyl cation. Interesting intermediates were observed via solid state electrochemistry through physical adsorption. We successfully modified a conductive surface (GC) by aromatic manganese carbonyl moiety using phenylenediamine as a linker; however, the heteroatom makes the electrochemistry of the target complicated. We are still working on permanent attachment using diazonium chemistry indirectly by changing the hapticity from eta 6 to eta 5.

6.5 References

1. S. Sun, L.K. Yeung, D. A. Sweigart*, T.-U. Lee, S.S.Lee, Y. K. Chung, S. R. Switzer, and R. D. Pike, *Organometallics*, **1995**, 14, 2613.
2. S. Sun, C. A. Dullaghan, and D. A. Sweigart*, *J. Chem. Soc., Dalton Trans.*, **1996**, 4493.
3. Catherine C. Neto, Carl D. Baer, Young K. Chung and Dwight A. Sweigart" *J. Chem. Soc., Chem. Comun.*, **1993** 816-818
4. Chapter 3.
5. P. R. Moses, L. Wier, and R. W. Murray, *Anal. Chem.*, 47, 1882 (**1975**).
6. Jannie C. Swarts, Derek Laws, and William E. Geiger* *Organometallics* **2005,** *24,* 341-343
7. Derek R. Laws, John Sheats, Arnold L. Rheingold and William E. Geiger*, *Langmuir* **2010**, 26(18), 15010 - 15021
8. Bernard, M.-C.; Chausse, A.; Cabet-Deliry, E.; Chehimi, M. M.; Pinson, J.; Podvorica, F.; Vautrin-Ul, C. *Chem. Mater.* **2003**, 15(18), 3450.
9. Michel Delamar, Rachid Hitmi, Jean Pinson, Jean Michel Saveant *J. Am. Chem. Soc.*; **1992**, 114(14), 5883
10. Bahr, J. L.; Yang, J.; Kosynkin, D. V.; Bronikowski, M. J.; Smalley, R. E.; Tour, J. M.

    J. Am. Chem. Soc., **2001**, 123(27), 6536
11. Abbou, J.; Anne, A.; Demaille, C. *J. Am. Chem. Soc*; **2004**, 126(32), 10095
12. Electrochemical Methods Allen J. Bard Larry R. Faulkner 2nd edition Charpter

14.

13. Hong, H.-G.; Park, W. *Langmuir*; **2001**, 17(8); 2485

Chapter 7

Synthesis and characterization of heterodinuclear complex with core structure of Mn-M metal metal bond

7.1 Introduction

The η^6-aromatic manganese dicarbonyl anion is strong nucleophile, it was proposed to be the important intermediate which catalyzed the proton reduction reaction (chapter 4). By introducing the dicarbonyl anion with the tricarbonyl cation stoichiometrically, Eyman reported the formation of an aromatic homodinuclear manganese complex with a Mn-Mn bond and bridged carbonyl ligands.[1] It would be interesting to check the reaction between the same manganese anion with $[(\eta^6\text{-HMB})Re(CO)_3]PF_6$. We want to explore the possibility of forming the heterodinuclear dimmer with a novel core structure of Mn-Re metal-metal bond. There is no report about the study of Mn-Re metal-metal bond; furthermore, heterodinuclear complex has potential applications in molecular catalysis.

The importance of this project:

The reaction between η^6-aromatic manganese dicarbonyl anion and other transition metal cation or neutral species might provide us a unique synthetic template for formation of Mn-M metal metal bond. This project was just initiated and I am still in the process of getting preliminary data of the first Mn-Re heterodinuclear compound. In order to make my thesis to be systematic, I need to include this project into my thesis. Any result will be discussed in my defense and further updates will be put into my thesis.

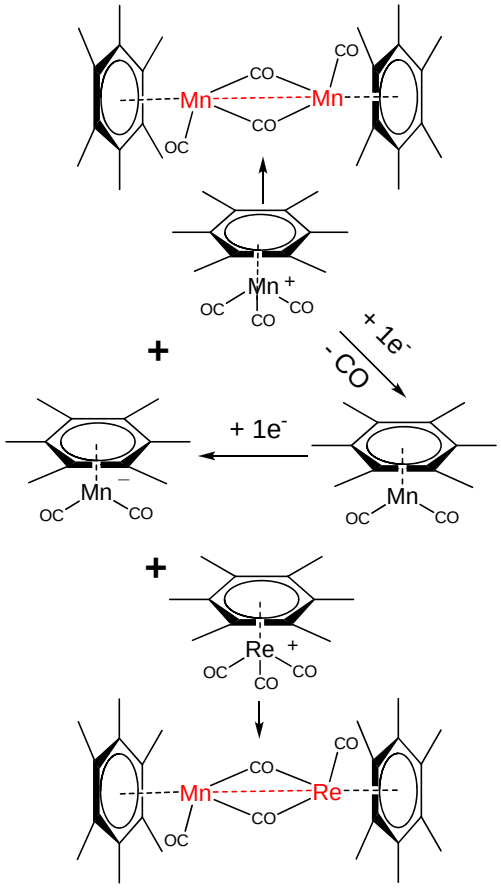

Scheme 7-1. Proposed scheme of formation of Mn-Re metal metal bond

7.2 Reference

1. Peter J. Schlom, Ann M. Morken, Darrell P. Eyman,' Norman C. Baenziger, and Steven J. Schauer *Organometallics* **1993**,12, 3461-3467